Investigation of Receptors for the Modulation of Neuronal Growth by Chondroitin Sulfate

Thesis by

Joshua Micah Brown

In Partial Fulfillment of the Requirements for the

degree of

Doctor of Philosophy

CALIFORNIA INSTITUTE OF TECHNOLOGY

Pasadena, California

2014

(Defended July 8, 2013)

Abstract

A major obstacle to neural regeneration after injury in the central nervous system (CNS) is the environment encountered by injured axons. This environment is inhibitory due to proteins expressed by the CNS myelin as well as molecules present in the glial scar. Experimental results have implicated chondroitin sulfate proteoglycans (CSPGs) as major inhibitors of axonal regeneration after CNS injury, but until recently, the mechanisms of this inhibition were not well understood. Furthermore, the complex nature of the chondroitin sulfate (CS) chains made it difficult to study their contribution to CSPG function. This thesis describes a specific carbohydrate epitope, CS-E, that is primarily responsible for the inhibition of CNS axonal regrowth in the presence of CSPGs. We show that removal or blocking of the CS-E motif via genetic elimination of the enzyme responsible for generating CS-E or a monoclonal antibody that binds specifically to the CS-E motif significantly reduces the inhibitory activity of CSPGs on axon growth. Furthermore, we show that CS-E functions as a protein recognition element to engage receptors, including the transmembrane protein tyrosine phosphatase PTPσ, which had been previously established to be a receptor for CSPGs. Finally, we show that the protein tyrosine kinase receptor EphA4 is a novel receptor for the CS-E motif, and as with PTPσ, neurons deficient in EphA4 exhibit reduced inhibition by CS-E. Our results demonstrate that a specific sugar epitope within chondroitin sulfate polysaccharides directs important physiological processes, and establish the importance of the chemical structure of CS chains in modulating the activity of CSPGs *in vivo*. The identification of receptors that mediate the inhibitory effect of CS-E advances our understanding of the

mechanisms of axon regeneration following injury to the CNS when CS-E expression is upregulated. These findings provide us with the opportunity to develop therapies for the recovery of axonal outgrowth after damage to the nervous system, which in conjunction with blocking approaches targeting the CS motif, can provide a powerful strategy for allowing recovery after injury to the CNS.

Table of Contents

List of Figures

Chapter 3

Chapter 4

Appendix 1

List of Abbreviations

Ab	antibody
Ac	acetyl, acetate
aq	aqueous
BDNF	brain-derived neurotrophic factor
BSA	bovine serum albumin
°C	degrees Celsius
$CaCl_2$	calcium chloride
cAMP	cyclic adenosine monophosphate
CGN	cerebellar granule neuron
CHO	chinese hamster ovary
CMF-HBSS	calcium- and magnesium-free Hank's balanced salt solution
CNS	central nervous system
CO_2	carbon dioxide
CS	chondroitin sulfate
ddH_2O	double distilled water
DIV	days in vitro
DMEM	Dulbecco's minimal Eagle's medium
DMSO	dimethylsulfoxide
DNA	deoxyribonucleic acid
DRG	dorsal root ganglion

DTT	dithiothreitol
E18	embryonic day 18
EDTA	ethylenediaminetetraacetic acid
Efn	ephrin
EGFR	epidermal growth factor receptor
EGTA	ethylene glycol tetraacetic acid
Fc	fragment crystallizable region of an antibody/immunoglobulin
FGF	fibroblast growth factor
g	gram, gravitational force
GAG	glycosaminoglycan
GalNAc	N-acetylgalactosamine
GDNF	glial cell line-derived neurotrophic factor
GlcA	D-glucuronic acid
GlcNAc	N-acetylglucosamine
h	hour
H_2O	water
HRP	horse-radish peroxidase
HS	heparan sulfate
IgG	immunoglobulin
IP	immunoprecipitated
Jak	Janus kinase
JNK	Jun-N-terminal kinase

K_D	dissociation constant
kDa	kilodalton
KO	knockout
L	liter
LCMS	liquid chromatography–mass spectrometry
m	milli or meter
M	molar
mAb	monoclonal antibody
MAPK	mitogen-associated protein kinase
MEM	minimal Eagle's medium
MeOH	methanol
$MgCl_2$	magnesium chloride
min	minutes
μ	micro
μg	microgram
mol	mole
MS	mass spectrometry
MWCO	molecular weight cut-off
n	nano
Na^+	sodium ion
NaCl	sodium chloride
NaOH	sodium hydroxide

NGF	nerve growth factor
NP-40	nonidet P-40 detergent
P0	post-natal day 0 mouse or rat pup
P7	post-natal day 7 mouse or rat pup
PAGE	polyacrylamide gel electrophoresis
PBS	phosphate buffered saline
PTPσ	protein tyrosine phosphatase sigma
PY	phosphotyrosine
PVDF	polyvinylidene difluoride
ROCK	rho-associated protein kinase
RNA	ribonucleic acid
rpm	revolutions per minute
rt	room temperature
SDS	sodium dodecyl sulfate
SEM	standard error of the mean
STAT	signal transducer and activator of transcription
TBST	tris-buffered saline with Tween-20
TNFα	tumor necrosis factor alpha
Tris-Cl	tris chloride
U	unit
UV	ultraviolet
vol	volume

w/v   weight per volume

WT   wild type

Chapter 1: Introduction to Chondroitin Sulfate and Inhibition in the Central Nervous System

Inhibition in the CNS

In the adult central nervous system (CNS), axons have very little ability to regenerate after injury. In contrast, neurons in the peripheral nervous system (PNS) and the embryonic CNS can regenerate, and this difference is explained by both the reduced capability for growth of mature neurons, and the presence of inhibitory molecules in the adult CNS.[1-5] A possible reason for the existence of these inhibitory molecules is that they are critical for pathfinding and axon guidance in the developing nervous system, and only present a problem in the mature organism after injury.[6] The chondroitin sulfate proteoglycans (CSPGs) are one of the main inhibitory components of the CNS, and can be found in the glial scar that forms after neuronal damage and acts as a barrier to axon regeneration.[6-8] The other inhibitory components are the members of a group of molecules known as the myelin-associated inhibitors (MAIs), which are expressed on the surface of oligodendrocytes.

It has long been known that CNS myelin inhibits neuronal growth, while PNS myelin does not have this property.[9] *In vitro* investigations of CNS myelin led to the isolation and cloning of the reticulon protein Nogo-A, which was found to be highly inhibitory to neuronal growth in culture.[10] Later studies identified myelin-associated glycoprotein (MAG) and oligodendrocyte myelin glycoprotein (OMgp), two additional inhibitory proteins that, like Nogo-A, are expressed by oligodendrocytes, and are strongly inhibitory to neuron regeneration.[11-13] These three proteins serve as independent ligands for

a common receptor complex, and all ligands bind to the Nogo receptor NgR,[13-15] providing an attractive target for blocking strategies. A more thorough discussion of these proteins and the receptors that mediate their activity can be found in Appendix 1. Findings by our lab and others have determined that there is overlap between the cellular mechanisms underlying the inhibitory effects of these two groups of molecules, and further research will provide a clearer picture of the interactions and interplay of these inhibitors. This thesis describes what we have discovered about both groups of molecules, with primary emphasis on the CSPGs.

CS Biosynthesis and Regulation

CSPGs, along with HSPGs, DSPGs, and KSPGs (chondroitin, heparan, dermatan, and keratan sulfate proteoglycans, respectively) are a type of protein with covalently attached carbohydrate chains known as glycosaminoglycans (GAGs).[7] These proteoglycans can be found in the extracellular matrix or expressed on the cell surface of many types of cells. The GAG chains on these proteins are comprised of linear chains of repeated disaccharide subunits, which differ among the GAG types (Figure 1.1).
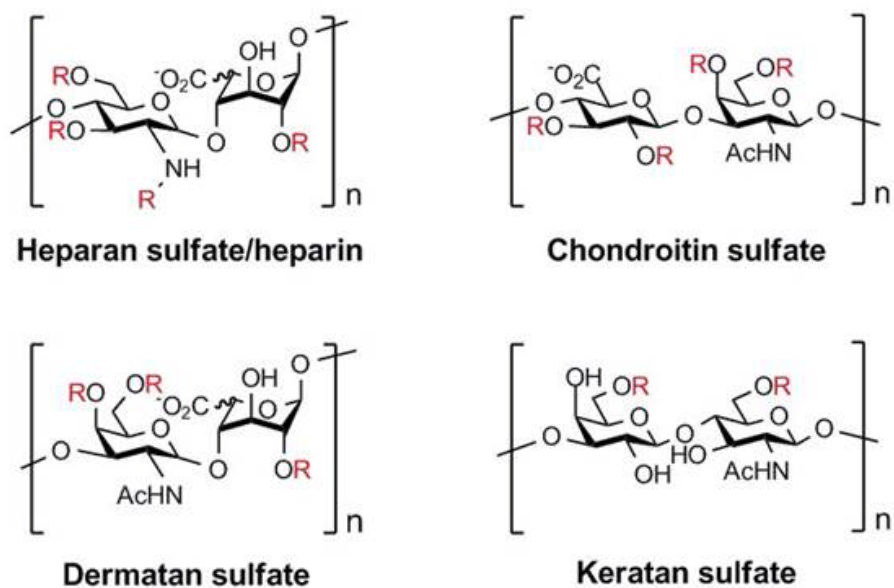
Figure 1.1. Representative classes of glycosaminoglycans, with potential sites of sulfation indicated.
$R=SO_3^-$ or H; $R_1 = SO_3^-$, H, or Ac; n= ~40-200.

The work described in this thesis focuses on the CSPGs and their interactions with protein receptors. Chondroitin sulfate (CS) is synthesized by the cell in the endoplasmic reticulum and the Golgi apparatus. This synthesis begins with the addition to the target protein of a tetrasaccharide linkage region, composed of xylose, two galactose molecules, and glucuronic acid. Xylose is first attached to a serine residue of the target protein via a xylosyl transferase, and this occurs in the endoplasmic reticulum, while the remaining sugars are attached in the Golgi apparatus.[16] Additional modifications can also take place here, and the glycosylated protein is then transported to the cell membrane via the trans-Golgi network.
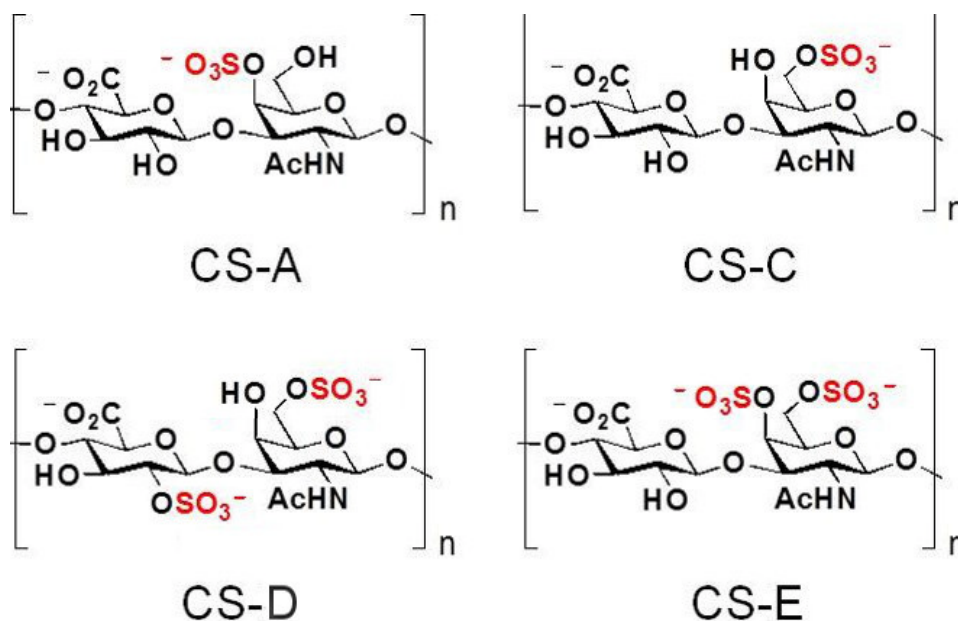
Figure 1.2. CS polysaccharides are composed of disaccharide repeating units of D-glucuronic acid (GlcA) and N-acetyl-D-galactosamine (GalNAc). The sugar hydroxyls are variably sulfated to give rise to diverse sulfation patterns. Chemical structures of major sulfation motifs found in the mammalian nervous system: CS-A (GlcA-4SGalNAc), CS-C (GlcA-6SGalNAc), CS-D (2SGlcA-6SGalNAc) and CS-E (GlcA-4S, 6SGalNAc). n = 20-200.

CS is comprised of an unbranched chain of alternating glucuronic acid (GlcA) and N-acetylgalactosamine (GalNAc). The CS chain is elongated by CS polymerases, and can range in length from 20-200 disaccharide units.[17-19] During elongation, the disaccharide motifs of CS can be sulfated in a variety of ways, and these sulfate groups are introduced via the CS sulfotransferases (STs) in the Golgi apparatus.[16] The most common CS motifs are shown in Figure 1.2. There have been seven sulfotransferases identified to date: three isoforms of C4ST,[20, 21] two isoforms of C6ST,[22, 23] a uronyl-2-sulfotransferase, which converts CS-C to CS-D,[24] and GalNAc4S-6ST, which converts CS-A to CS-E.[25] The two most common CS motifs, CS-A and CS-C, are generated by the sulfation of the C4 and C6 hydroxyl of GalNAc, respectively.[16] The CS-C motif can be further modified by the addition of a sulfate group to the C2 hydroxyl of GlcA to produce CS-D, while the CS-A

motif can be modified by the addition of a second sulfate group to the C4 hydroxyl of GalNAc to form CS-E (Figure 1.3).

Different sulfated motifs of CS occur in specific brain regions and tracts, and are expressed in an age-dependent manner, supporting the notion of CS serving as a cue or boundary for axon guidance.[26, 27] This is correlated with the expression of sulfotransferases in specific brain regions, with several of these enzymes being highly expressed in the embryo, with less expression in the neonatal brain.[28] The expression of CS is important for the guidance of axons in the development of tracts, and a loss of CS results in aberrant growth of axons in the embryonic nervous system and the retina.[29, 30]
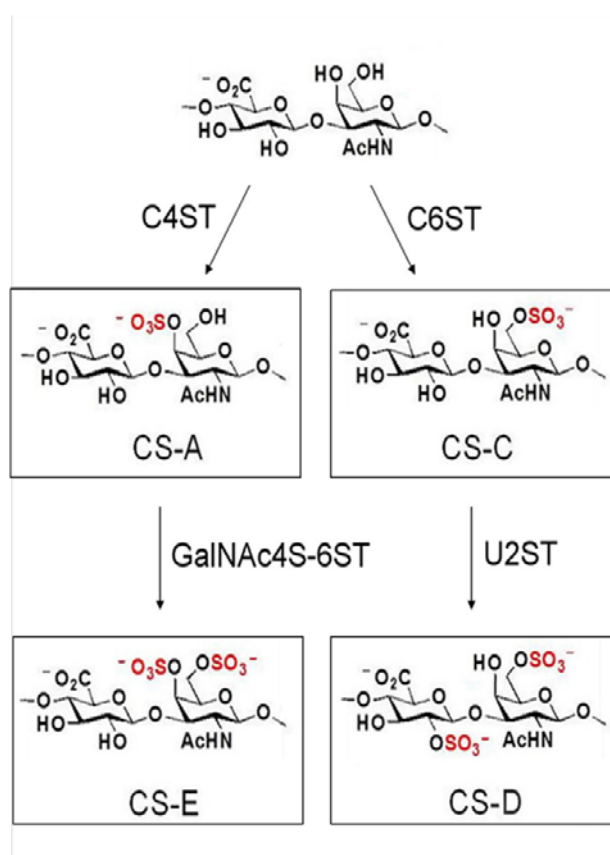
Figure 1.3. Biosynthesis of chondroitin sulfate by the sulfotransferases.

Since it is known that CSPGs are a major contributor to the inhibition of regeneration after injury, various groups have investigated the time-dependent upregulation of CSPGs after a lesion is introduced. Increased immunostaining of the CSPGs neurocan, NG2, brevican, and versican is observed after injury to the spinal cord, and peak detection of this increase occurs rapidly, within a week or less.[31-33] In some cases, increased expression is observed within 24 hours.[31] Increased expression of neurocan and versican has also been observed in injuries to the cortex,[34, 35] again with peak increases observed within a week or less. These results show that certain types of CSPGs become more prevalent after injury, and these CSPGs may prove to be particularly inhibitory. It is known that the growth inhibition effect is due mostly or completely to the CS chains of proteoglycans, rather than the protein cores.[36, 37] Therefore, some groups have investigated whether changes occur to the CS side chains after injury. One group studied the ratio of different CS motifs in uninjured or injured mouse cortex. In uninjured animals, CS-A was the dominant motif, but became significantly reduced after injury. On the other hand, CS-C became more prevalent, and the CS-D and CS-E motifs were present in observable amounts, which was not the case prior to injury.[38] This difference in motif abundance is likely due to the differential expression of sulfotransferases, the expression of which has been shown to be modified after injury.[27]

The work described in this thesis shows that the CS-E motif is one of the main contributors to neuron outgrowth inhibition after injury to the CNS, and is the element present on CSPGs responsible for their inhibitory effect. Work by our collaborators has shown that CS-E is strongly and rapidly upregulated after injury; in the optic nerve, CS-E expression increased soon after injury, with intense staining visible within 24 hours (see

Chapter 3). Furthermore, blocking of CS-E via a monoclonal antibody reversed the inhibitory effect. Subsequent research by others has supported our finding: recently, it was shown that localized upregulation of GalNAc46ST occurs in the cortex after lesioning. This study also found that astrocytes that had been treated with siRNA to downregulate the expression of C4ST or GalNAc46ST, thus reducing or eliminating the presence of CS-A and CS-E or CS-E alone, respectively, resulted in astrocytes that were less inhibitory to cortical neurite outgrowth.[39] Taken together, these results suggest that the CS-E motif becomes more prevalent concurrent with the upregulation of CSPGs, and provides most if not all of the inhibitory effect of CSPGs.

The CS-E motif

The CS-E motif has been shown to be widely expressed in the developing nervous system and in the cerebellum and olfactory bulb of postnatal mice.[40] In certain contexts, this CS motif promotes the growth of neurons.[41, 42] This effect was first observed in embryonic hippocampal neurons, the growth of which is also increased by the CS-D motif, although to a lesser degree than that seen with CS-E.[41] This growth-promoting effect was further confirmed by our group, which used a chemically synthesized CS-E tetrasaccharide to demonstrate the result, eliminating the possibility of mixed disaccharide subunits being responsible for the effect.[42] The growth-promoting effect was found to be due to the protein-binding properties unique to CS-E, as certain growth factors were shown to bind specifically to this motif, and not to other CS motifs. This selective binding provides a mechanism in which CS-E is able to increase the local concentration of growth factors present *in vivo*, and thereby increase neuronal growth.[43, 44]

As mentioned previously, in other contexts CS-E is potently inhibitory, and overcoming this inhibition is critical for regeneration after injury. In the postnatal nervous system, CS-E is typically not present in measurable amounts, and is only observed after injury.[38] In contrast to the embryonic nervous system, in which CS-E recruits factors to stimulate growth, CS-E that is upregulated after injury engages protein receptors on the surface of neurons to transmit downstream inhibitory signaling. The work described in this thesis shows the specific binding partners of CS-E that we have discovered, and how the inhibitory effect can be eliminated by blocking the CS-E motif and thus disrupting receptor binding.

A valuable tool for elucidating the role of CS-E is mice that are deficient in GalNAc4S-6ST, the enzyme that catalyzes the formation of CS-E. These knockout animals are born healthy and fertile, and have no obvious physical defects. One possible effect is a decreased litter size in homozygous crosses that perhaps suggests some degree of embryonic lethality, although this has not been systematically studied.[43] Recent results from our group show that axon pathfinding is altered in these embryos, with ectopic retinal axon terminations in the superior colliculus (C. Rogers, unpublished results). Furthermore, it is expected that these animals will exhibit enhanced recovery after spinal cord injury, as the CS-E motif is a major contributor to this inhibition (see Chapter 3). These mice that are genetically deficient in CS-E provide the opportunity to study a system that is completely devoid of the motif, giving valuable insights into the functions for which CS-E is essential. However, there are some drawbacks to using these mice for studying regeneration of growth after injury. By genetically removing the GalNAc4S-6ST enzyme, we may introduce subtle variations into the CS chains, or cause changes to the developing animal

that obfuscate recovery studies. Furthermore, removing the CS-E motif may influence the expression or localization of other molecules that are involved in inhibition and growth promotion.

Interestingly, the group that generated the knockout animals observed that the mast cells of CS-E-deficient mice had reduced protease activity. Mast cells are inflammation-mediating cells of the immune system, and can be found in the adult CNS localized around lesion sites.[44] These cells have been found to contain intracellular CS-E,[45, 46] and could be responsible for delivering CS-E to the injury site. Any subsequent release of CS-E, along with stimulation of the immune system, could contribute to the lack of regeneration. The reduced protease activity observed in the knockout animals, along with the lack of CS-E, could together contribute to enhance regeneration in these animals. On the other hand, there could be as-yet-unobserved effects in the immune systems that will prove to be detrimental to injury recovery; furthermore, mast cells are known to produce factors with regenerative properties,[47] so it is unclear what the dominant effect will be. Future studies with these animals will more clearly describe the role of CS-E in development and in recovery after lesions to the CNS.

CS Receptors

Before the discovery of specific proteins that interact with and mediate the inhibitory effects of CSPGs,[48-50] there were several observations that implicated a receptor-based mechanism. An early clue was the finding that CSPGs elevate cytoplasmic Ca^{2+} levels,[51] and this effect was associated with growth inhibition and the reorganization of growth cone actin. It has been known for some time that like the myelin inhibitors, CSPGs induce the activation of RhoA.[52-55] Activation of this GTPase leads to growth cone collapse

and the retraction of neurites via the downstream destabilization of the actin cytoskeleton,[54] via ROCK1 (Rho-associated, coiled-coil containing protein kinase 1).[56] In another convergence of signaling, both the myelin inhibitors and CSPGs induce the activation of protein kinase C (PKC).[57] This activation is thought to be necessary for RhoA activation, as PKC inhibition eliminates the activation of Rho by either CSPGs or the myelin inhibitors. It was also discovered that CSPGs activate the mitogen-activated protein kinase (MAPK) pathway via the epidermal growth factor receptor (EGFR). It was observed that a MAPK inhibitor or EGFR inhibitor blocked the effects of CSPGs on neurite outgrowth.[58] Furthermore, it was found that MAPK was phosphorylated in response to CSPGs, and this phosphorylation was lost upon the inhibition of EGFR. EGFR was also found to be phosphorylated in response to CSPGs, and these phosphorylated sites are known to be involved in PKC signaling, further establishing that PKC activation induced by the CSPGs is dependent on the activation of EGFR.[58] This activation of EGFR is thought to occur via trans-activation, in which other signaling pathways activate the receptor and its downstream targets.[59]

The first discovered receptor that directly interacts with CSPGs and becomes activated in response was the protein tyrosine phosphatase receptor PTPσ.[48] This protein is a member of the leukocyte antigen-related (LAR) receptor family, and PTPσ as well as other members of this family had previously been identified as receptors for heparan sulfate proteoglycans.[60-62] Subsequent work by our group showed that the CS-E motif is responsible for mediating the interaction between PTPσ and CSPGs, and that neurons deficient in PTPσ are less inhibited by CS-E.[56] Recent work has shown that HS and CS share a common binding site on PTPσ, and their differing effects on cell growth (promoting

and inhibiting, respectively) may be dependent on the nature of the GAG chain, and whether or not binding to the receptor allows growth-promoting receptor clusters.[63] PTPσ contains intracellular phosphatase domains that interact with the guanine nucleotide exchange factor Trio, a protein that activates the Rho family of small GTPases,[64, 65] providing evidence of further convergence at RhoA.

Another phosphatase receptor that is related to PTPσ, the leukocyte common antigen-related phosphatase receptor (LAR), was next identified as a receptor that directly engages the CSPGs to inhibit neuron growth.[66] Deletion of this receptor led to the elimination of RhoA activation in response to CSPGs, showing the role of this molecule in the downstream signaling of LAR. Similar results were seen with the protein kinase Akt, which was found to be dephosphorylated in response to CSPGs. Removal of LAR led to sustained phosphorylation of this kinase upon treatment with CSPGs, further elucidating the downstream effects of CSPGs.

It was recently found that CSPGs engage the Nogo receptor isoforms NgR1 and NgR3, representing a convergence in signaling for CSPGs and the myelin inhibitory proteins.[50] Additionally, it was found that removing both NgR and PTPσ resulted in even greater reduction of inhibition by CSPGs, demonstrating that the inhibitory effect is exerted on multiple receptors simultaneously. Our lab has found that NgR binds to CS-E polysaccharides with remarkably high affinity and specificity, with at least two independent, high-affinity NgR binding sites within CS-E polysaccharides (unpublished data; see Appendix 1). No binding was seen with other CS motifs, once again showing that CS-E is the critical binding and functional element with CS chains of CSPGs for receptor activation.

Finally, the guidance molecule semaphorin 5A (Sema5A) has been shown to modulate the effects of CSPGs.[67] As in the case of PTPσ, Sema5A interacts with both CSPGs and HSPGs. It was found that when growth cones of expanding axons encounter Sema5A, HS or CS present on the axon surface were responsible for determining whether Sema5a was attractive or repellant, respectively. This suggests that HSPGs and CSPGs form a functional receptor complex with unidentified Sema5A receptors, and GAGs on the neuronal surface could be involved in the modulation of growth of these neurons.

It was also shown that CSPGs could inhibit growth by disruption of the adhesion between neurons and their substrate. One group found that CSPGs inhibited axon growth through the inactivation of the attachment-mediating receptor integrin on substrates of laminin, demonstrating the importance of cell adhesion molecules in neuronal growth.[68] Future studies will continue to elucidate how these multiple receptors interact with the various molecules already implicated in CSPG-mediated inhibition of growth. Combinations of inhibitory strategies against these molecules may completely eliminate CSPG suppression of growth in the CNS to achieve axonal regeneration after injury *in vivo*.

Overcoming Inhibition

Since the discovery of the myelin-associated inhibitors, strategies have been devised to overcome the inhibitory effect of these proteins. One technique for overcoming inhibition of regeneration after injury is by blocking the inhibitory molecules with antibodies specific to either the ligand or receptor, effectively preventing them from exerting their effect. It was found that antibodies against the myelin inhibitors are able to increase neurite outgrowth in response to myelin *in vitro*, and to improve recovery after injuries to the nervous system *in vivo*.[69]

In particular, antibodies against Nogo-A have been shown to increase regeneration in several injury models. Rats had lesions to their spinal cords administered, after which an antibody against Nogo was delivered immediately and continuously for two weeks. Animals receiving this antibody showed increased functional recovery compared to control, and were shown to have more axons extending past the injury site.[70] In addition to problems with movement, other issues such as muscle spasms are observed with less severe injuries to the spinal cord. The Nogo antibody was also able to relieve this effect.[71] It is hoped that this treatment strategy can be applied to humans with injuries to the spinal cord, and efforts are underway to make this a viable treatment strategy.[72] Studies have shown that the effect of the antibody treatment is observed when administered immediately or within one week after injury. Treatment administered two weeks after injury does not give the beneficial effect.[73] This is likely related to the timing of upregulation of inhibitory molecules, as Nogo expression increases within days after injury to the spinal cord.[74] Similar results were found in cortical injury models, with improvements in both axonal projections and test of skilled limb functions.[75, 76] In another study, a small peptide, which was identified as blocking the interaction between Nogo and NgR, was administered after injury, and was found to found to improve functional recovery in spinal cord injury models.[77]

In spite of these promising results, it has been found that genetically deleting either NgR or p75, a co-receptor that is necessary for the downstream signaling of NgR, does not result in significant recovery after spinal cord injury.[78] Similarly, genetic deletion of all Nogo isoforms does not result in enhanced regeneration after injury.[79] One possible explanation is that the study with NgR did not account for all isoforms of NgR, and at least

two of the isoforms have been shown to be critical for the mediation of inhibition by CSPGs, which could also apply to the myelin inhibitors.[50] Furthermore, it has been shown that the p75 co-receptor critical for NgR activity can be replaced by another functional equivalent,[80] explaining the lack of effect in p75-deficient animals. Finally, other groups have speculated that the blocking agents used to neutralize Nogo and its receptor may themselves have some additional growth-promoting effects beyond their specific blocking capability, or that genetically deleting Nogo or its receptors could result in neurons that are less likely to regenerate based on other functions of these proteins.[81]

Another method of improving recovery after injury is to stimulate the intrinsic growth capability of the neurons. One such means of doing this is via the second messenger molecule cyclic adenosine monophosphate (cAMP). Endogenous cAMP is present in much higher levels in young neurons compared to older neurons, and this level correlates with the neurons' ability to regenerate.[82] Exogenous cAMP has been shown to increase survival of neurons,[83] and to block the effects of myelin-associated inhibitors.[84] Furthermore, it has been previously shown that the application of cAMP analogs (CPT-cAMP) can increase regeneration in the injured optic nerve or spinal cord.[85, 86]

As with the myelin inhibitors, an antibody against inhibitory CS motifs could potentially help to overcome inhibition by blocking the motifs and preventing them from interacting with their receptor proteins. Previously, a variety of methods have been used to generate antibodies against chondroitin sulfate. The antigens used to generate antibodies in the past have included proteoglycans, glycoproteins, and CSPGs, all derived from natural sources.[87-93] In these cases, the CS antigens have a mixture of sulfation motifs present, making it difficult to determine which motifs are being detected, and which motifs are

present on a particular sample being analyzed by antibody for immunostaining studies. Analysis of the specificity of these antibodies usually has occurred via competition assays with known standards.[87-91, 94, 95] The Hsieh-Wilson lab has generated and characterized mouse monoclonal antibodies that were raised against CS tetrasaccharides synthesized by the lab.[96] With these antibodies, specific detection of natural polysaccharides bearing the relevant motif is possible, allowing the study of endogenous CS motif expression, and the blocking of specific motifs *in vitro* and *in vivo* (See Chapter 3).

Conclusions

Chondroitin sulfate has been shown to serve many diverse roles in the developing and mature organism, but its role in inhibiting growth after injury is still emerging. After injury to the adult CNS, axon regeneration is inhibited, due in large part to the effects of CSPGs present in the glial scar. CSPGs can interact with a variety of cell-surface molecules to exert an inhibitory effect, and this effect is dependent upon the complex CS chains of CSPGs. The work in this thesis shows that the effects of CSPGs are due to the CS-E motif, which itself it highly inhibitory and is the critical element for binding to receptors and for inducing downstream inhibition of growth. This work also describes our efforts at finding novel proteins that interact with CS-E and thus serve as CSPG receptors. Elucidating the complex mechanisms of neuronal inhibition in the CNS will allow these interactions to be blocked or attenuated, such that regeneration in the CNS can be achieved.

References

1. Schwab, M. E. & Bartholdi, D. Degeneration and regeneration of axons in the lesioned spinal cord. *Physiol. Rev.* **1996,** 76, (2), 319-370.

2. Horner, P. J. & Gage, F. H. Regenerating the damaged central nervous system. *Nature* **2000,** 407, (6807), 963-970.

3. Spencer, T., Domeniconi, M., Cao, Z. & Filbin, M. T. New roles for old proteins in adult CNS axonal regeneration. *Curr. Opin. Neurobiol.* **2003,** 13, (1), 133-139.

4. McGee, A. W. & Strittmatter, S. M. The Nogo-66 receptor: focusing myelin inhibition of axon regeneration. *Trends Neurosci.* **2003,** 26, (4), 193-198.

5. Yiu, G. & He, Z. Signaling mechanisms of the myelin inhibitors of axon regeneration. *Curr. Opin. Neurobiol.* **2003,** 13, (5), 545-551.

6. Yiu, G. & He, Z. Glial inhibition of CNS axon regeneration. *Nat. Rev. Neurosci.* **2006,** 7, (8), 617-627.

7. Busch, S. A. & Silver, J. The role of extracellular matrix in CNS regeneration. *Curr. Opin. Neurobiol.* **2007,** 17, (1), 120-127.

8. Carulli, D., Laabs, T., Geller, H. M. & Fawcett, J. W. Chondroitin sulfate proteoglycans in neural development and regeneration. *Curr. Opin. Neurobiol.* **2005,** 15, (1), 116-120.

9. Schwab, M. E. & Thoenen, H. Dissociated neurons regenerate into sciatic but not optic nerve explants in culture irrespective of neurotrophic factors. *J. Neurosci.* **1985,** 5, (9), 2415-2423.

10. Chen, M. S*., et al.* Nogo-A is a myelin-associated neurite outgrowth inhibitor and an antigen for monoclonal antibody IN-1. *Nature* **2000,** 403, (6768), 434-439.

11. Mukhopadhyay, G., Doherty, P., Walsh, F. S., Crocker, P. R. & Filbin, M. T. A novel role for myelin-associated glycoprotein as an inhibitor of axonal regeneration. *Neuron* **1994,** 13, (3), 757-767.

12. McKerracher, L*., et al.* Identification of myelin-associated glycoprotein as a major myelin-derived inhibitor of neurite growth. *Neuron* **1994,** 13, (4), 805-811.

13. Wang, K. C*., et al.* Oligodendrocyte-myelin glycoprotein is a Nogo receptor ligand that inhibits neurite outgrowth. *Nature* **2002,** 417, (6892), 941-944.

14. Fournier, A. E., GrandPre, T. & Strittmatter, S. M. Identification of a receptor mediating Nogo-66 inhibition of axonal regeneration. *Nature* **2001,** 409, (6818), 341-346.

15. Liu, B. P., Fournier, A., GrandPre, T. & Strittmatter, S. M. Myelin-associated glycoprotein as a functional ligand for the Nogo-66 receptor. *Science* **2002,** 297, (5584), 1190-1193.

16. Silbert, J. E. & Sugumaran, G. Biosynthesis of chondroitin/dermatan sulfate. *IUBMB Life* **2002,** 54, (4), 177-186.

17. Sugahara, K. & Kitagawa, H. Recent advances in the study of the biosynthesis and functions of sulfated glycosaminoglycans. *Curr. Opin. Struct. Biol.* **2000,** 10, (5), 518-527.

18. Kitagawa, H., Uyama, T. & Sugahara, K. Molecular cloning and expression of a human chondroitin synthase. *J. Biol. Chem.* **2001,** 276, (42), 38721-38726.

19. Yada, T.*, et al.* Chondroitin sulfate synthase-2. Molecular cloning and characterization of a novel human glycosyltransferase homologous to chondroitin sulfate glucuronyltransferase, which has dual enzymatic activities. *J. Biol. Chem.* **2003,** 278, (32), 30235-30247.

20. Hiraoka, N., Misra, A., Belot, F., Hindsgaul, O. & Fukuda, M. Molecular cloning and expression of two distinct human N-acetylgalactosamine 4-O-sulfotransferases that transfer sulfate to GalNAc beta 1-->4GlcNAc beta 1-->R in both N- and O-glycans. *Glycobiology* **2001,** 11, (6), 495-504.

21. Kang, H. G., Evers, M. R., Xia, G., Baenziger, J. U. & Schachner, M. Molecular cloning and characterization of chondroitin-4-O-sulfotransferase-3. A novel member of the HNK-1 family of sulfotransferases. *J. Biol. Chem.* **2002,** 277, (38), 34766-34772.

22. Tsutsumi, K., Shimakawa, H., Kitagawa, H. & Sugahara, K. Functional expression and genomic structure of human chondroitin 6-sulfotransferase. *FEBS Lett.* **1998,** 441, (2), 235-241.

23. Kitagawa, H., Fujita, M., Ito, N. & Sugahara, K. Molecular cloning and expression of a novel chondroitin 6-O-sulfotransferase. *J. Biol. Chem.* **2000,** 275, (28), 21075-21080.

24. Kobayashi, M.*, et al.* Molecular cloning and characterization of a human uronyl 2-sulfotransferase that sulfates iduronyl and glucuronyl residues in dermatan/chondroitin sulfate. *J. Biol. Chem.* **1999,** 274, (15), 10474-10480.

25.	Ito, Y. & Habuchi, O. Purification and characterization of N-acetylgalactosamine 4-sulfate 6-O-sulfotransferase from the squid cartilage. *J. Biol. Chem.* **2000,** 275, (44), 34728-34736.

26.	Fernaud-Espinosa, I., Nieto-Sampedro, M. & Bovolenta, P. Developmental distribution of glycosaminoglycans in embryonic rat brain: relationship to axonal tract formation. *J. Neurobiol.* **1996,** 30, (3), 410-424.

27.	Properzi, F.*, et al.* Chondroitin 6-sulphate synthesis is up-regulated in injured CNS, induced by injury-related cytokines and enhanced in axon-growth inhibitory glia. *Eur. J. Neurosci.* **2005,** 21, (2), 378-390.

28.	Kitagawa, H., Tsutsumi, K., Tone, Y. & Sugahara, K. Developmental regulation of the sulfation profile of chondroitin sulfate chains in the chicken embryo brain. *J. Biol. Chem.* **1997,** 272, (50), 31377-31381.

29.	Masuda, T.*, et al.* Developmental regulation of notochord-derived repulsion for dorsal root ganglion axons. *Molecular & Cellular Neurosciences* **2004,** 25, (2), 217-227.

30.	Brittis, P. A., Canning, D. R. & Silver, J. Chondroitin sulfate as a regulator of neuronal patterning in the retina. *Science* **1992,** 255, (5045), 733-736.

31.	Jones, L. L., Yamaguchi, Y., Stallcup, W. B. & Tuszynski, M. H. NG2 is a major chondroitin sulfate proteoglycan produced after spinal cord injury and is expressed by macrophages and oligodendrocyte progenitors. *J. Neurosci.* **2002,** 22, (7), 2792-2803.

32.	Jones, L. L., Margolis, R. U. & Tuszynski, M. H. The chondroitin sulfate proteoglycans neurocan, brevican, phosphacan, and versican are differentially regulated following spinal cord injury. *Exp. Neurol.* **2003,** 182, (2), 399-411.

33.	Tang, X., Davies, J. E. & Davies, S. J. Changes in distribution, cell associations, and protein expression levels of NG2, neurocan, phosphacan, brevican, versican V2, and tenascin-C during acute to chronic maturation of spinal cord scar tissue. *J. Neurosci. Res.* **2003,** 71, (3), 427-444.

34.	Asher, R. A.*, et al.* Neurocan is upregulated in injured brain and in cytokine-treated astrocytes. *J. Neurosci.* **2000,** 20, (7), 2427-2438.

35.	Asher, R. A.*, et al.* Versican is upregulated in CNS injury and is a product of oligodendrocyte lineage cells. *J. Neurosci.* **2002,** 22, (6), 2225-2236.

36.	Bradbury, E. J.*, et al.* Chondroitinase ABC promotes functional recovery after spinal cord injury. *Nature* **2002,** 416, (6881), 636-640.

37. Moon, L. D., Asher, R. A., Rhodes, K. E. & Fawcett, J. W. Regeneration of CNS axons back to their target following treatment of adult rat brain with chondroitinase ABC. *Nat. Neurosci.* **2001,** 4, (5), 465-466.

38. Gilbert, R. J.*, et al.* CS-4,6 is differentially upregulated in glial scar and is a potent inhibitor of neurite extension. *Molecular & Cellular Neurosciences* **2005,** 29, (4), 545-558.

39. Karumbaiah, L.*, et al.* Targeted downregulation of N-acetylgalactosamine 4-sulfate 6-O-sulfotransferase significantly mitigates chondroitin sulfate proteoglycan-mediated inhibition. *Glia* **2011,** 59, (6), 981-996.

40. Sugahara, K. & Mikami, T. Chondroitin/dermatan sulfate in the central nervous system. *Curr. Opin. Struct. Biol.* **2007,** 17, (5), 536-545.

41. Clement, A. M., Sugahara, K. & Faissner, A. Chondroitin sulfate E promotes neurite outgrowth of rat embryonic day 18 hippocampal neurons. *Neurosci. Lett.* **1999,** 269, (3), 125-128.

42. Tully, S. E.*, et al.* A chondroitin sulfate small molecule that stimulates neuronal growth. *J. Am. Chem. Soc.* **2004,** 126, (25), 7736-7737.

43. Ohtake-Niimi, S.*, et al.* Mice deficient in N-acetylgalactosamine 4-sulfate 6-o-sulfotransferase are unable to synthesize chondroitin/dermatan sulfate containing N-acetylgalactosamine 4,6-bissulfate residues and exhibit decreased protease activity in bone marrow-derived mast cells. *J. Biol. Chem.* **2010,** 285, (27), 20793-20805.

44. Silver, R., Silverman, A. J., Vitkovic, L. & Lederhendler, II Mast cells in the brain: evidence and functional significance. *Trends. Neurosci.* **1996,** 19, (1), 25-31.

45. Razin, E., Stevens, R. L., Akiyama, F., Schmid, K. & Austen, K. F. Culture from mouse bone marrow of a subclass of mast cells possessing a distinct chondroitin sulfate proteoglycan with glycosaminoglycans rich in N-acetylgalactosamine-4,6-disulfate. *J. Biol. Chem.* **1982,** 257, (12), 7229-7236.

46. Stevens, R. L., Fox, C. C., Lichtenstein, L. M. & Austen, K. F. Identification of chondroitin sulfate E proteoglycans and heparin proteoglycans in the secretory granules of human lung mast cells. *Proc. Natl. Acad. Sci. U S A* **1988,** 85, (7), 2284-2287.

47. Leon, A.*, et al.* Mast cells synthesize, store, and release nerve growth factor. *Proc. Natl. Acad. Sci. U S A* **1994,** 91, (9), 3739-3743.

48. Shen, Y.*, et al.* PTPsigma is a receptor for chondroitin sulfate proteoglycan, an inhibitor of neural regeneration. *Science* **2009,** 326, (5952), 592-596.

49.   Brown, J. M*., et al.* A sulfated carbohydrate epitope inhibits axon regeneration after injury. *Proc Natl Acad Sci U S A* **2012,** 109, (13), 4768-4773.

50.   Dickendesher, T. L*., et al.* NgR1 and NgR3 are receptors for chondroitin sulfate proteoglycans. *Nat. Neurosci.* **2012,** 15, (5), 703-712.

51.   Snow, D. M., Atkinson, P. B., Hassinger, T. D., Letourneau, P. C. & Kater, S. B. Chondroitin sulfate proteoglycan elevates cytoplasmic calcium in DRG neurons. *Dev. Biol.* **1994,** 166, (1), 87-100.

52.   Schweigreiter, R*., et al.* Versican V2 and the central inhibitory domain of Nogo-A inhibit neurite growth via p75NTR/NgR-independent pathways that converge at RhoA. *Mol. Cell. Neurosci.* **2004,** 27, (2), 163-174.

53.   Fournier, A. E., Takizawa, B. T. & Strittmatter, S. M. Rho kinase inhibition enhances axonal regeneration in the injured CNS. *J. Neurosci.* **2003,** 23, (4), 1416-1423.

54.   Lehmann, M*., et al.* Inactivation of Rho signaling pathway promotes CNS axon regeneration. *J. Neurosci.* **1999,** 19, (17), 7537-7547.

55.   Monnier, P. P., Sierra, A., Schwab, J. M., Henke-Fahle, S. & Mueller, B. K. The Rho/ROCK pathway mediates neurite growth-inhibitory activity associated with the chondroitin sulfate proteoglycans of the CNS glial scar. *Mol. Cell. Neurosci.* **2003,** 22, (3), 319-330.

56.   Maekawa, M*., et al.* Signaling from Rho to the actin cytoskeleton through protein kinases ROCK and LIM-kinase. *Science* **1999,** 285, (5429), 895-898.

57.   Sivasankaran, R*., et al.* PKC mediates inhibitory effects of myelin and chondroitin sulfate proteoglycans on axonal regeneration. *Nat. Neurosci.* **2004,** 7, (3), 261-268.

58.   Kaneko, M., Kubo, T., Hata, K., Yamaguchi, A. & Yamashita, T. Repulsion of cerebellar granule neurons by chondroitin sulfate proteoglycans is mediated by MAPK pathway. *Neurosci. Lett.* **2007,** 423, (1), 62-67.

59.   Koprivica, V*., et al.* EGFR activation mediates inhibition of axon regeneration by myelin and chondroitin sulfate proteoglycans. *Science* **2005,** 310, (5745), 106-110.

60.   Aricescu, A. R., McKinnell, I. W., Halfter, W. & Stoker, A. W. Heparan sulfate proteoglycans are ligands for receptor protein tyrosine phosphatase sigma. *Molecular & Cellular Biology* **2002,** 22, (6), 1881-1892.

61. Fox, A. N. & Zinn, K. The heparan sulfate proteoglycan syndecan is an in vivo ligand for the Drosophila LAR receptor tyrosine phosphatase. *Curr. Biol.* **2005,** 15, (19), 1701-1711.

62. Johnson, K. G*., et al.* The HSPGs Syndecan and Dallylike bind the receptor phosphatase LAR and exert distinct effects on synaptic development. *Neuron* **2006,** 49, (4), 517-531.

63. Coles, C. H*., et al.* Proteoglycan-specific molecular switch for RPTPsigma clustering and neuronal extension. *Science* **2011,** 332, (6028), 484-488.

64. Debant, A*., et al.* The multidomain protein Trio binds the LAR transmembrane tyrosine phosphatase, contains a protein kinase domain, and has separate rac-specific and rho-specific guanine nucleotide exchange factor domains. *Proc. Natl. Acad. Sci. U S A* **1996,** 93, (11), 5466-5471.

65. Johnson, K. G. & Van Vactor, D. Receptor protein tyrosine phosphatases in nervous system development. *Physiol. Rev.* **2003,** 83, (1), 1-24.

66. Fisher, D*., et al.* Leukocyte common antigen-related phosphatase is a functional receptor for chondroitin sulfate proteoglycan axon growth inhibitors. *J. Neurosci.* **2011,** 31, (40), 14051-14066.

67. Kantor, D. B*., et al.* Semaphorin 5A is a bifunctional axon guidance cue regulated by heparan and chondroitin sulfate proteoglycans. *Neuron* **2004,** 44, (6), 961-975.

68. Tan, C. L*., et al.* Integrin activation promotes axon growth on inhibitory chondroitin sulfate proteoglycans by enhancing integrin signaling. *J. Neurosci.* **2011,** 31, (17), 6289-6295.

69. Fouad, K., Dietz, V. & Schwab, M. E. Improving axonal growth and functional recovery after experimental spinal cord injury by neutralizing myelin associated inhibitors. *Brain Res. Rev.* **2001,** 36, (2-3), 204-212.

70. Liebscher, T*., et al.* Nogo-A antibody improves regeneration and locomotion of spinal cord-injured rats. *Ann. Neurol.* **2005,** 58, (5), 706-719.

71. Gonzenbach, R. R*., et al.* Nogo-A antibodies and training reduce muscle spasms in spinal cord-injured rats. *Ann. Neurol.* **2010,** 68, (1), 48-57.

72. Zorner, B. & Schwab, M. E. Anti-Nogo on the go: from animal models to a clinical trial. *Ann. N. Y. Acad. Sci.* **2010,** 1198 Suppl 1, E22-34.

73. Gonzenbach, R. R*., et al.* Delayed anti-nogo-a antibody application after spinal cord injury shows progressive loss of responsiveness. *J. Neurotrauma* **2012,** 29, (3), 567-578.

74.   Hunt, D., Coffin, R. S., Prinjha, R. K., Campbell, G. & Anderson, P. N. Nogo-A expression in the intact and injured nervous system. *Molecular & Cellular Neurosciences* **2003,** 24, (4), 1083-1102.

75.   Emerick, A. J. & Kartje, G. L. Behavioral recovery and anatomical plasticity in adult rats after cortical lesion and treatment with monoclonal antibody IN-1. *Behav. Brain Res.* **2004,** 152, (2), 315-325.

76.   Emerick, A. J., Neafsey, E. J., Schwab, M. E. & Kartje, G. L. Functional reorganization of the motor cortex in adult rats after cortical lesion and treatment with monoclonal antibody IN-1. *J. Neurosci.* **2003,** 23, (12), 4826-4830.

77.   GrandPre, T., Li, S. & Strittmatter, S. M. Nogo-66 receptor antagonist peptide promotes axonal regeneration. *Nature* **2002,** 417, (6888), 547-551.

78.   Zheng, B*., et al.* Genetic deletion of the Nogo receptor does not reduce neurite inhibition in vitro or promote corticospinal tract regeneration in vivo. *Proc. Natl. Acad. Sci. U S A* **2005,** 102, (4), 1205-1210.

79.   Zheng, B*., et al.* Lack of enhanced spinal regeneration in Nogo-deficient mice. *Neuron* **2003,** 38, (2), 213-224.

80.   Shao, Z*., et al.* TAJ/TROY, an orphan TNF receptor family member, binds Nogo-66 receptor 1 and regulates axonal regeneration. *Neuron* **2005,** 45, (3), 353-359.

81.   Teng, F. Y. & Tang, B. L. Why do Nogo/Nogo-66 receptor gene knockouts result in inferior regeneration compared to treatment with neutralizing agents? *J. Neurochem.* **2005,** 94, (4), 865-874.

82.   Cai, D*., et al.* Neuronal cyclic AMP controls the developmental loss in ability of axons to regenerate. *J. Neurosci.* **2001,** 21, (13), 4731-4739.

83.   Rydel, R. E. & Greene, L. A. cAMP analogs promote survival and neurite outgrowth in cultures of rat sympathetic and sensory neurons independently of nerve growth factor. *Proc. Natl. Acad. Sci. U S A* **1988,** 85, (4), 1257-1261.

84.   Cai, D., Shen, Y., De Bellard, M., Tang, S. & Filbin, M. T. Prior exposure to neurotrophins blocks inhibition of axonal regeneration by MAG and myelin via a cAMP-dependent mechanism. *Neuron* **1999,** 22, (1), 89-101.

85.   Cui, Q., Yip, H. K., Zhao, R. C., So, K. F. & Harvey, A. R. Intraocular elevation of cyclic AMP potentiates ciliary neurotrophic factor-induced regeneration of adult rat retinal ganglion cell axons. *Molecular & Cellular Neurosciences* **2003,** 22, (1), 49-61.

86. Qiu, J*., et al.* Spinal axon regeneration induced by elevation of cyclic AMP. *Neuron* **2002,** 34, (6), 895-903.

87. Couchman, J. R., Caterson, B., Christner, J. E. & Baker, J. R. Mapping by monoclonal antibody detection of glycosaminoglycans in connective tissues. *Nature* **1984,** 307, (5952), 650-652.

88. Yamagata, M*., et al.* A monoclonal antibody that specifically recognizes a glucuronic acid 2-sulfate-containing determinant in intact chondroitin sulfate chain. *J. Biol. Chem.* **1987,** 262, (9), 4146-4152.

89. Yamagata, M., Suzuki, S., Akiyama, S. K., Yamada, K. M. & Kimata, K. Regulation of cell-substrate adhesion by proteoglycans immobilized on extracellular substrates. *J. Biol. Chem.* **1989,** 264, (14), 8012-8018.

90. Mikecz, K., Glant, T. T. & Poole, A. R. Immunity to cartilage proteoglycans in BALB/c mice with progressive polyarthritis and ankylosing spondylitis induced by injection of human cartilage proteoglycan. *Arthritis & Rheumatism* **1987,** 30, (3), 306-318.

91. Mark, M. P., Butler, W. T. & Ruch, J. V. Transient expression of a chondroitin sulfate-related epitope during cartilage histomorphogenesis in the axial skeleton of fetal rats. *Dev. Biol.* **1989,** 133, (2), 475-488.

92. Watanabe, E., Fujita, S. C., Murakami, F., Hayashi, M. & Matsumura, M. A monoclonal antibody identifies a novel epitope surrounding a subpopulation of the mammalian central neurons. *Neuroscience* **1989,** 29, (3), 645-657.

93. Caterson, B., Christner, J. E. & Baker, J. R. Identification of a monoclonal antibody that specifically recognizes corneal and skeletal keratan sulfate. Monoclonal antibodies to cartilage proteoglycan. *J. Biol. Chem.* **1983,** 258, (14), 8848-8854.

94. Mark, M. P., Baker, J. R., Kimata, K. & Ruch, J. V. Regulated changes in chondroitin sulfation during embryogenesis: an immunohistochemical approach. *Int. J. Dev. Biol.* **1990,** 34, (1), 191-204.

95. Ito, Y*., et al.* Structural characterization of the epitopes of the monoclonal antibodies 473HD, CS-56, and MO-225 specific for chondroitin sulfate D-type using the oligosaccharide library. *Glycobiology* **2005,** 15, (6), 593-603.

96. Tully, S. E., Rawat, M. & Hsieh-Wilson, L. C. Discovery of a TNF-alpha antagonist using chondroitin sulfate microarrays. *J. Am. Chem. Soc.* **2006,** 128, (24), 7740-7741.

Chapter 2: Chondroitin Sulfate Proteoglycans and Protein Binding*†

Introduction

Glycosaminoglycans are sulfated polysaccharides that play important roles in fundamental biological processes, such as cell division, viral invasion, cancer and neuroregeneration. The multivalent presentation of multiple glycosaminoglycan chains on proteoglycan scaffolds may profoundly influence their interactions with proteins and subsequent biological activity. Carbohydrates possess greater structural diversity than either nucleic acids or proteins. Although they participate in a wide range of critical processes and alterations in their structure have been linked to a number of human diseases, they remain under-explored targets for chemical biology and pharmaceutical chemistry. We have embarked on a program to study a large class of sulfated polysaccharides known as glycosaminoglycans, with the goals of understanding their structure-function relationships and gaining insight into the molecular mechanisms underlying their biological activity.
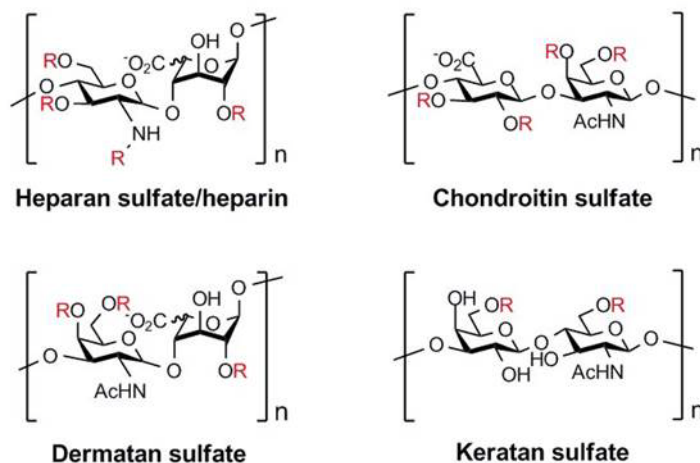
Figure 2.1. Representative classes of glycosaminoglycans, with potential sites of sulfation indicated. $R=SO_3^-$ or H; $R_1 = SO_3^-$, H, or Ac; n= ~40-200.

Figure 2.2. CS polysaccharides are composed of 20-200 units of the repeating disaccharide D-glucuronic acid (GlcA) and N-acetyl-D-galactosamine (GalNAc). The sugar hydroxyls are variably sulfated to give rise to diverse sulfation patterns. Chemical structures of major sulfation motifs found in the mammalian nervous system: CS-A (GlcA-4SGalNAc), CS-C (GlcA-6SGalNAc) and CS-E (GlcA-4S, 6SGalNAc). n = 20-200.

Glycosaminoglycans (GAGs) are polymers, composed of 10–200 repeating sulfated disaccharide units (Figure 2.1).[1-3] They contain regions of high and low sulfation,[4, 5] with highly sulfated regions serving as binding sites for proteins,[6-10] and these interactions endow GAGs with the ability to regulate essential processes such as cell division, viral invasion, blood coagulation and neuronal regeneration.[1, 2, 6, 11-13] The CS-A, CS-C and CS-E disaccharides represent major sulfation motifs in the mammalian CNS (Figure 2.2), and our

lab has previously shown that the CS-E motif in particular can serve as a recognition unit for proteins such as growth factors, thus regulating cellular growth.[14] The CS-E motif can also act as a ligand to engage receptors and trigger downstream cellular events (see Chapters 3 and 4).

GAGs are covalently attached to various proteoglycan proteins, with some proteoglycans bearing as many as 100 sugar chains (Figure 2.3).[15] It has been established using synthetic glycopolymers and oligosaccharides for other systems that the relative position and density of sugars can impact the avidity and specificity of glycan-protein interactions.[16-20] However, despite these advancements, the role of the multivalent architecture found in native GAG structures has remained largely unexplored.
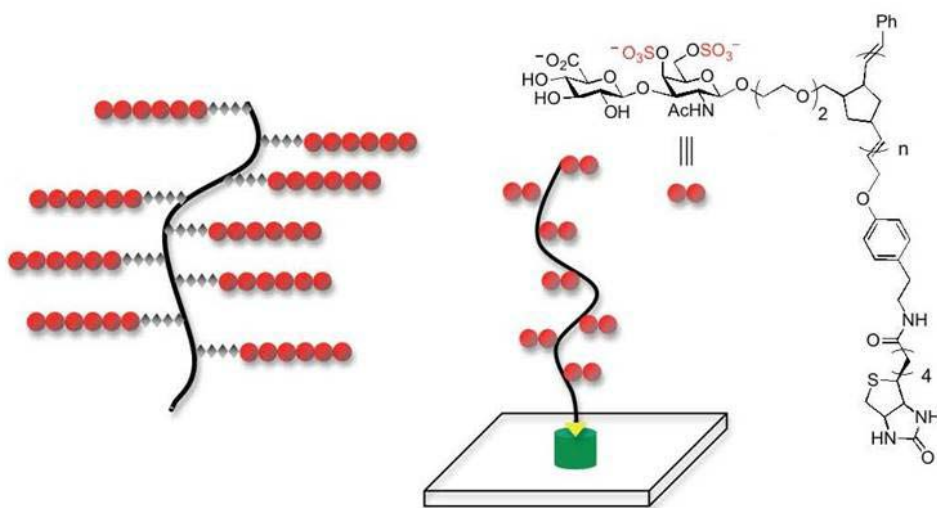
Figure 2.3. Schematic representation of a proteoglycan, which typically consists of multiple GAG chains attached to a protein core (left); Biotin end-functionalized ROMP polymers as mimetics of CS proteoglycans. n = ~80-280 (right).

Results

      To mimic the orientation of the sugar chains on proteoglycans, we designed a CS glycopolymer, which has an end-functionalized biotin moiety to achieve the desired orientation of the pendant sugars and to facilitate attachment of the polymer to surfaces (Figure 2.4). We chose a norbornene-based backbone to allow for multivalent display of

CS-E polymer: $R_1 = SO_3^-$, $R_2 = SO_3^-$
Unsulfated polymer: $R_1 = H$, $R_2 = H$
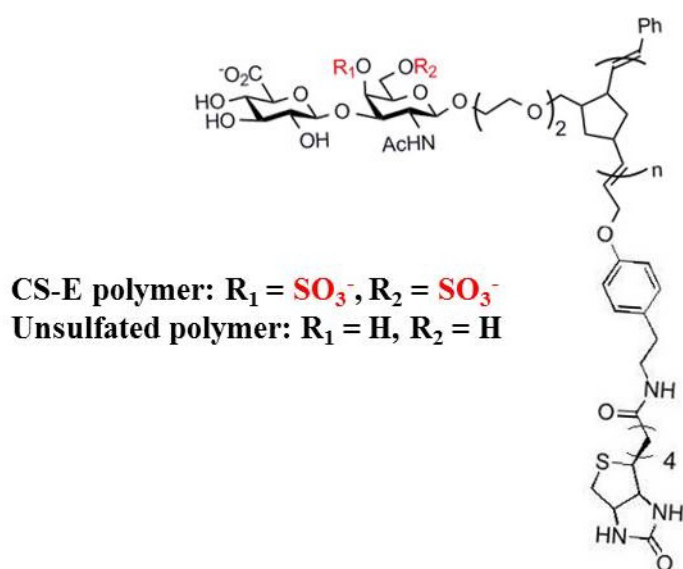
Figure 2.4. Biotin End-Functionalized CS Glycopolymers.

the sugar chains at defined, chemically controlled intervals and to confer a degree of rigidity to the structure. Previous studies in our laboratory have demonstrated that glycopolymers containing complex, highly anionic di- and tetrasaccharides can be generated using ring-opening metathesis polymerization (ROMP) chemistry, although more flexible cis-cyclooctene monomers were employed.[21] In addition to increasing the structural rigidity of the resultant polymer, norbornene-based monomers would have the advantage of enabling access to block copolymers for controlling the sulfation motifs

between GAG chains. We next investigated end-functionalization of the glycopolymers with a biotin moiety. Addition of the biotin terminating agent to the reaction mixture after completion of the living polymerization resulted in the desired end-capping of the glycopolymer.
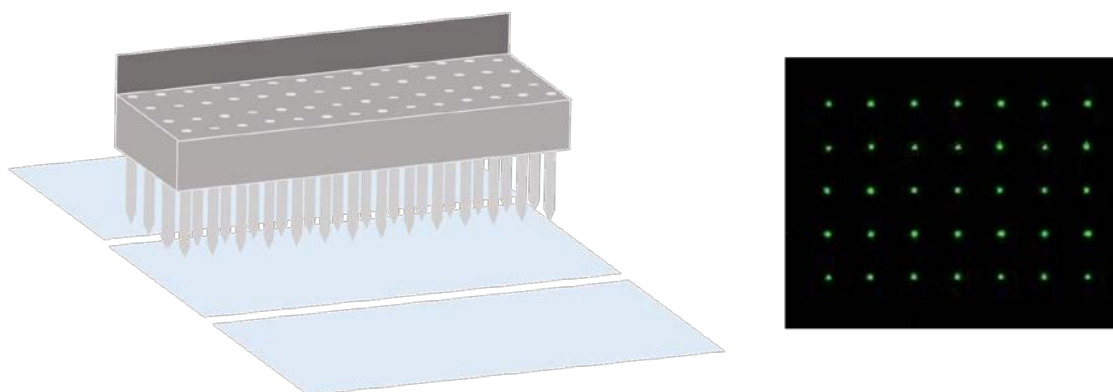
Figure 2.5. Depiction of the microarray printing robot adding carbohydrate solutions to the glass slide surface (left). A representative experimental slide is shown on the right, where areas of fluorescence indicate protein binding to the carbohydrates on the surface after the addition of a fluorescent antibody specific to the protein being investigated.

To explore the ability of the glycopolymers to interact with proteins of interest, the unsulfated and CS-E sulfated biotin glycopolymers (Figure 2.4) were attached to microarray surfaces. A high-precision contact-printing robot was used to deliver nanoliter volumes of the biotin-labeled glycopolymers to streptavidin-coated slides, yielding spots approximately 200 μm in diameter (Figure 2.5). We examined the binding of monoclonal antibodies 2D11 and 2D5, which are selective for the CS-E and CS-C sulfation motifs, respectively.[7, 14] The microarrays were incubated with each antibody (70 nM), and protein binding was visualized using a secondary Cy3-conjugated goat anti-mouse antibody.
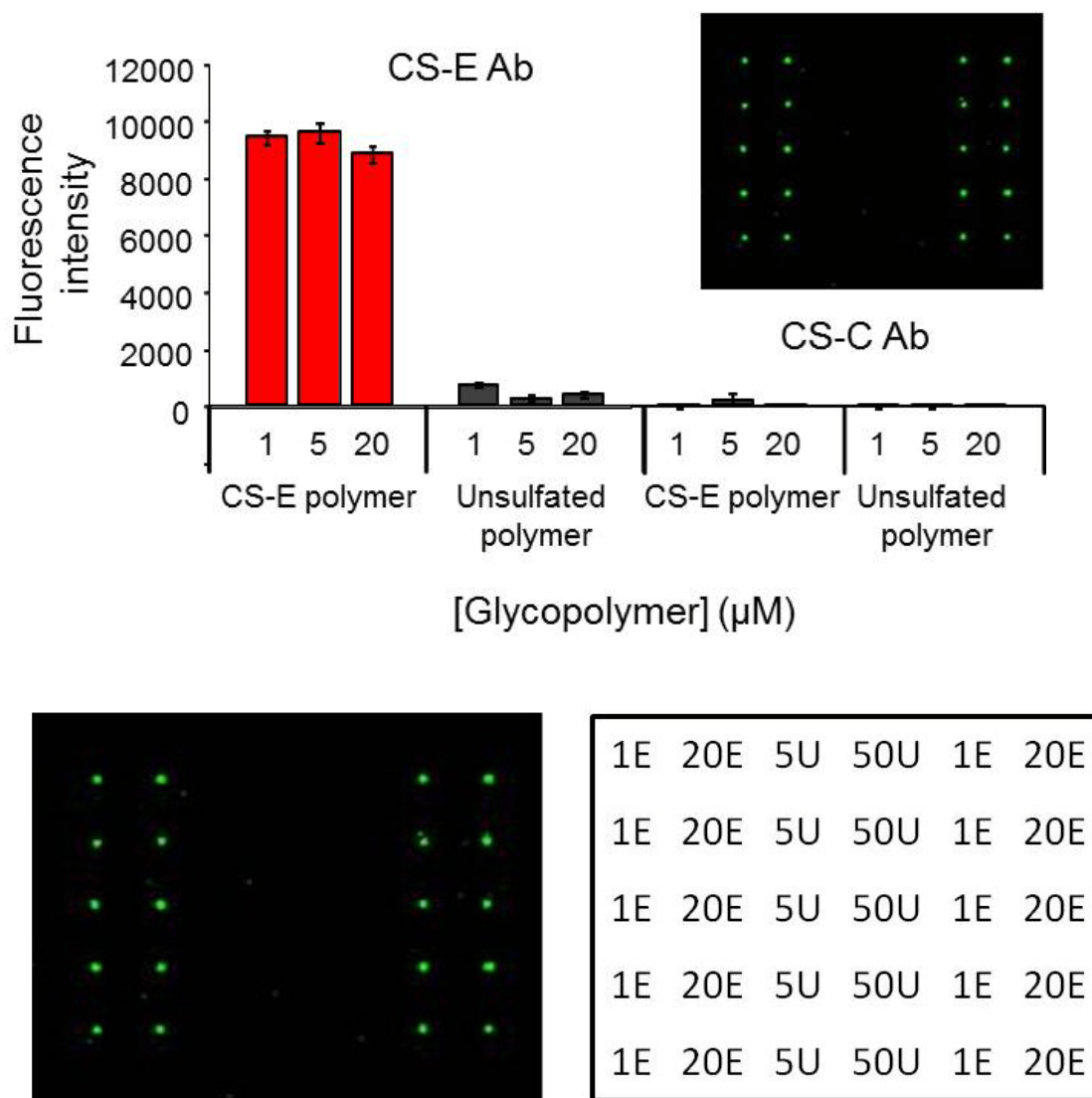
Figure 2.6. Top: Binding of the CS-E mAb (left) and the CS-C mAb (right) to unsulfated and CS-E sulfated polymer. A representative portion of the array is shown (inset). The CS-C mAb did not bind to either polymer on the array; Bottom: Representative portion of the microarray, illustrating spot morphology and fluorescence intensity after incubation with the CS-E antibody. Note that only a small portion of the microarray is shown. The panel on the right indicates the corresponding polymers and their concentrations for each spot shown. Values are in µM. E = CS-E sulfated polymer, U = Unsulfated polymer.
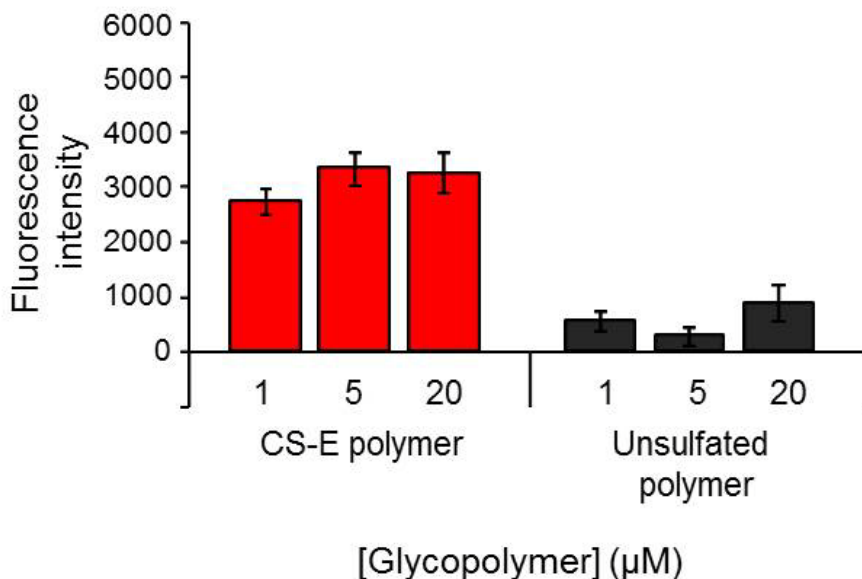
Figure 2.7. Relative binding of GDNF to glycopolymers on the biotinylated polymer microarray.

Antibody 2D11 bound selectively to the CS-E sulfated glycopolymer and showed no detectable binding to the unsulfated glycopolymer (Figure 2.6).

Moreover, no binding of the CS-C antibody 2D5 to either glycopolymer was observed, consistent with the selective recognition of specific sulfated epitopes. We also examined the binding of several growth factors, including glial cell-derived neurotrophic factor (GDNF), a growth factor important for the survival and differentiation of dopaminergic neurons.[22, 23] Although the binding of GDNF to a highly sulfated mixture of chondroitin and dermatan sulfate chains has been studied,[8] its ability to recognize homogeneous, well-defined CS structures has not been explored. Significant binding of GDNF to the CS-E sulfated glycopolymer, but not the unsulfated glycopolymer, was observed (Figure 2.7), indicating a clear preference of GDNF for the sulfated sugar epitope.

Finally, we investigated whether the end-functionalized glycopolymers could be used to facilitate quantitative, real-time analysis of GAG-protein interactions using surface

plasmon resonance (SPR). The unsulfated and CS-E sulfated glycopolymers were

immobilized on streptavidin-conjugated CM5 sensor chips at low density (RL ≈ 25 RU)
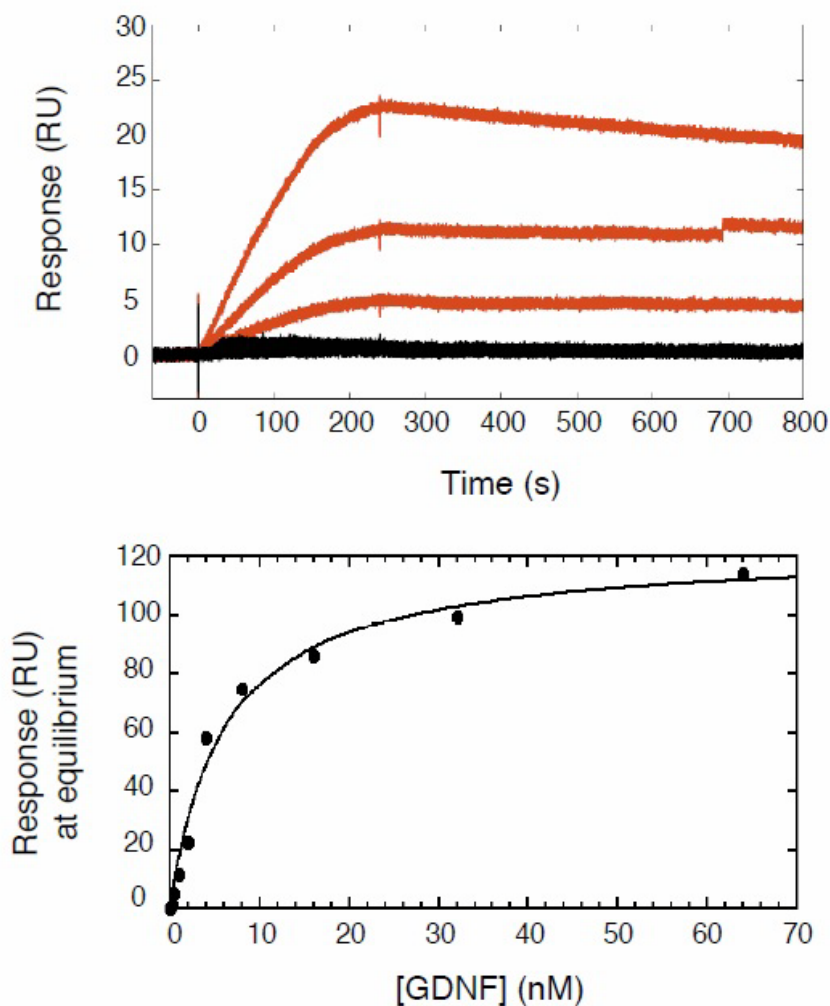
Figure 2.8. Top: Surface plasmon resonance of GDNF binding to CS glycopolymers. GDNF at varying concentrations (2, 1, and 0.5 nM) binds to the CS-E sulfated glycopolymer (red), but not the unsulfated polymer (black); Bottom: The dissociation constant (K_D) for the interaction between the CS-E sulfated polymer and GDNF was measured by plotting 5 the response at equilibrium for varying concentrations of GDNF. Nonlinear regression analysis gave a K_D of 6 ± 1 nM.

to prevent mass transfer-limited kinetics. Binding of GDNF to the glycopolymers was

assessed by flowing GDNF over the chip at various concentrations (2, 1, 0.5 nM) and

recording the SPR sensorgrams (50 µL/min, 25 ºC). As shown in Figure 2.8, GDNF

interacted with the CS-E sulfated glycopolymer, but not with the unsulfated glycopolymer,

consistent with the microarray results.   Binding of GDNF to the CS-E sulfated

glycopolymer was characterized by a slow initial rate of association that rapidly reached
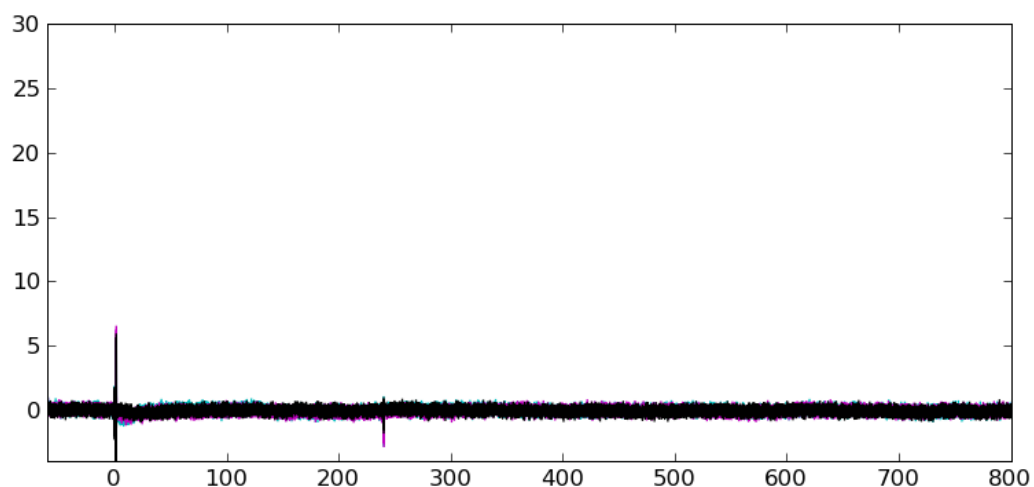
Figure 2.9. SPR sensorgram of the interaction between GDNF and a monovalent, biotinylated CS-E disaccharide at various GDNF concentrations (2 nm, cyan; 1 nm, magenta; 0.5 nm, black). No significant binding to the monovalent CS-E disaccharide was observed.

equilibrium, followed by a slow rate of dissociation.   By plotting the response at

equilibrium for varying concentrations of GDNF (0.25–62 nM), we obtained a dissociation

constant (K_D) of 6 ± 1 nM for the interaction between GDNF and the CS-E sulfated

glycopolymer.   It is well known that monovalent CS and heparan sulfate disaccharides

exhibit weak binding affinity for proteins and minimal biological activity.[21, 24-26] Indeed,

binding of GDNF to a biotinylated CS-E disaccharide could not be detected under these

conditions (Figure 2.9). Thus, the observation that our glycopolymers interact strongly with

proteins suggests that the multivalent display of sulfated epitopes between GAG chains

plays a critical role in enhancing their interactions with proteins.   Together, our studies

demonstrate that end-functionalized ROMP glycopolymers can effectively engage glycosaminoglycan-binding proteins and function as novel mimetics for CS glycosaminoglycans.

In order to study the effects of spacing on the binding capability of the glycopolymers, our group also generated norbornene polymers in which the norborne-dissacharide units are separated on the polymer chain by unconjugated norbornene linkers (Figure 2.10).
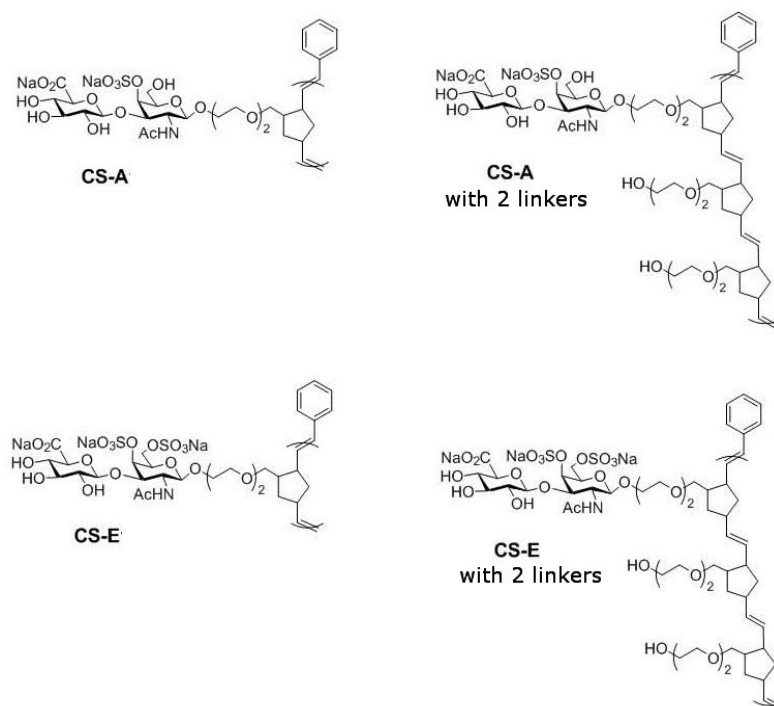
Figure 2.10. CS glycopolymers with linkers to increase distance between CS disaccharide units.

Microarrays were generated as described above, by spotting biotin-labeled glycopolymers to streptavidin-coated slides. In addition, biotinylated CS polysaccharides were also added, to compare the binding of the proteins to the naturally occurring CS motifs. Initial testing

of these arrays with the CS-E antibody revealed highly preferential binding to the CS-E glycopolymer and the polymer with two norbornene linkers (Figure 2.11). A much lower level of binding of the antibody to the CS-E polysaccharide was observed, which could be due to competitive effects of the CS polymers on the array surface.
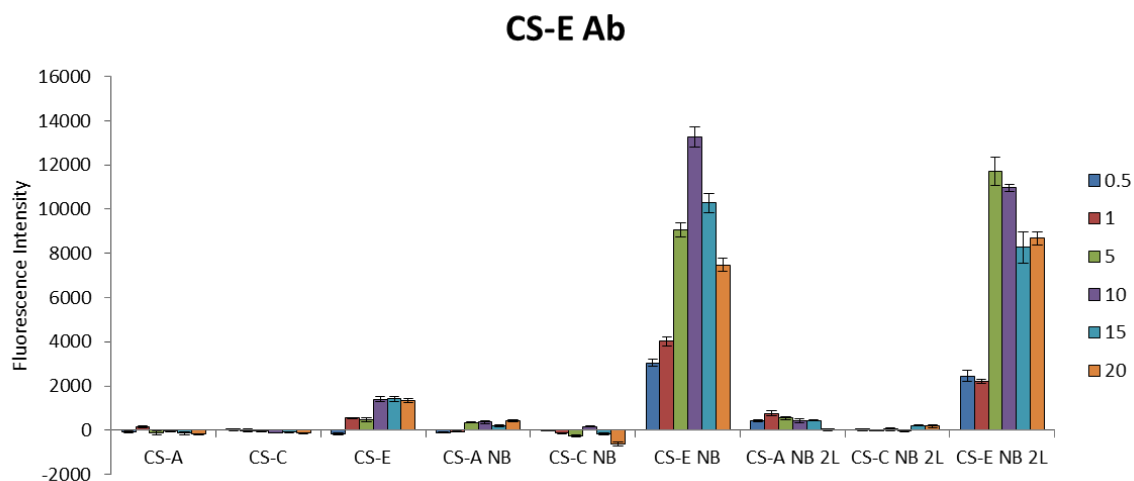
Figure 2.11. The CS-E antibody preferentially binds to the CS-E norbornene polymer (CS-E NB) and the CS-E norbornene polymer with two norbornene linkers (CS-E NB 2L). No binding was observed to other CS polysaccharide motifs, or to CS-A or CS-C polymers. Concentration of the polysaccharides/polymers is shown at right (μM).

Next, we investigated the binding of several proteins on the microarray. These included midkine, a growth factor involved in the development in the nervous system[27], and TNFα, a cytokine that induces inflammation and is implicated in a variety of human diseases.[28, 29] Both midkine and TNFα have been shown previously to bind specifically to CS-E.[7, 14, 30] TNFα appeared to bind preferentially to the CS-E polysaccharide and the CS-E norbornene polymer, but not to the polymer with two linkers (Figure 2.12). Midkine bound

to the CS-E polysaccharide preferentially, but also seemed to bind to all of the polymers on the array to some degree. This may be explained by the reduced specificity of midkine to the CS polysaccharides, as it also appeared to bind to both CS-A and CS-C polysaccharides. Midkine is also known to bind to heparin and to various CS motifs[31] supporting the observation of non-specific anionic binding with this protein. GDNF was also tested on these arrays, and was observed to bind to the CS-E polysaccharide and to the CS-E norbornene polymer, but not to the polymer with two linkers.
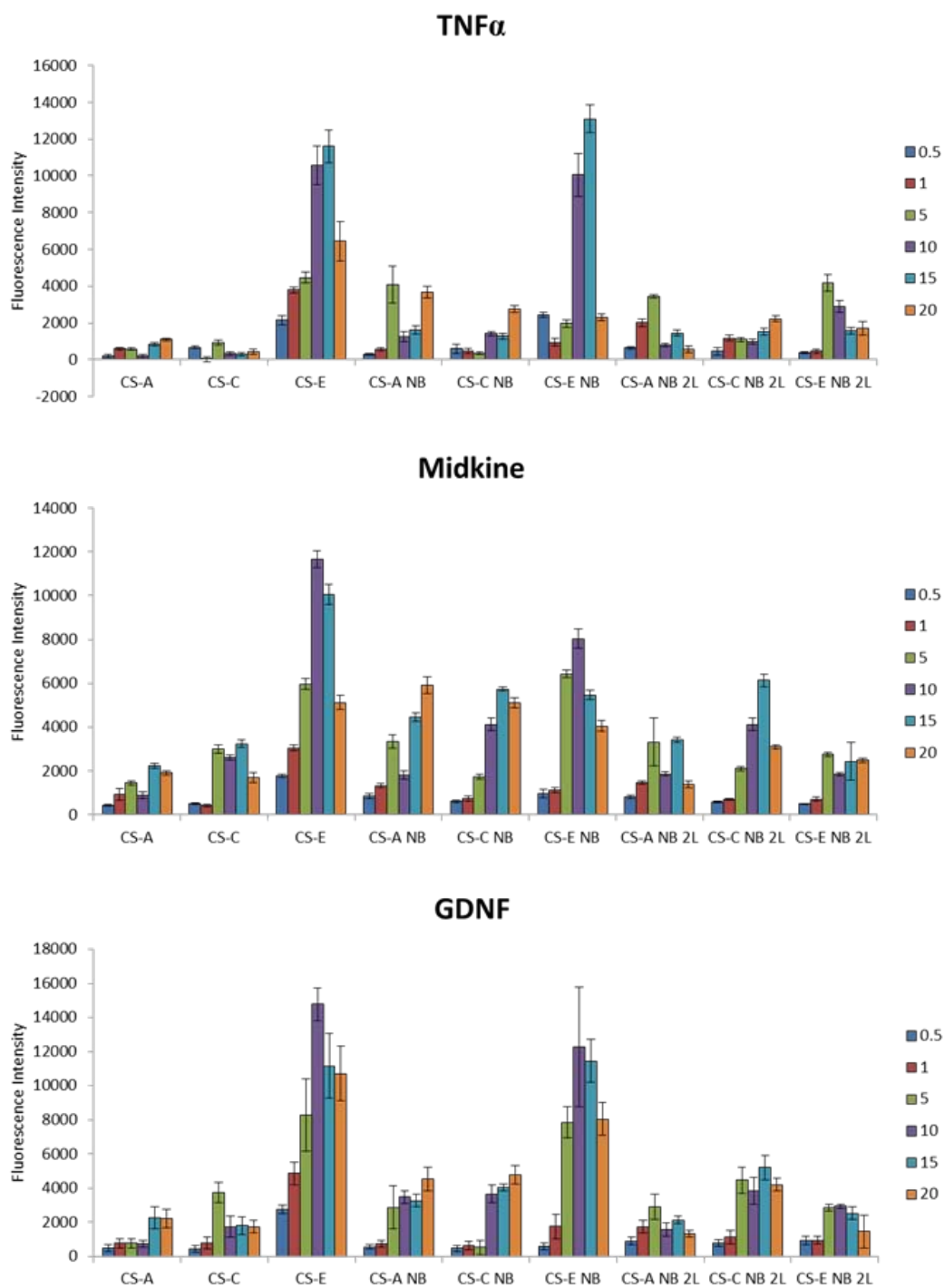
Figure 2.12. Binding of proteins to CS polysaccharides, norbornene polymers (NB) and norbornene polymers with two norbornene linkers (CS NB 2L). Concentration of the polysaccharides/polymers is shown at right (μM).

Conclusions

We have generated a new class of CS glycomimetic polymers that display defined sulfation motifs, while mimicking the multivalent architecture of native GAG chains. Our studies demonstrate that these glycopolymers can be efficiently attached to surfaces, where they approximate physiological cell-cell and cell-extracellular matrix interactions and retain the ability to engage proteins. ROMP-based glycopolymers are part of a growing arsenal of chemical tools for studying the structure-activity relationships of GAGs. We anticipate that they will prove valuable for understanding how multivalency, not only within but also between, GAG chains enhances the avidity, specificity and cooperativity of GAG-protein interactions. Future studies will focus on extending the methodology reported herein to polymers and block co-polymers with varied sulfation patterns and applying them as tools to manipulate CS activity in various biological contexts. The results with CS polymers incorporating norbornene linkers show that the spacing of the motifs on the polymer chain can retain the binding seen with some proteins, while the binding is lost in other proteins. This data, along with future experiments, can provide insight into the CS binding sites of proteins of interest and how different protein surfaces can interact with the CS motifs.

Materials and Methods

Determination of glycopolymer concentrations. Concentrations of the glycopolymers were determined by measuring their relative uronic acid content using the carbazole reaction.[32] Briefly, the acid borate reagent (1.5 ml of 0.80 g sodium tetraborate, 16.6 ml H_2O, and 83.3 ml H_2SO_4) was added to 15-ml glass test tubes. The glycopolymers (5 µl of a 10 mg/ml stock in 3.5 M NaCl) were added and the solution placed in a boiling H_2O bath for 10 min. Following addition of the carbazole reagent (50 µl of 0.1% w/v carbazole in 100% EtOH), the solution was boiled for 15 min. The absorbance was read at 530 nm and compared to a D-glucuronolactone standard in H_2O.

Polysaccharide biotinylation. Chondroitin sulfate polysaccahrides were biotinylated as previousy described.[33] Briefly, CS polysaccharides (2 mg; Seikagaku) were dissolved in 1 ml of 0.05 M $NaHCO_3$ for 30 min at room temperature. EZ-Link Sulfo-NHS-LC-LC-Biotin (0.25 mg; Pierce) was dissolved in 1 ml of H_2O, and added to each CS sample. The mixture was incubated at room temperature for 3 h while mixing end-over-end, and then dialyzed into PBS using 13,500 MW cutoff dialysis tubing.

Biotin quantification. Incorporation of biotin into the polymers was quantified using the Fluorescence Biotin Quantitation Kit (Thermo Scientific). Briefly, the biotinylated polymers were dissolved in PBS, and DyLight Reporter (fluorescent avidin and HABA premix) was added to the biotinylated samples and a range of diluted biocytin standards. The avidin in this reporter fluoresces when the weakly interacting HABA (4′-hydroxyazobenzene-2-carboxylic acid) is displaced by the biotin. The amount of biotin in the polymer samples was then determined by comparing the sample's fluorescence to the

biocytin standard curve. The amount of biotin in the sample was compared to the predetermined polymer concentration to determine the extent of biotinylation.

Microarray assays. Carbohydrate microarrays were generated by spotting stock solutions of glycopolymers in PBS (1 nl) onto streptavidin coated slides (Xenopore) using a Microgrid II arrayer (Biorobotics; Cambridge, UK) at room temperature and 50% humidity. The concentrations of the stock solutions, which ranged from 500 nM to 50 µM, were determined using the carbazole assay as described above and were corrected for the percentage of biotinylation. A given concentration of each polymer was spotted ten times at different positions on the array. A boundary was created around the polymer spots on the slides using a hydrophobic slide marker (Super Pap Pen, Research Products International), and the slides were blocked with 10% fetal bovine serum (FBS) in PBS (pH 7.4, unless otherwise indicated) with gentle rocking at 37 °C for 1 h, followed by a brief rinse with PBS. Human GDNF (Peprotech) was reconstituted in 1% Triton X-100 in PBS, added to the bound region on the slides at a concentration of 2 µM (100 µL), and incubated at room temperature for 3 h. The slides were briefly rinsed three times with PBS, and then incubated with a rabbit anti-human GDNF antibody (Peprotech; 1:1000 in 1% Triton X-100 in PBS) for 1 h at room temperature. The slides were again rinsed with PBS, and then incubated with an anti-rabbit antibody conjugated to Cy3 (Jackson ImmunoResearch; 1:5000 in PBS) for 1 h in the dark with gentle rocking. After rinsing two times with PBS and once with H_2O, the microarray was analyzed at 532 nm using a GenePix 5000a scanner, and fluorescence quantification was performed using GenePix 6.0 software. Binding of the anti-CS-C (2D5-1D2) and anti-CS-E (2D11-2A10) antibodies[7, 14] was evaluated as described above using 100 µL of a 10 µg/ml (or ~70nM) solution of the

antibody and a goat anti-mouse IgG secondary antibody conjugated to Cy3 (Jackson ImmunoResearch; 1:5000 in PBS). The experiments were performed in duplicate, and data representing the average of 20 spots per concentration were shown. Error bars represent the standard error of the mean.

References

1. Capila, I. & Linhardt, R. J. Heparin-protein interactions. *Angew. Chem. Int. Ed. Engl.* **2002,** 41, (3), 391-412.

2. Sugahara, K.*, et al.* Recent advances in the structural biology of chondroitin sulfate and dermatan sulfate. *Curr. Opin. Struct. Biol.* **2003,** 13, (5), 612-620.

3. Gama, C. I. & Hsieh-Wilson, L. C. Chemical approaches to deciphering the glycosaminoglycan code. *Curr. Opin. Chem. Biol.* **2005,** 9, (6), 609-619.

4. Desaire, H., Sirich, T. L. & Leary, J. A. Evidence of block and randomly sequenced chondroitin polysaccharides: sequential enzymatic digestion and quantification using ion trap tandem mass spectrometry. *Anal. Chem.* **2001,** 73, (15), 3513-3520.

5. Turnbull, J. E. & Gallagher, J. T. Distribution of iduronate 2-sulphate residues in heparan sulphate. Evidence for an ordered polymeric structure. *Biochem. J.* **1991,** 273 (Pt 3), 553-559.

6. Raman, R., Sasisekharan, V. & Sasisekharan, R. Structural insights into biological roles of protein-glycosaminoglycan interactions. *Chem. Biol.* **2005,** 12, (3), 267-277.

7. Tully, S. E., Rawat, M. & Hsieh-Wilson, L. C. Discovery of a TNF-alpha antagonist using chondroitin sulfate microarrays. *J. Am. Chem. Soc.* **2006,** 128, (24), 7740-7741.

8. Nandini, C. D., Itoh, N. & Sugahara, K. Novel 70-kDa chondroitin sulfate/dermatan sulfate hybrid chains with a unique heterogeneous sulfation pattern from shark skin, which exhibit neuritogenic activity and binding activities for growth factors and neurotrophic factors. *J. Biol. Chem.* **2005,** 280, (6), 4058-4069.

9. Deepa, S. S., Umehara, Y., Higashiyama, S., Itoh, N. & Sugahara, K. Specific molecular interactions of oversulfated chondroitin sulfate E with various heparin-binding growth factors. Implications as a physiological binding partner in the brain and other tissues. *J. Biol. Chem.* **2002,** 277, (46), 43707-43716.

10. Shipp, E. L. & Hsieh-Wilson, L. C. Profiling the sulfation specificities of glycosaminoglycan interactions with growth factors and chemotactic proteins using microarrays. *Chem. Biol.* **2007,** 14, (2), 195-208.

11. Mizuguchi, S.*, et al.* Chondroitin proteoglycans are involved in cell division of Caenorhabditis elegans. *Nature* **2003,** 423, (6938), 443-448.

12. Trowbridge, J. M. & Gallo, R. L. Dermatan sulfate: new functions from an old glycosaminoglycan. *Glycobiology* **2002,** 12, (9), 117r-125r.

13. Shen, Y. J*., et al.* PTP sigma Is a Receptor for Chondroitin Sulfate Proteoglycan, an Inhibitor of Neural Regeneration. *Science* **2009,** 326, (5952), 592-596.

14. Gama, C. I*., et al.* Sulfation patterns of glycosaminoglycans encode molecular recognition and activity. *Nat. Chem. Biol.* **2006,** 2, (9), 467-473.

15. Kjellen, L. & Lindahl, U. Proteoglycans: structures and interactions. *Annu. Rev. Biochem.* **1991,** 60, 443-475.

16. Gestwicki, J. E., Cairo, C. W., Strong, L. E., Oetjen, K. A. & Kiessling, L. L. Influencing receptor-ligand binding mechanisms with multivalent ligand architecture. *J. Am. Chem. Soc.* **2002,** 124, (50), 14922-14933.

17. Horan, N., Yan, L., Isobe, H., Whitesides, G. M. & Kahne, D. Nonstatistical binding of a protein to clustered carbohydrates. *Proc. Natl. Acad. Sci. U S A* **1999,** 96, (21), 11782-11786.

18. Lewallen, D. M., Siler, D. & Iyer, S. S. Factors affecting protein-glycan specificity: effect of spacers and incubation time. *Chembiochem.* **2009,** 10, (9), 1486-1489.

19. Dhayal, M. & Ratner, D. M. XPS and SPR analysis of glycoarray surface density. *Langmuir* **2009,** 25, (4), 2181-2187.

20. Branderhorst, H. M., Ruijtenbeek, R., Liskamp, R. M. J. & Pieters, R. J. Multivalent carbohydrate recognition on a glycodendrimer-functionalized flow-through chip. *Chembiochem.* **2008,** 9, (11), 1836-1844.

21. Rawat, M., Gama, C. I., Matson, J. B. & Hsieh-Wilson, L. C. Neuroactive chondroitin sulfate glycomimetics. *J. Am. Chem. Soc.* **2008,** 130, (10), 2959-2961.

22. Lin, L. F., Doherty, D. H., Lile, J. D., Bektesh, S. & Collins, F. GDNF: a glial cell line-derived neurotrophic factor for midbrain dopaminergic neurons. *Science* **1993,** 260, (5111), 1130-1132.

23. Tomac, A*., et al.* Protection and repair of the nigrostriatal dopaminergic system by GDNF in vivo. *Nature* **1995,** 373, (6512), 335-339.

24. Tully, S. E*., et al.* A chondroitin sulfate small molecule that stimulates neuronal growth. *J. Am. Chem. Soc.* **2004,** 126, (25), 7736-7737.

25. de Paz, J. L., Noti, C., Bohm, F., Werner, S. & Seeberger, P. H. Potentiation of fibroblast growth factor activity by synthetic heparin oligosaccharide glycodendrimers. *Chem. Biol.* **2007,** 14, (8), 879-887.

26. Ostrovsky, O*., et al.* Differential effects of heparin saccharides on the formation of specific fibroblast growth factor (FGF) and FGF receptor complexes. *J. Biol. Chem.* **2002,** 277, (4), 2444-2453.

27. Muramatsu, T. Midkine and pleiotrophin: two related proteins involved in development, survival, inflammation and tumorigenesis. *J. Biochem.* **2002,** 132, (3), 359-371.

28. Palladino, M. A., Bahjat, F. R., Theodorakis, E. A. & Moldawer, L. L. Anti-TNF-alpha therapies: the next generation. *Nat. Rev. Drug Discov.* **2003,** 2, (9), 736-746.

29. Raza, A. Anti-TNF therapies in rheumatoid arthritis, Crohn's disease, sepsis, and myelodysplastic syndromes. *Microsc. Res. Tech.* **2000,** 50, (3), 229-235.

30. Ueoka, C*., et al.* Neuronal cell adhesion, mediated by the heparin-binding neuroregulatory factor midkine, is specifically inhibited by chondroitin sulfate E. Structural ans functional implications of the over-sulfated chondroitin sulfate. *J. Biol. Chem.* **2000,** 275, (48), 37407-37413.

31. Zou, K*., et al.* A heparin-binding growth factor, midkine, binds to a chondroitin sulfate proteoglycan, PG-M/versican. *Eur. J. Biochem.* **2000,** 267, (13), 4046-4053.

32. Taylor, K. A. & Buchanan-Smith, J. G. A colorimetric method for the quantitation of uronic acids and a specific assay for galacturonic acid. *Anal. Biochem.* **1992,** 201, (1), 190-196.

33. Saito, A. & Munakata, H. Detection of chondroitin sulfate-binding proteins on the membrane. *Electrophoresis* **2004,** 25, (15), 2452-2460.

Chapter 3: A Sulfated Carbohydrate Epitope Inhibits Axon Regeneration after Injury[*]

Introduction

A major obstacle to functional recovery after CNS injury is the inhibitory environment encountered by regenerating axons. Chondroitin sulfate (CS) polysaccharides and their associated proteoglycans (CSPGs) are the principal inhibitory components of the glial scar, which forms after neuronal damage and acts as a barrier to axon regeneration.[1-3] It is well established that the inhibitory activity of CSPGs is derived from their CS chains, as chondroitinase ABC (ChABC) treatment promotes axon regeneration, sprouting, and functional recovery after injury *in vivo*.[4-7] However, the mechanisms by which CS polysaccharides inhibit axon growth are poorly understood. Dissection of the structural determinants and mechanisms underlying CS activity is essential for understanding the barriers to axon regeneration and for developing new treatments to promote regeneration and functional recovery after spinal cord and other CNS injuries.
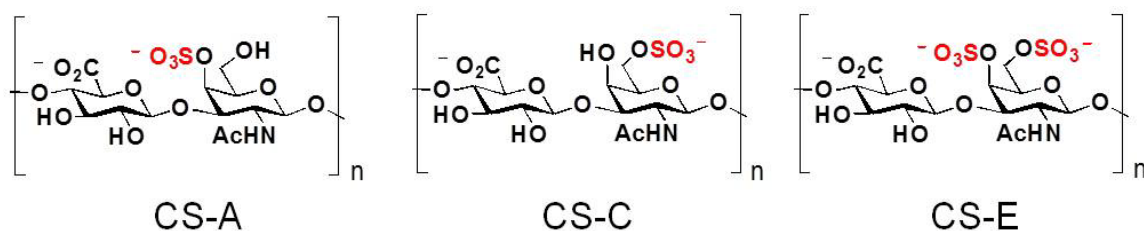
Figure 3.1. CS polysaccharides are composed of 20-200 units of the repeating disaccharide D-glucuronic acid (GlcA) and N-acetyl-D-galactosamine (GalNAc). The sugar hydroxyls are variably sulfated to give rise to diverse sulfation patterns. Chemical structures of major sulfation motifs found in the mammalian nervous system: CS-A (GlcA-4SGalNAc), CS-C (GlcA-6SGalNAc) and CS-E (GlcA-4S, 6SGalNAc). n = 20-200.

CS polysaccharides are composed of repeating disaccharide units, which undergo regiochemical sulfation during development and after injury.[8-11] The CS-A (GlcA-4SGalNAc), CS-C (GlcA-6SGalNAc) and CS-E (GlcA-4S, 6SGalNAc) disaccharides represent major sulfation motifs in the mammalian CNS (Figure 3.1). Although the diverse sulfation patterns of CS polysaccharides lie at the heart of their biological activity, these complex sulfation patterns have also hampered efforts to understand the biological functions of CS. For example, genetic approaches are challenged by the presence of multiple sulfotransferase isoforms with overlapping specificities, and deletion of a single sulfotransferase gene can propagate global changes throughout the carbohydrate chain.[12] The structural complexity of CS has also thwarted biochemical efforts to isolate well-defined, sulfated molecules. As such, only heterogeneous mixtures or purified samples biased toward abundant, readily isolable sequences have been available for biological investigations.[8, 9] Although studies have suggested that the CS-A, CS-E, and CS-C motifs are upregulated after neuronal injury and may play roles in axon regeneration,[8, 10, 13] only heterogeneous polysaccharides were utilized for those studies, and there has been conflicting data, confounding the question of whether specific sulfation sequences are

important. Indeed, because of the lack of structure-activity relationships, relatively nonspecific mechanisms have also been proposed, such as those brought about by steric blockage of the extracellular space,[14] arrays of negatively charged sulfate,[8] or obstruction of substrate adhesion molecules.[15]

Here, we exploited chemically synthesized CS oligosaccharides and glycopolymers to examine systematically the role of specific sulfation sequences in neural regeneration. Our studies demonstrate that the CS-E sulfation motif is a key structural determinant responsible for the inhibitory activity of CSPGs. Moreover, we provide the first mechanistic insights into how CS-E enables CSPGs to inhibit axon growth through the identification of a specific neuronal receptor for CS-E. Finally, we show that blocking the inhibitory CS-E sugar motif can reverse CSPG-mediated inhibition and promote axon regeneration *in vivo*, providing a novel therapeutic approach to neural regeneration.

Results

CS-E-Enriched Polysaccharides Inhibit Neurite Outgrowth and Repel Axons. To understand the role of specific sulfation motifs, we used CS polysaccharides enriched in particular motifs and exploited our ability to chemically synthesize defined CS-A, CS-C and CS-E oligosaccharides. First, we compared the inhibitory effects of CSPGs and CS polysaccharides enriched in CS-A, CS-C or CS-E disaccharide units on neurite outgrowth. Neurite outgrowth of dissociated dorsal root ganglion (DRG) neurons was inhibited by 58% of untreated control levels when grown on CSPGs (Figure 3.2A).
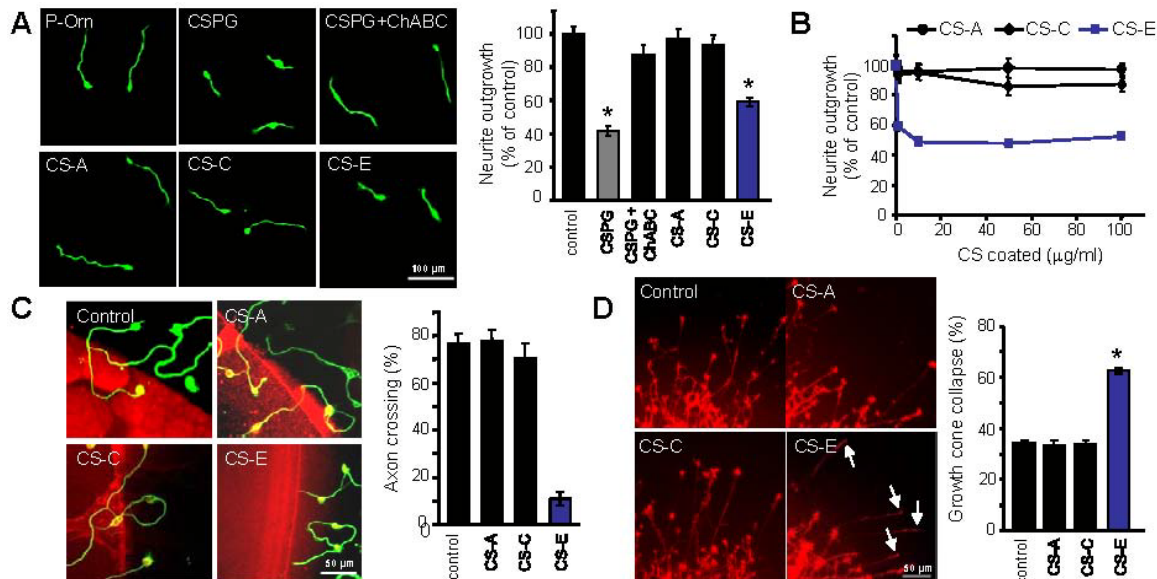
Figure 3.2. CS-E-enriched polysaccharides inhibit DRG neurite outgrowth and induce growth cone collapse. (A) Dissociated chick E7 DRGs were cultured on a substratum of poly-DL-ornithine (P-Orn control), CSPGs, chondroitinase ABC-treated CSPGs, or CS polysaccharides enriched in the CS-A, CS-C or CS-E sulfation motifs. Representative images and quantitation of average neurite length (± SEM, error bars) from three experiments (n = 50-200 cells per experiment). **(B)** Polysaccharides enriched in the CS-E sulfation motif, but not the CS-A or CS-C motifs, inhibit DRG neurite outgrowth in a dose-dependent manner. **(C)** CS-E-enriched polysaccharides repel axon crossing in a boundary assay. Polysaccharides (1 mg/ml) or PBS control were mixed with Texas Red and spotted on P-Orn coated coverslips. Dissociated rat P5-9 CGN neurons were immunostained with an anti-β-tubulin antibody. Representative images and quantitation of percentage of axon crossing (± SEM, error bars) from two experiments (n = 30-50 axons per experiment). **(D)** CS-E-enriched polysaccharides induce growth cone collapse. DRG explants from chick E7-9 embryos were grown on a P-Orn/laminin substratum, treated with medium (control) or the indicated polysaccharides, and stained with rhodamine-phalloidin. Representative images and quantitation of growth cone collapse (± SEM, error bars) from five experiments (n = 50-100 growth cones per experiment). Arrows indicate collapsed growth cones. All statistical analyses were performed using the one-way ANOVA (*P < 0.0001, relative to control).

ChABC digestion largely abolished the effects, confirming the importance of the CS chains.[16] CS polysaccharides enriched in the CS-E motif potently inhibited neurite outgrowth to ~50% of untreated control levels as suggested previously[8] and in a dose-dependent manner (Figure 3.2A and 2.2B). In contrast, polysaccharides enriched in the

CS-A or CS-C motif had no appreciable inhibitory effects on neurite outgrowth at the same glucuronic acid concentrations. The lack of inhibition observed for CS-A and CS-C, even when used at 100-fold higher concentrations than CS-E (Figure 3.2B), suggests that the inhibitory activity of CS-E polysaccharides is not simply due to their high overall negative charge. Similar results were obtained with cerebellar granule neurons (CGNs; Figure 3.3), whose neurite growth is inhibited by CSPGs.[16]
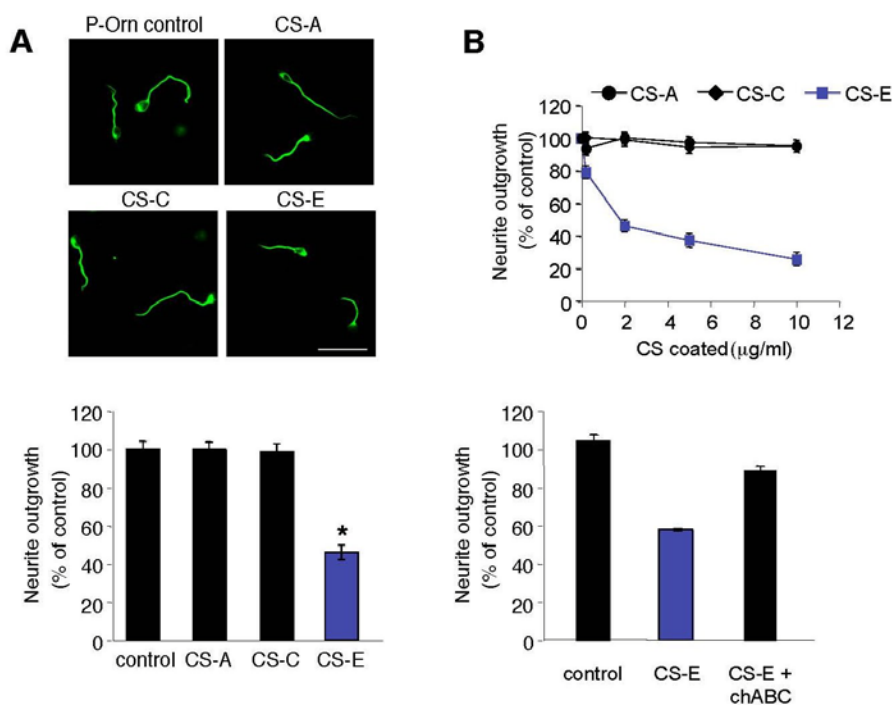
Figure 3.3. Polysaccharides enriched in the CS-E sulfation motif (60% CS-E content), but not CS-A or CS-C (90% CS-A and CS-C content, respectively), inhibit the neurite outgrowth of cerebellar granule neurons (CGNs). (A) Dissociated P5-9 rat CGNs were cultured on a substratum of polysaccharides enriched in the CS-A, CS-C or CS-E sulfation motifs (1 µg/ml) for 24 h. Cells were immunostained using an anti-βIII-tubulin antibody, imaged and quantified using the NIH software ImageJ. Representative images are shown on the top, and quantitation of the average neurite length (± SEM, error bars) from at least three experiments is shown on the bottom (One-way ANOVA, *P < 0.0001, relative to P-Orn control; n = 50–200 cells per experiment). (B) Polysaccharides enriched in the CS-E sulfation motif, but not the CS-A or CS-C motifs, inhibit CGN outgrowth in a dose-dependent manner (top). Chondroitinase ABC digestion abolishes the inhibitory properties of CS-E-enriched polysaccharides in CGNs (bottom).
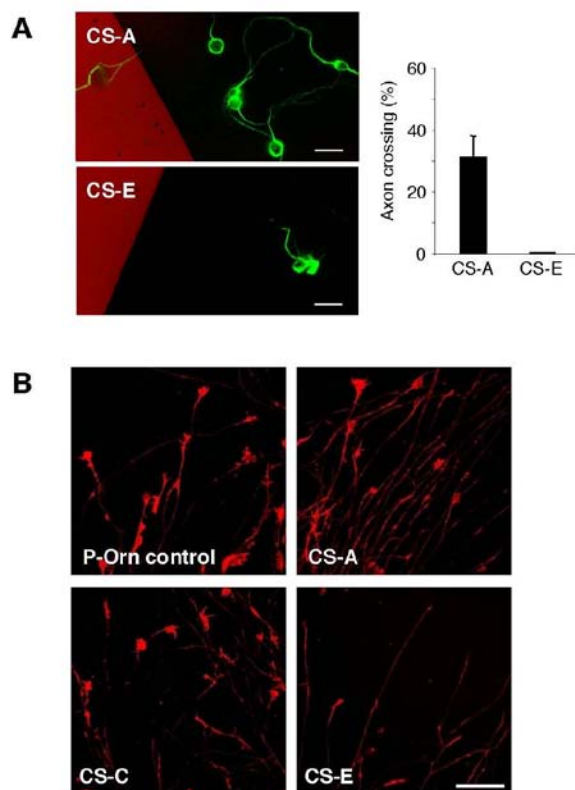
Figure 3.4. Representative images of the (A) axon repellant activity of CS-A and CS-E polysaccharides at high sugar concentrations (10 mg/ml) and (B) growth cone collapse in rat P7-9 CGN explants induced by CS-E polysaccharides. Scale bars, 30μm.

As CSPGs in the glial scar form an inhibitory boundary to growing axons, we examined whether polysaccharides enriched in the CS-E sulfation motif could repel axons in a boundary assay. Like CSPGs,[17] CS-E-enriched polysaccharides formed an inhibitory zone that was strongly repellent to CGN axons (Figure 3.2C). In contrast, axons freely crossed into boundaries enriched in the CS-A or CS-C motifs. CS-A-enriched polysaccharides also exhibited repulsive behavior as reported,[9] but much higher concentrations of sugar were required (Figure 3.4A).

It is known that CSPGs can acutely collapse growth cones to form dystrophic axonal structures that no longer extend, thus leading to long-term inhibition of regrowth.[18] To examine whether CS-E is involved in the acute phase of the inhibitory response, we performed growth cone collapse assays. Application of CS-E-enriched polysaccharides to DRG or CGN explants significantly increased the number of collapsed growth cones within minutes (Figure 3.2D and Fig. 2.4B), whereas CS-A- and CS-C-enriched polysaccharides had no effect. Taken together, these results indicate that CS polysaccharides are sufficient to recapitulate the inhibitory effects of CSPGs on neurons, and this activity depends critically on the CS sulfation pattern.
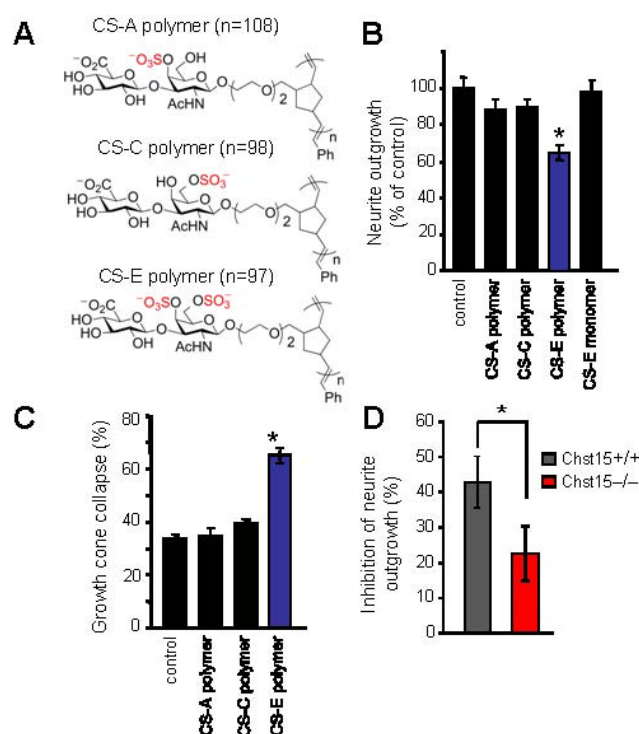
Figure 3.5. The CS-E motif is a potent inhibitor of axon growth. (A) Structures of synthetic glycopolymers displaying pure CS-A, CS-C and CS-E disaccharides. **(B)** The synthetic CS-E glycopolymer inhibits neurite outgrowth of chick E7 DRGs, whereas the CS-A glycopolymer, CS-C glycopolymer, and monovalent CS-E disaccharide have little effect. **(C)** The synthetic CS-E glycopolymer induces DRG growth cone collapse. **(D)** CSPGs from CS-E-deficient mice show significant loss of inhibitory activity on DRG neurite outgrowth. Mouse P8 DRGs were cultured on CSPGs purified from Chst15 knockout or wild-type mice. Statistical analyses were performed using the one-way ANOVA (*$P < 0.0001$, relative to control).

Pure CS-E Potently Inhibits Neurite Outgrowth and Collapses Growth Cones.
Although natural polysaccharides enriched in CS-E shed light on how specific sulfation
motifs function in CSPG-mediated axon inhibition, these data should be interpreted
cautiously because polysaccharides containing a single, pure sulfation sequence have not
traditionally been isolated from natural sources, and thus the possibility that the inhibitory
activity is due to minor, contaminating motifs cannot be eliminated. Indeed, about 40% of
the CS-E-enriched polysaccharide contains other sulfation motifs, and rare sulfation
sequences are likely to be biologically important, as in the case of heparan sulfate
glycosaminoglycans.[19, 20] As such, the intrinsic structural complexity and heterogeneity of
CS pose a major obstacle to understanding structure-activity relationships.

To overcome this problem, we synthesized homogeneously sulfated glycopolymers
displaying only the CS-A, CS-C or CS-E sulfation motifs (Figure 3.5A). Norbornene-
linked CS-A, CS-C or CS-E disaccharides were polymerized using ruthenium-catalyzed
ring-opening metathesis polymerization (ROMP) chemistry. This approach generates
glycopolymers of pure, defined sulfation sequence with molecular weights and biological
activities comparable to natural CS polysaccharides.[21] Previously, we showed that these
molecules were powerful tools to study the roles of specific CS motifs in promoting neurite
outgrowth of developing hippocampal neurons.[22] In the context of DRG neurons,
glycopolymers containing pure CS-E inhibited neurite outgrowth, whereas those containing
pure CS-A or CS-C had minimal activity (Figure 3.5B and Figure 3.6). Moreover, the
monovalent CS-E disaccharide at the same uronic acid concentration did not inhibit neurite
outgrowth, confirming that the multivalent presentation of CS-E is critical for biological
activity. Similarly, we found that glycopolymers containing pure CS-E potently induced

growth cone collapse in DRG explants (Figure 3.5C), whereas CS-A or CS-C glycopolymers had no effect. As CS polysaccharides are found as a complex mixture of different sulfation patterns *in vivo*, we also examined the activity of a glycopolymer mixture. A 1:1 mixture of CS-A and CS-E glycopolymers had no further effects on
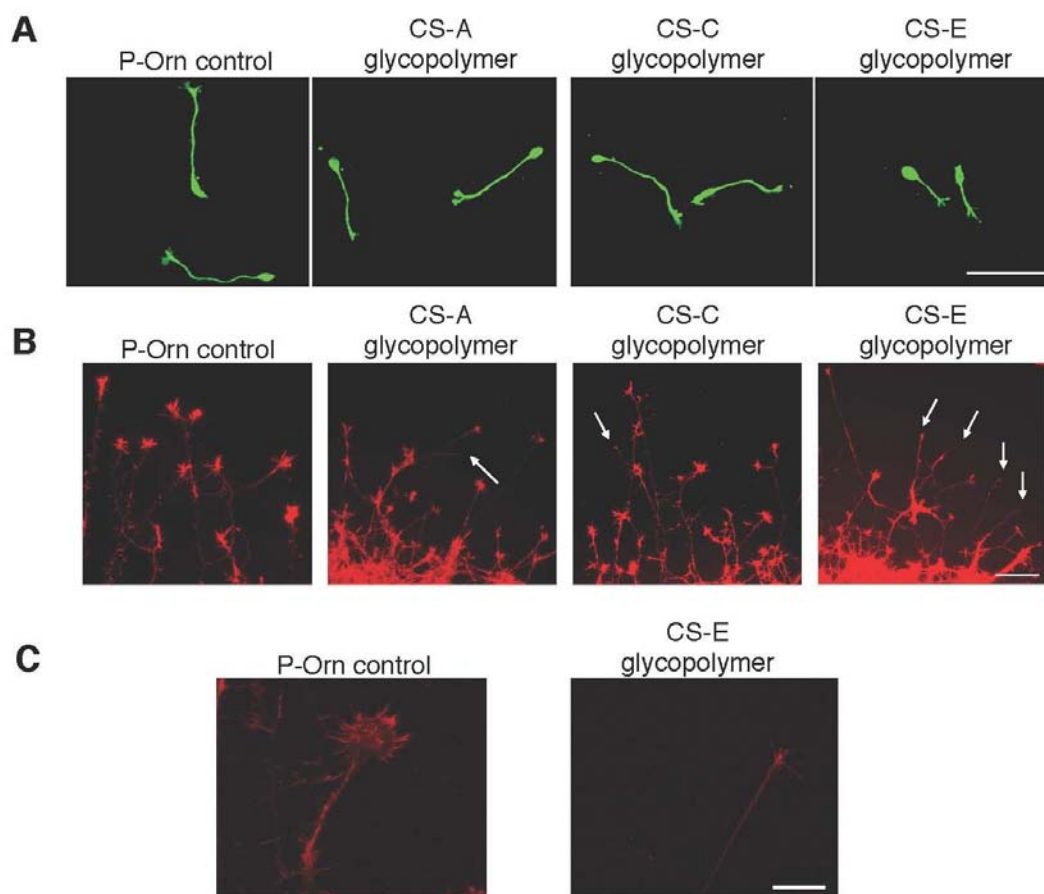
Figure 3.6. Representative images of the (A) inhibition of chick E7 DRG outgrowth by the synthetic glycopolymers, and (B) growth cone collapse of chick E7-9 DRG explants induced by the synthetic glycopolymers. Arrows indicate collapsed growth cones. (C) Higher magnification images (60x) of intact and collapsed growth cones. Scale bars A and B: 100 µm; C: 20 µm.

neurite outgrowth compared to the pure CS-E glycopolymer alone, confirming that sulfated

mixtures do not confer additional inhibitory properties (Figure 3.7).

To complement our chemical approaches, we also investigated the contribution of

the CS-E motif using genetic methods. We isolated CSPGs from mice containing a

targeted gene disruption of *N*-acetylgalactosamine 4-sulfate 6-*O* sulfotransferase 15

(Chst15), the enzyme that generates CS-E via addition of a sulfate group to the 6-*O*

position of GalNAc on CS-A.[23] Consistent with potent inhibitory activity for CS-E,
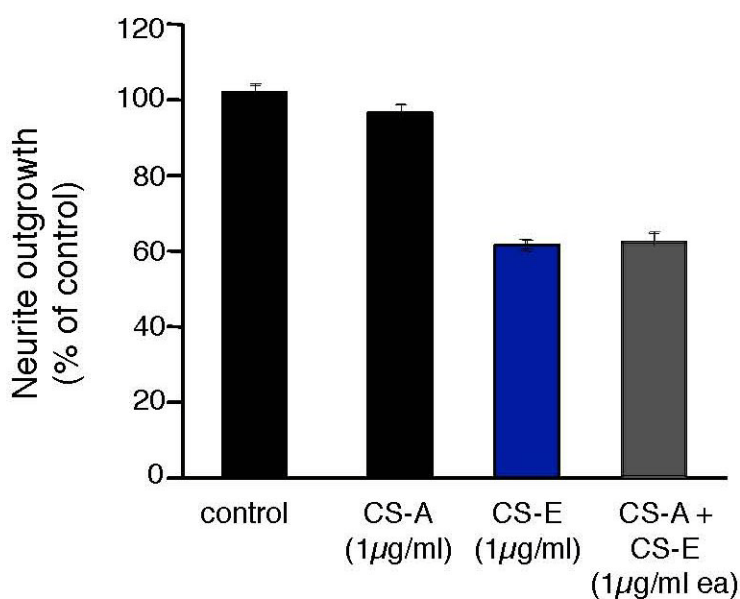
Figure 3.7. A mixture of the CS-A and CS-E synthetic glycopolymers does not confer additional inhibitory properties compared to the pure CS-E glycopolymer. Dissociated E7 chick DRGs were cultured on the indicated substrates for 12-14 h. Cells were immunostained using an anti-βIII-tubulin antibody, imaged, and quantified using the NIH software ImageJ. Quantitation of average neurite length (± SEM, error bars) from three experiments (n = 100-150 cells per experiment) is shown.
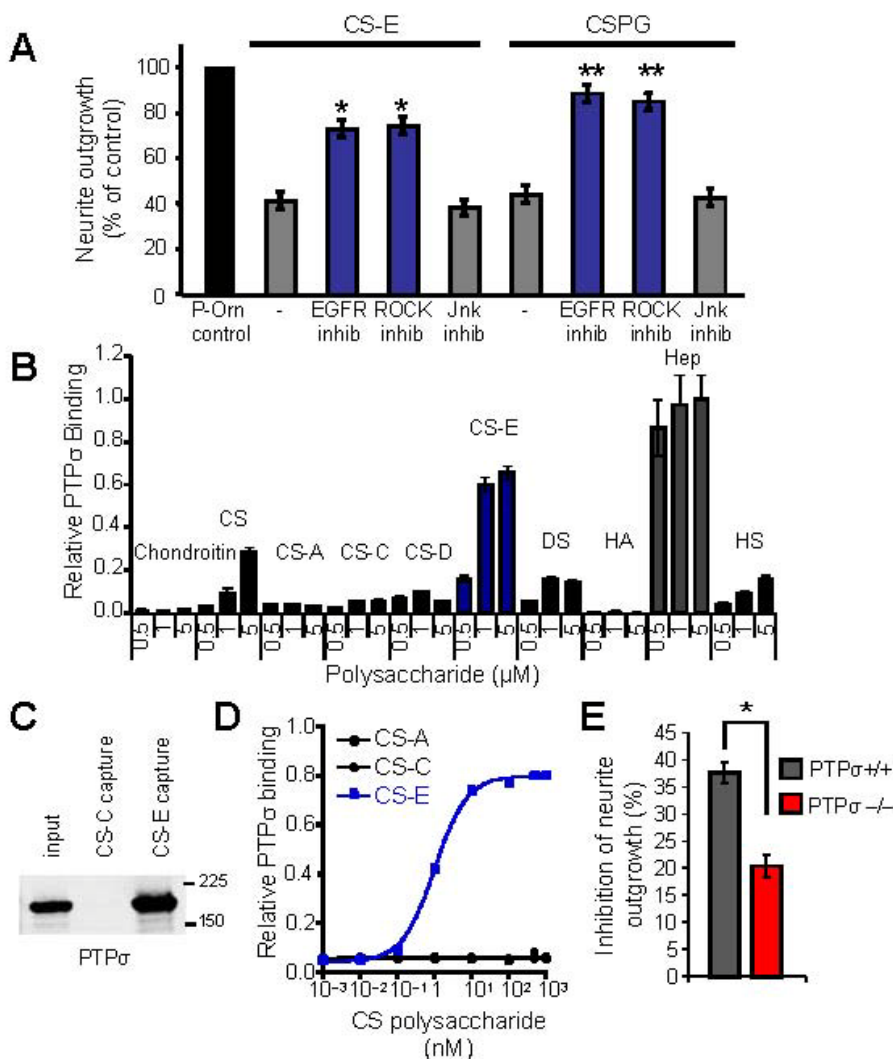
Figure 3.8. The CS-E sulfation motif inhibits axon growth via PTPσ. **(A)** Inhibitors against EGFR (AG1478, 15 nM) and ROCK (Y27632, 5 μM) rescued CS-E- and CSPG-mediated inhibition of neurite outgrowth in dissociated rat P5-9 CGN cultures, whereas JNK inhibitor II (10 μM) had no effect. Quantitation of neurite outgrowth from three experiments is reported. (One-way ANOVA, *P < 0.0001, relative to CS-E control without inhibitors, **P < 0.0001, relative to CSPG control without inhibitors; n = 50-200 cells per experiment). **(B)** PTPσ binds selectively to CS-E-enriched polysaccharides on glycosaminoglycan microarrays. Microarrays were incubated with PTPσ-Fc, followed by a Cy3-conjugated anti-human IgG secondary antibody, and analyzed using a GenePix 5000a scanner. Graphs show quantification from three experiments (n = 10 per condition). **(C)** Co-precipitation of CS-E and PTPσ. Full-length PTPσ-mycHis was expressed in COS-7 cells and incubated with biotinylated CS-E or CS-C polysaccharides bound to streptavidin beads. PTPσ binding was detected by immunoblotting with an anti-myc antibody. **(D)** Specific, high affinity binding of CS-E polysaccharides to PTPσ. **(E)** PTPσ-/- neurons show significantly less inhibition by CS-E than wild-type control neurons. For each genotype, the percentage inhibition of neurite outgrowth is plotted relative to neurons treated with only P-Orn. Quantification from three experiments is shown. (One-way ANOVA, *P < 0.005, relative to control; n = >200 cells per experiment).

removal of CS-E from CSPGs resulted in significant loss of inhibitory activity on DRG neurite outgrowth (Figure 3.5D). The remaining inhibitory effect of CSPGs from $Chst15^{-/-}$ mice is likely due to the proteoglycan core protein or other proteins in the mixture, as treatment with ChABC to remove CS chains did not reduce the inhibitory effects any further. Taken together, our chemical and genetic studies demonstrate conclusively that the CS-E motif is a potent inhibitor of axon growth and a critical inhibitory structure on CSPGs.

The CS-E Motif Activates Inhibitory Signaling Pathways. To investigate the molecular mechanisms by which CS-E inhibits axon growth, we examined the ability of CS-E to activate signaling pathways associated with inhibition of axon regeneration. CSPGs and myelin inhibitors have been shown to activate Rho/Rho-kinase (ROCK) and epidermal
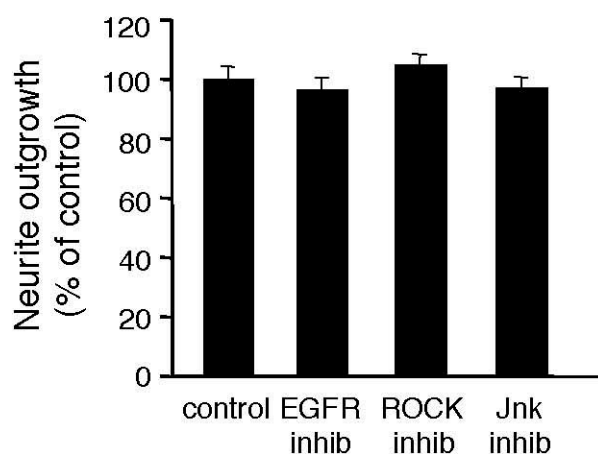
Figure 3.9. Inhibitors to EGFR, ROCK, and JNK alone have no effect on CGN outgrowth in the absence of CS-E or CSPGs. Dissociated rat P5-9 CGN neurons were cultured on a P-Orn substratum in the presence or absence of inhibitors against EGFR (AG1478, 15 nM), ROCK (Y27632, 5 μM), and JNK (inhibitor II, 10 μM) for 24 h. Neurites were visualized by staining with an anti-β-tubulin III antibody, and quantitation of neurite outgrowth from at least three independent experiments is shown (n = 50–200 cells per experiment).

growth factor receptor (EGFR) pathways.[9, 16, 17, 24] Pharmacological inhibition of these signaling pathways effectively reversed the inhibitory effects of CSPGs on CGN neurons (Figure 3.8A and Figure 3.9). Specifically, the EGFR competitive inhibitor AG1478and the ROCK inhibitor Y27632 restored neurite outgrowth to within 79-88% of untreated control levels, in agreement with previous studies.[16, 17, 24] Importantly, we found that the EGFR and ROCK inhibitors also neutralized the inhibitory activity of CS-E polysaccharides and rescued neurite outgrowth to a similar extent. In contrast, inhibition of c-Jun N-terminal kinase (JNK) pathways using JNK inhibitor II showed no effect on either CS-E- or CSPG-mediated neurite inhibition, as expected.[17] Moreover, treatment of COS-7 cells with CS-E or CSPGs led to activation of RhoA (Figure 3.10).
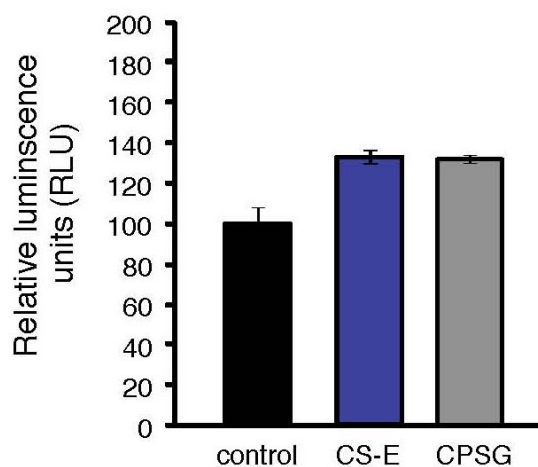
Figure 3.10. CS-E and CSPGs activate RhoA. Serum starved COS-7 cells treated with CS-E polysaccharides or CSPGs (10 μg/ml) for 10 min. Cell lysates were standardized for total protein concentration and then added to a 96-well plate containing immobilized rhotekin-RBD, which binds the active (GTP-bound) form of RhoA. Bound RhoA was detected using a RhoA antibody followed by a horseradish peroxidase-labeled secondary antibody. Relative luminescence units (RLU) are plotted relative to that of the untreated control (cell medium alone) for two experiments.

Thus, CS-E activates intracellular signaling pathways involved in CSPG-mediated inhibition of axon regeneration, further supporting the notion that this sugar epitope is a major inhibitory component of CSPGs.

The CS-E Motif Inhibits Neurite Outgrowth via PTPσ. The ability of CS-E to trigger downstream signaling pathways suggests that CS-E may directly engage protein receptors
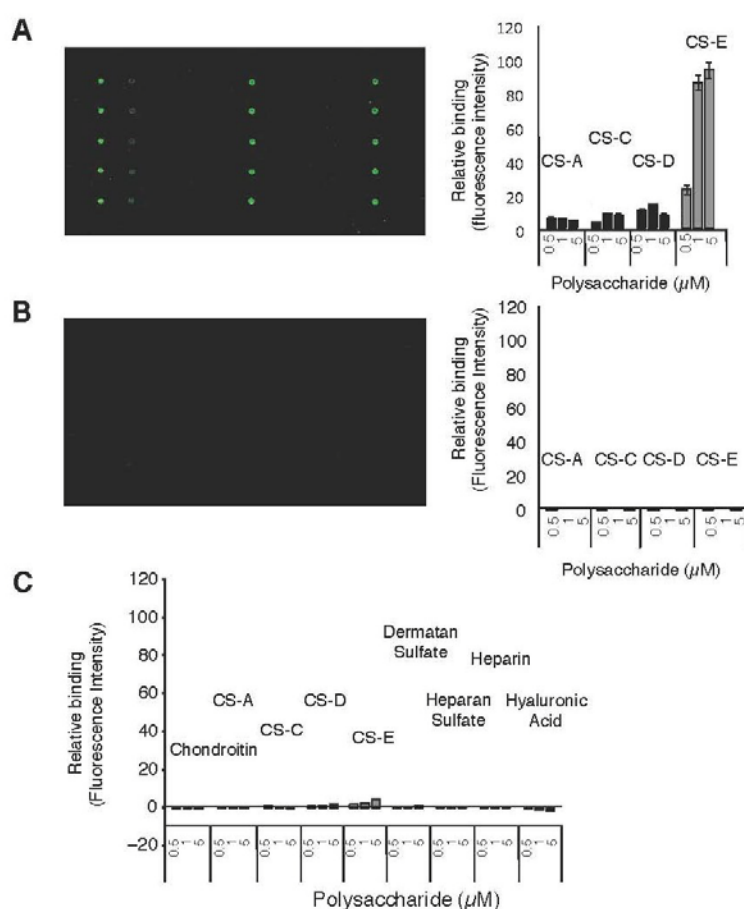
Figure 3.11. PTPσ-Fc but not Fc alone or EphA2-Fc bind preferentially to CS-E-enriched polysaccharides. Representative portion of the microarray after binding to PTPσ-Fc (A, left) or Fc control (B, left). Quantitation from three experiments is shown on the right. Each bar (A and B, right) represents an average of 10 spots per carbohydrate concentration. (C) EphA2-Fc binding to carbohydrate microarrays. Binding relative to PTPσ-Fc is shown.

at the cell surface, thereby initiating intracellular signaling. Recently, CSPGs were shown to interact with protein tyrosine phosphatase PTPσ, a transmembrane receptor known to bind heparan sulfate proteoglycans.[6, 25] PTPσ gene disruption reduced axon inhibition by CSPGs in culture[6] and enhanced regeneration in sciatic, facial, optic, and spinal cord nerves *in vivo.*[6, 26-28] However, it remains unknown whether (and which) specific sulfation motifs on CS mediate the interactions of CSPGs with PTPσ.

In light of our results showing that CS-E is a major inhibitory motif on CSPGs, we examined the potential interaction between CS-E and PTPσ using carbohydrate microarrays.[29] A soluble PTPσ-Fc fusion protein, but not other receptors such as EphA2-Fc or Fc alone, bound efficiently to CS-E polysaccharides arrayed on poly-lysine-coated glass slides (Figure 3.8B and Figure 3.11). PTPσ showed strong binding to heparin and CS-E polysaccharides, with weaker binding to chondroitin sulfate and dermatan sulfate (both of which contain some CS-E) and heparan sulfate. Little or no binding to CS-A, CS-C, or CS-D polysaccharides was observed, highlighting the specificity of PTPσ for the CS-E sulfation motif.

To confirm further the PTPσ-CS-E interaction, biotinylated CS-E or CS-C polysaccharides were conjugated to streptavidin beads and incubated with COS-7 cell lysates expressing full-length PTPσ. We found that CS-E polysaccharides were capable of pulling down PTPσ, whereas CS-C polysaccharides showed no interaction (Figure 3.8C). In addition to this heterologous cell system, we captured PTPσ from a rat brain membrane protein-enriched fraction and identified the protein by mass spectrometry analysis (Figure 3.12). Lastly, we showed that biotinylated CS-E, but not CS-A or CS-C, polysaccharides bind immobilized PTPσ with high affinity according to a Langmuir binding model (Figure

3.8D). The apparent dissociation constant ($K_{D, app}$) of approximately 1 nM is similar to values reported for the association of PTPσ with the CSPGs neurocan and aggrecan.[6]

Having demonstrated that CS-E interacts specifically with PTPσ, we next tested whether CS-E and PTPσ form a functional association. Deletion of PTPσ significantly attenuated CS-E-induced inhibition of neurite outgrowth in DRG neurons (Figure 3.8E), indicating that PTPσ is required for CS-E to inhibit neurite outgrowth. Interestingly, residual inhibition by CS-E (~22%) remained in PTPσ-deficient neurons, consistent with previous observations with CSPGs.[6] These results suggest that CS-E may also engage other receptors, possibly leukocyte common antigen-related phosphatase (LAR)[30] and as-yet-undiscovered receptors, although we cannot rule out additional receptor-independent mechanisms, such as charge repulsion or reduced cell adhesion. Together, these studies demonstrate that the fine structure of CS chains mediates interactions with receptors involved in axon regeneration, and they identify PTPσ as a critical functional receptor for CS-E.
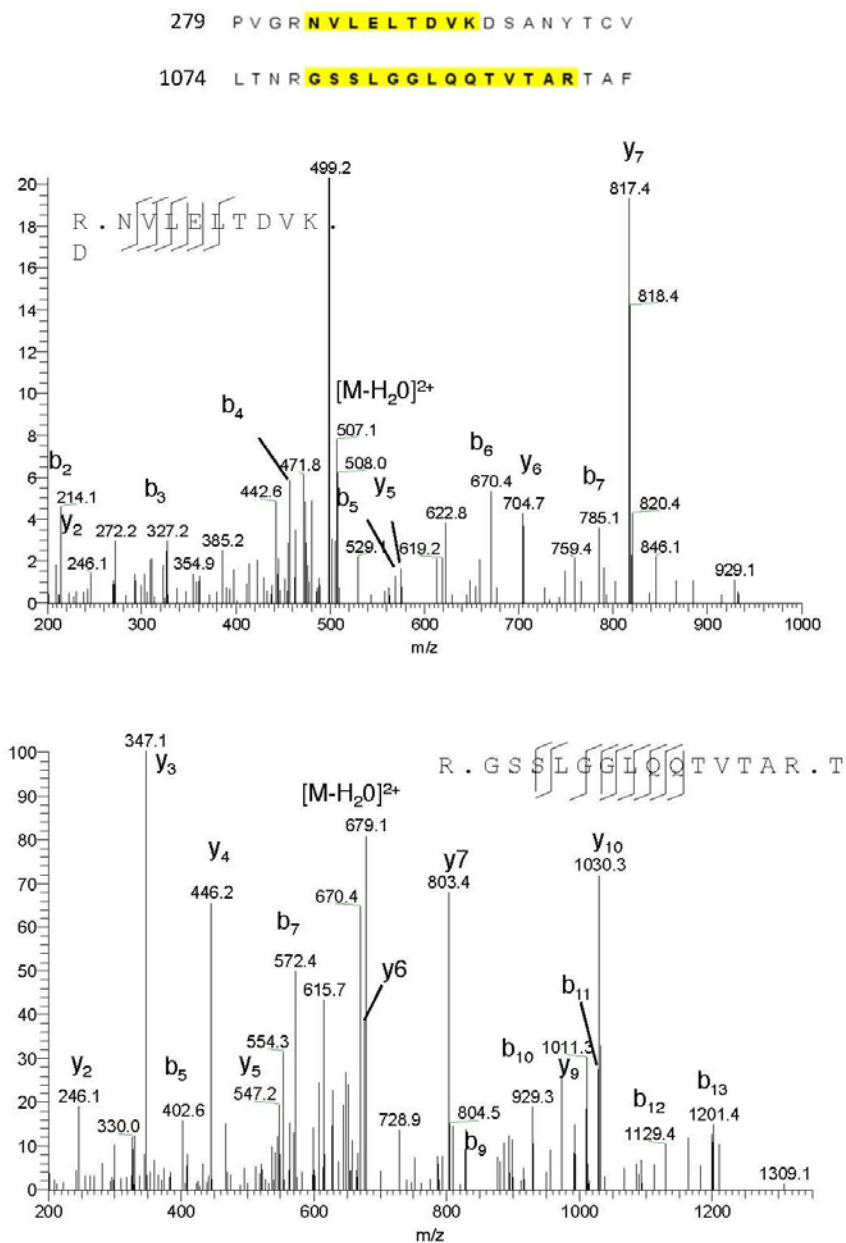
Figure 3.12. PTPσ peptides identified by LC-MS/MS analysis. PTPσ from rat brain lysates was pulled down using CS-E and resolved by SDS-PAGE. In-gel tryptic digestion and LC-MS/MS analysis revealed two unique peptides within PTPσ. The annotated spectra from collision-activated dissociation mass spectrometry (CAD-MS) of the peptides show the y and b fragment ions enabling identification.
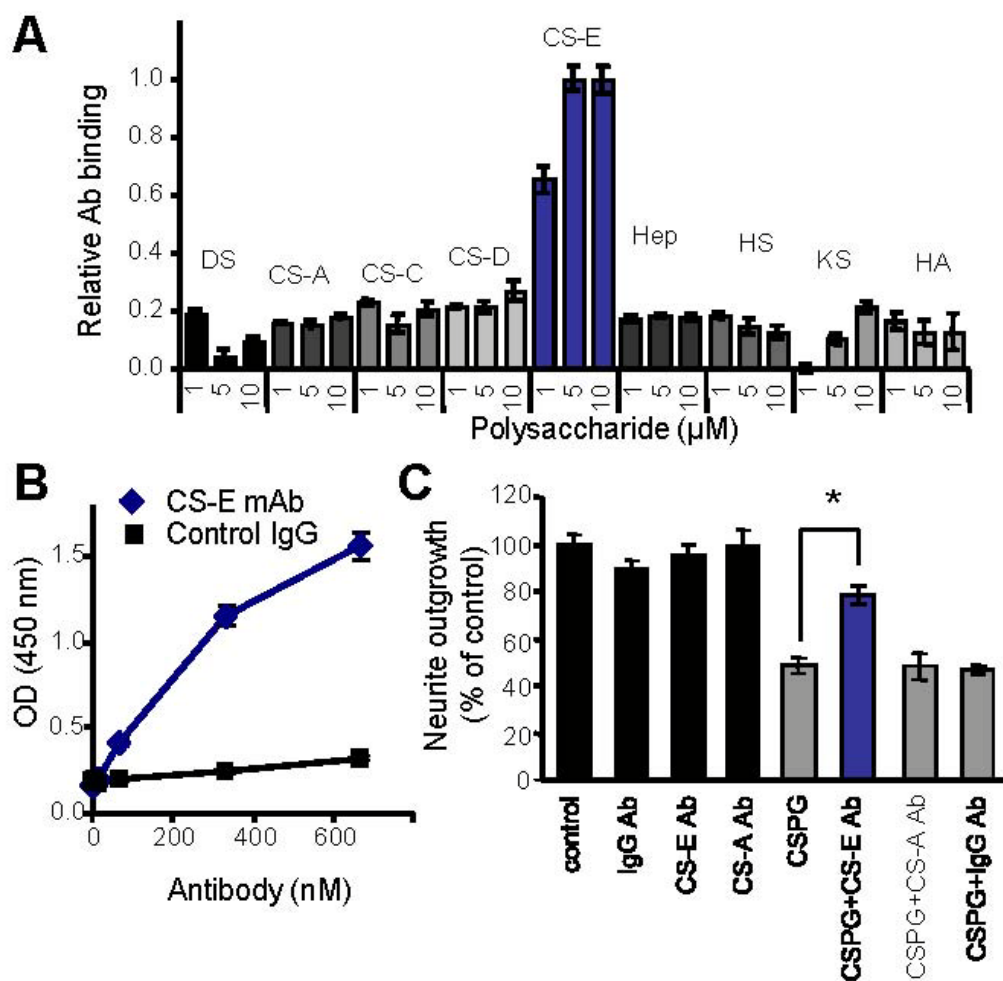
Figure 3.13. A monoclonal antibody binds specifically to CS-E and blocks CSPG-mediated neurite inhibition. (A) Binding of the CS-E antibody to carbohydrate microarrays. Little binding to other sulfated CS polysaccharides or glycosaminoglycan classes was detected. Experiments were performed in triplicate (n =10 per condition). (B) Dose-dependent binding of the anti-CS-E antibody to CSPGs, as shown by an enzyme-linked immunosorbent assay. The experiment was performed in triplicate, and average values (± SD, error bars) are shown for one representative experiment. (C) The CS-E antibody blocks CSPG-mediated inhibition of neurite outgrowth. Dissociated chick E7 DRGs were cultured on a substratum of P-Orn (control) or CSPGs (0.5 μg/ml) in the presence of the indicated antibodies (0.1 mg/ml) for 12 h. Quantitation from three experiments is shown (One-way ANOVA, *P < 0.0001, relative to CSPG without antibody treatment control; n = 50–200 cells per experiment).

Generation of a Selective CS-E Blocking Antibody. An important implication of these results is that blocking CS-E interactions may prevent the inhibition caused by CSPGs and promote axon regeneration. To generate a CS-E blocking agent, we raised a monoclonal antibody against a pure synthetic CS-E tetrasaccharide.[31] Although antibodies have been generated previously using CS polysaccharides as antigens,[32, 33] their specificity has been limited by the structural heterogeneity of natural polysaccharides. Synthetic chemistry has the advantage of providing defined molecules of precise sulfation sequence, which can be used as antigens, for screening antibodies, and for characterizing binding specificities. An antibody generated in this manner was highly selective for the CS-E sulfation motif, as measured by dot blot, ELISA, carbohydrate microarrays, and surface plasmon resonance (Figure 3.13A, Figure 3.14, and Figure 3.15). Strong binding to pure CS-E tetrasaccharides and natural CS-E polysaccharides was observed, with minimal binding to CS-A or CS-C tetrasaccharides and other glycosaminoglycan classes. Notably, this antibody also bound a mixture of CSPGs derived from chick brain (Figure 3.13B), confirming the presence of the CS-E epitope on CSPGs, and blocked the interaction of CS-E polysaccharides with PTPσ (Figure 3.16).
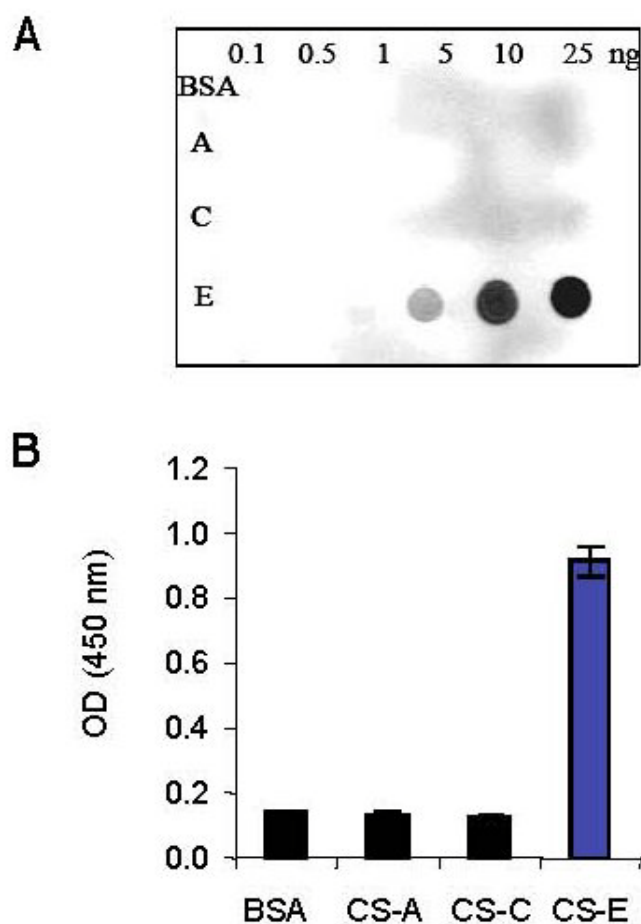
Figure 3.14. The anti-CS-E antibody selectively binds to a pure CS-E tetrasaccharide and natural CS-E-enriched polysaccharides, whereas it does not bind to CS-A or CS-C tetrasaccharides or natural polysaccharides. (A) Tetrasaccharides containing pure CS-A, CS-C or CS-E motifs were conjugated to bovine serum albumin (BSA) and spotted on nitrocellulose membranes at the indicated amounts. Binding of the antibody to the membrane was detected using an Alexa Fluor 680-conjugated goat anti-mouse secondary antibody. The anti-CS-E antibody bound in a concentration-dependent manner to the BSA-CS-E tetrasaccharide conjugate but did not bind significantly to BSA-CS-A, BSA-CS-C, or BSA alone. **(B)** Binding of the anti-CS-E antibody to biotinylated CS polysaccharides enriched in the CS-A, CS-C, or CS-E sulfation motifs. Biotinylated CS polysaccharides were absorbed on streptavidin-coated plates, and antibody binding to the plate was detected using a goat anti-mouse secondary antibody conjugated to horseradish peroxidase. Experiments were repeated in triplicate.

k_{a1} ($M^{-1} s^{-1}$)	k_{d1} (s^{-1})	k_{a2} ($RU^{-1} s^{-1}$)	k_{d2} (s^{-1})	R_{max} (RU)	χ^2 (RU^2)
$3.77 (\pm 0.00) \times 10^4$	$6.41 (\pm 0.01) \times 10^{-5}$	$4.71 (\pm 0.84)$	$11.9 (\pm 2.1)$	$22.6 \pm (0.02)$	0.059
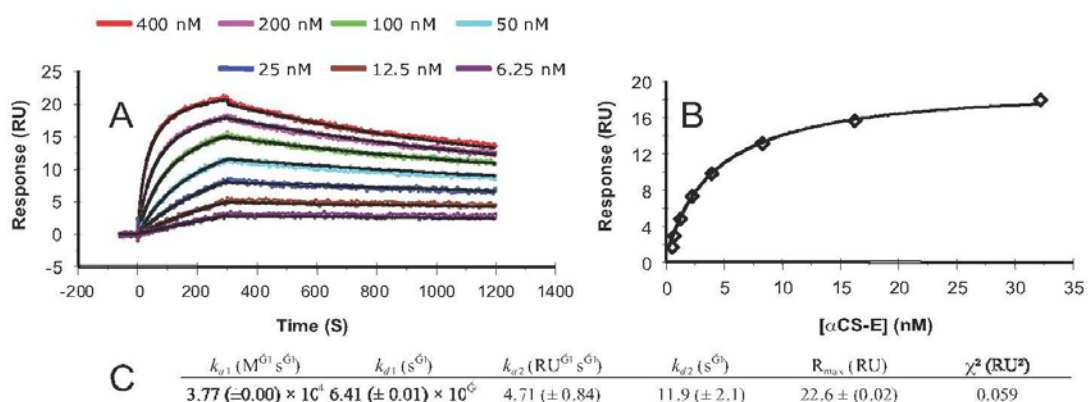
Figure 3.15. Kinetic analysis of the interaction between the anti-CS-E antibody and CS-E tetrasaccharide by surface plasmon resonance. (A) The synthetic CS-E tetrasaccharide was covalently immobilized onto the surface via reductive amination chemistry. Kinetics were monitored at 25 ºC by injecting the CS-E antibody over the surface for 300 s at 30 μl/min and recording the disassociation for 900 s before the surface was regenerated with 6 M guanidine HCl. The resulting sensorgrams were fit to the bivalent analyte model. According to this model, a surface-bound analyte can bind another ligand molecule with the free binding site. The kinetic parameters of the fit, with standard errors in parentheses, are tabulated in (C). The affinity was also measured by injecting the antibody over the surface for 3600 s to give sufficient time to reach equilibrium. The response at equilibrium was plotted versus concentration to give a K_D of 4.3 nM (B).
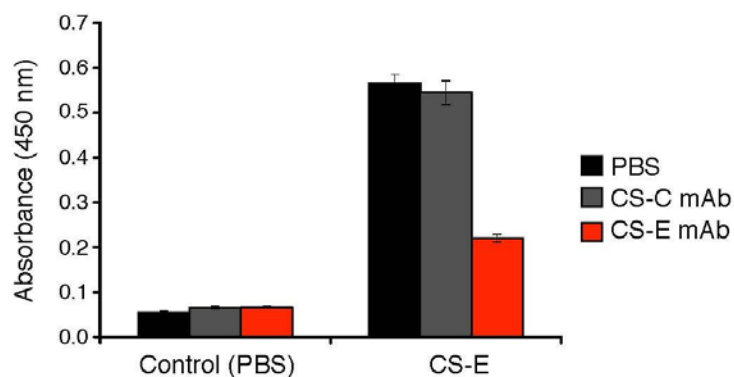
Figure 3.16. The CS-E monoclonal antibody (mAb) attenuates binding of CS-E polysaccharides to PTPσ-Fc. PTPσ-Fc was immobilized in protein A-coated 96-well plates. Biotinylated CS-E (10 nM) in PBS was added in the presence of PBS (control), CS-C mAb (10 μM), or CS-E mAb (10 μM). Binding of CS-E was detected using a streptavidin-horseradish peroxidase conjugate. The experiment was performed in duplicate.
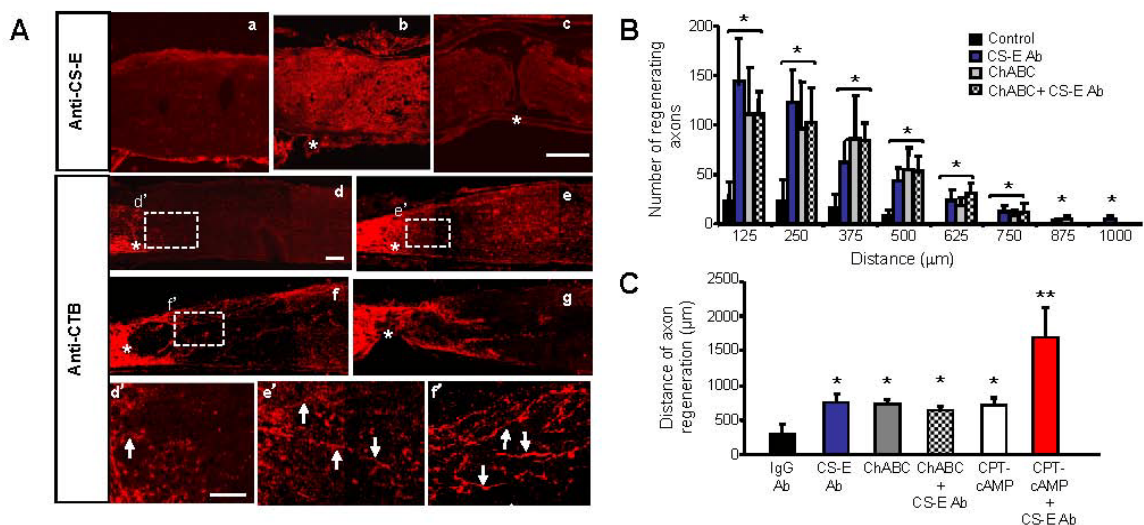
Figure 3.17. CS-E neutralizing antibodies promote optic nerve regeneration. (A) a-c: Immunofluorescence labeling of CS-E expression in optic nerve sections at day 1 sham-operation (a), optic nerve crush injury (b) or optic nerve crush injury plus ChABC treatment. Note upregulation of CS-E around the injury site (b) that was removed by ChABC treatment (c). d-g: Representative epifluorescence photomicrographs of optic nerve sections taken from mice treated with control IgG (d), CS-E antibody (e), ChABC (f) or ChABC plus CS-E antibody (g). Asterisk indicates the crush site. Retinal ganglion cell axons (red) are labeled by an anterograde axon tracer, CTB, which was injected into the vitreous 3 days prior to scarify, followed by immunostaining with goat-anti-CTB antibody. In control antibody-treated mice (d), few regenerating axons are evident. In contrast, numerous regenerating axons were seen extending pass the crush site in CS-E antibody, ChABC or the combine-treated groups (e-g). Scale bars: 75 μm (a-g); 25 μm (d'-f'). Arrowheads indicate growth cone structures. (g) Quantification of the numbers of regenerating axons at different distances from the injury site. (B) Quantification of axon regeneration in vivo. Nerve fibers were counted at 125-μm intervals from the crush site from three non-consecutive sections, and the number of fibers at a given distance was calculated (± SEM, error bars). Both the anti-CS-E- and ChABC-treated groups showed significantly more regenerating axons as compared with the control IgG antibody-treated group (ANOVA with Bonferroni posttests at each distance, *P < 0.001 as compared to controls; n = 6 for each group). (C) Quantification of the distances of axon regeneration. Longest distance of axon regeneration was measured from at least four non-consecutive optic nerve sections from each mouse (± SEM, error bars). Combined treatment of CS-E mAb and CPT-cAMP more than doubled the distance of axon regeneration but did not affect the number of regenerating axons compared to the anti-CS-E or CPT-cAMP treatment alone (Fig. 3.18).

CS-E Blocking Antibody Promotes Axon Regeneration. To test whether blocking the CS-E epitope reverses the inhibitory effects of CSPGs, we added the CS-E antibody to DRG neurons grown on a substratum of CSPGs. Neurite inhibition by CSPGs was significantly decreased by addition of the CS-E antibody, with neurite outgrowth returning to 79% of control levels (Figure 3.13C). In contrast, neither a CS-A monoclonal antibody nor an IgG control antibody had any effect on CSPG-mediated neurite outgrowth.

Having demonstrated specific blocking of CSPG activity *in vitro*, we next examined whether the CS-E antibody could promote axon regeneration *in vivo*. We performed an optic nerve crush injury in mice,[34] which causes focal damage and glial scarring in the optic nerve[35] and thus presents an ideal model for evaluating the effects of local application of the CS-E antibody on axon regeneration. Supporting the notion that CS-E is a prominent inhibitory component associated with CSPGs, pronounced upregulation of CS-E was rapidly observed around the lesion site within 1 day after the injury (Figure 3.17A). To examine the effects of the CS-E antibody on axon regeneration, gelfoam soaked in a solution containing the CS-E or control IgG antibody was placed around the crush site of the nerve immediately after the injury and replaced twice at day three and six. The extent of axonal regrowth was assessed 2 weeks after injury by anterograde axon tracing with choleratoxin-B subunit (CTB), which was injected intravitreally 3 days before mice were sacrificed. Little axon regeneration was observed in the control antibody-treated group. In contrast, the CS-E antibody treatment resulted in substantial axonal regrowth, with a six-fold increase in the number of regenerating axons when counted at 0.25 mm beyond the injury site, as compared with control antibody-treated mice (Figure 3.17B). Notably, the extent of axon regeneration observed after CS-E

antibody treatment was comparable to that seen in mice treated with ChABC alone (50

U/ml) or with ChABC and CS-E antibody applied simultaneously (50 U/ml and 1.7 mg/ml,

respectively).   Thus, blockade of CS-E activity induced a similar extent of axon

regeneration as complete removal of CS chains from the CSPGs, underscoring the

inhibitory potency of CS-E *in vivo*. To rule out the possibility that the observed axon

regrowth after CS-E antibody treatment was simply due to improved cell survival, we

stained retinal sections with an anti-β-tubulin antibody to image retinal ganglion cells and

counted the number of surviving cells. No detectable increase in retinal ganglion cell
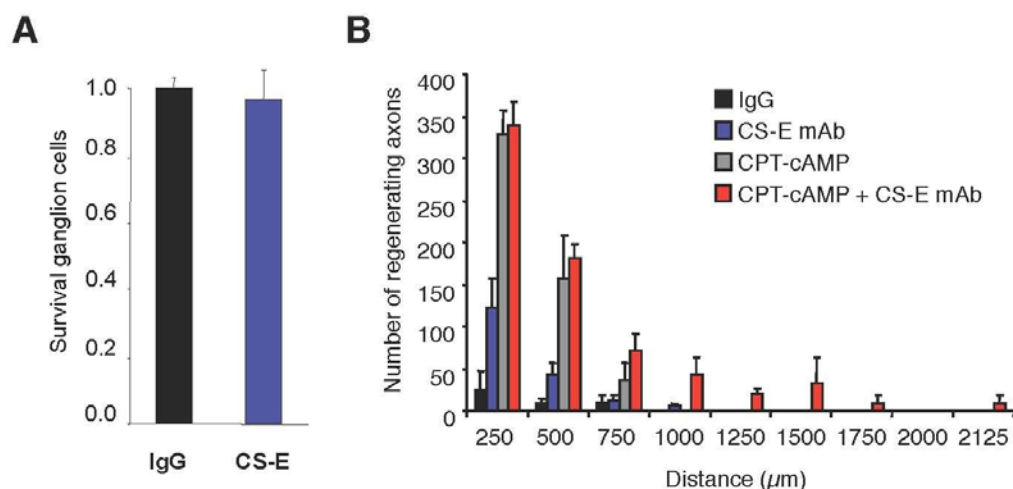
Figure 3.18. The CS-E antibody does not affect the survival or intrinsic growth status of retinal ganglion cells. (A) Application of the CS-E antibody does not change retinal ganglion cell survival after optic nerve injury. Bar graph indicates relative survival of retinal ganglion cells in control IgG or CS-E antibody treated mice that were quantified at 14 days post-optic nerve injury. (B) Comparison of axon regeneration in vivo induced by the CS-E antibody and/or CPT-cAMP. Retinal ganglion cell axons were counted at 125-μm intervals from the crush site from three nonconsecutive sections, and the number of fibers at a given distance was calculated as previously described (5) (± SEM, error bars). (ANOVA with Bonferroni posttests at each distance, *P < 0.001 as compared to controls; n=6 for each group.

survival was found in the CS-E antibody-treated mice, as compared with control antibody-treated mice (Figure 3.18). Remarkably, these results indicate that the complex process of CSPG-mediated neuronal inhibition can be broken down into discrete, active components, which when blocked are sufficient to promote axonal regeneration *in vivo*.

Combining the CS-E Blocking Antibody with Other Treatments. The failure of axons to regenerate has been attributed to inhibitory molecules in the extrinsic environment and a reduced intrinsic regenerative capacity of mature CNS neurons.[1, 2, 36, 37] We therefore examined the ability of the CS-E antibody to enhance axon regrowth *in vivo* when used in combination with 8-(4-chlorophenylthio)-cyclic AMP (CPT-cAMP), a cAMP analog known to penetrate the cell membrane and activate the intrinsic growth state of neurons.[38] In agreement with stimulation of the growth potential of retinal ganglion cell axons, treatment of CPT-cAMP increased the number of regenerating axons by 12-fold compared to the control treated group (Figure 3.18). Combined delivery of the CS-E antibody and CPT-cAMP stimulated longer axonal regrowth than either drug treatment alone, increasing the distance of regeneration by more than 3-fold (Figure 3.17C). The number of regenerating axons compared to the CPT-cAMP treatment alone was not affected (Figure 3.18), further supporting the notion that CS-E contributes to the environmental inhibition, but not the intrinsic growth status, of retinal ganglion cell axons. These results demonstrate the potential of combining the CS-E antibody to block inhibitory CSPGs in the extracellular matrix with growth-promoting treatments to enhance the regenerative outcome.

Conclusions

It has long been recognized that CSPGs are one of the major inhibitors of neural regeneration, but until recently, the structural determinants and mechanisms underlying their activity have been poorly understood. In particular, the precise role of the CS sugars and the importance of specific sulfation motifs have been unclear, limiting the development of molecular approaches to counteract CSPGs. Our studies identify a sugar epitope on CSPGs that is primarily responsible for the inhibitory effects of CSPGs. We show for the first time that the CS-E motif interacts directly with the PTPσ receptor and activates signaling pathways involved in inhibiting axon growth. These findings defy the conventional view that CSPGs function primarily as a mechanical barrier to axon regrowth[14] and that chondroitin sulfate sugars play non-specific, passive roles. The ability to upregulate particular sulfated epitopes on the sugar side chains may be essential for regulating CSPG activity by allowing for more precise control beyond mere expression of the core protein. Further, the concerted expression of diverse sulfated epitopes on different CSPGs could provide an elegant mechanism to coordinate the activities of various proteoglycan core proteins.

These studies also provide a new potential strategy for promoting axon regeneration and neural plasticity after injury. We show that CS-E blocking strategies can increase axon regeneration *in vivo* and can be combined effectively with other treatments, such as stimulation of neuronal growth, to further improve the regenerative outcome. Previous studies have demonstrated that antibodies delivered to the spinal cord can improve function after spinal cord injury,[39, 40] and new techniques may even allow antibodies into the brain for the treatment of neurodegenerative diseases.[41, 42] Additionally, the development of

small-molecule antagonists of CS-E function should also be feasible by inhibiting the sulfotransferases responsible for CS-E biosynthesis.[43, 44] Targeting specific CS sugar epitopes using antibodies, small molecules, or other approaches may offer fewer undesirable side effects and a more stable, selective, and less immunogenic alternative to chondroitinase ABC, which is currently being evaluated as a therapeutic treatment for spinal cord injury. Given that CS-E appears to interact with multiple protein receptors and activate multiple signaling pathways, strategies that block the sulfated CS-E epitope may also prove more effective at neutralizing CSPGs than targeting individual CSPG receptors or pathways.

More broadly, our results demonstrate the importance of the fine structure of CS chains in modulating the activity of CSPGs *in vivo*. In contrast to heparan sulfate, where a handful of important sequences have been identified,[19, 20] much less is known about the roles of CS sulfation. We provide the first *in vivo* evidence that a specific CS-E sulfation motif within CS polysaccharides signals through protein receptors so as to direct important physiological responses. Our studies underscore the power of synthetic chemistry to deliver sulfated sequences with precise spacing and orientation to assess an underappreciated component of the mechanism. Given the importance of glycosaminoglycans in processes ranging from development to viral invasion and spinal cord injury, an expanded view of these sulfated sugars may provide new insights into many critical biological processes.

Materials and Methods

Neurite outgrowth assays. Glass coverslips were coated with poly-DL-ornithine (P-Orn) in pH 8.5 borate buffer (0.5 mg/ml) for 2 h at 37 °C and 5% CO_2, followed by CS-A, -C, -E polysaccharides (Seikagaku), CSPGs derived from chick brains (Millipore), digested CSPGs treated with ChABC (Seikagaku; 4 mU ChABC per μg CSPG), or synthesized polymers[21] (polysaccharides and polymers at 1 μg/ml based on uronic acid content[45] in PBS) for 2 h at 37 °C and 5% CO_2. For mixed polymer assays, the polymers were mixed at the given concentrations immediately prior to coating. DRGs were dissected from day 7 chick embryos, incubated in 0.125% trypsin w/ EDTA (Invitrogen) for 15 min at 37 °C, triturated to dissociate to single cell suspensions, and grown on the coverslips coated with the above-mentioned substrata. Cells were grown in a growth medium composed of DMEM/F12, 10% horse serum, 50 ng/ml NGF (Sigma-Aldrich), and Insulin-Transferrin-Selenium-X supplement (Invitrogen) for 12 h. For CGNs, cerebella were dissected from P5-9 Sprague Dawley rats, incubated in 0.125% trypsin w/ EDTA for 15 min at 37 °C, triturated to dissociate to single cell suspensions, and purified on discontinuous 35%-60% Percoll gradient. For the signaling pathway inhibitor studies, inhibitors against EGFR (AG1478, 15 nM; Calbiochem), ROCK (Y27632, 5 μM; Calbiochem) and JNK (JNK Inhibitor II, 10 μM; Calbiochem) were added in solution at the start of culturing, and neurons were grown for 24 h in in DMEM/F12, 1% FBS, and N1 supplement at 37 °C and 5% CO_2. For the antibody blocking studies, anti-CS-E, anti-CS-A,[31] or IgG control antibodies (0.1 mg/ml) were added at the start of culturing to chick E7 DRGs, which were cultured as described above on glass slides with a substratum of P-Orn or CSPGs (0.5 μg/ml) for 12 h.

For inhibition studies using CSPGs derived from Chst15$^{-/-}$ mice,[23] 96-well Poly-D-Lysine Cellware plates (BD BioCoat™) were coated with CSPGs in phosphate buffered saline (PBS; 1 mM KH_2PO_4, 155 mM NaCl, 3 mM Na_2HPO_4, pH 7.4) overnight at 37 °C and 10% CO_2. The plates were then washed with PBS and coated with laminin (Invitrogen; 10 µg/ml) in Neurobasal medium (Invitrogen) for 2 h at 37 °C and 10% CO_2. DRGs were dissected from P8 wild-type (WT) mouse pups, incubated in 0.125% trypsin w/ EDTA for 15 min at 37 °C, followed by collagenase (Worthington; 4 mg/ml) for 15 min at 37 °C, triturated to dissociate to single cell suspensions, filtered using a 40-µm cell strainer (Fisher) to remove non-dissociated cells, and seeded at approximately 2000 cells per well. Cells were cultured for 2 days in Neurobasal medium supplemented with B27 and GlutaMAX™ (Invitrogen).

For inhibition studies using neurons from PTPσ$^{-/-}$ mice,[46] Poly-D-Lysine Cellware plates were coated with laminin (10 µg/ml) in Neurobasal medium (Invitrogen) for 2 h at 37 °C and 10% CO_2. DRGs were dissected from adult knockout (KO) mice or WT controls, dissociated, and cultured as described above. CS-E was biotinylated as described[8] and conjugated to streptavidin agarose beads (200 µg of CS in 400 µl PBS incubated with 100 µl agarose resin for 1 h at room temperature), which were then co-plated with the cells (5 µg of 50% slurry per well). Unconjugated beads at the same concentration were used as a control. Cells were grown in Neurobasal medium supplemented with B27 and GlutaMAX™ (Invitrogen) for 2 days. For all neurite outgrowth experiments, we performed statistical analysis using the one-way ANOVA; n = 50-200 cells per experiment, and results from at least three independent experiments were reported.

Growth cone collapse assays. DRG explants were dissected from E7-9 chick embryos and grown in DMEM/F12 medium supplemented with horse serum (10%), Insulin-Transferrin-Selenium-G supplement, and NGF (50 ng/ml) on 8-well Lab-Tek® II CC2™ slides (Electron Microscopy Sciences) that were coated with P-Orn in pH 8.5 borate buffer, followed by laminin (10 µg/ml) in PBS for 2 h at 37 °C and 5% CO_2. CGN explants were dissected from P7-9 rats, chopped with a razor blade into approximately 1-mm^2 pieces, and cultured on P-Orn-coated glass coverslips in DMEM/F12 medium supplemented with horse serum (10%), FBS (5%), and N1 supplement. After 24 h, explants were treated with the indicated polysaccharides or glycopolymers (10 µg/ml based on uronic acid content in media; initial stock: 200 µg/ml in PBS) for 30 min. *P*-values were determined using one-way ANOVA; n = 50-100 growth cones per experiment, and results from at least five independent experiments were reported.

Boundary assays. CS polysaccharides (1 mg/ml based on uronic acid content) were mixed with Texas Red (0.5 mg/ml; Invitrogen) in PBS, spotted at the center of P-Orn-coated coverslips (5 µl), and incubated for 2 h at 37 °C and 5% CO_2. Cerebella were dissected from P5-9 Sprague Dawley rats, incubated in 0.125% trypsin w/ EDTA for 15 min at 37 °C, triturated to dissociate to single cell suspensions, and purified on a discontinuous 35%-60% Percoll gradient. These cells were then cultured on the coated coverslips for 48 h. After immunostaining for neurite outgrowth, axons growing toward the boundary and within 10 µm distance of the boundary were evaluated. The percentage of axons that crossed the boundary over the total axons was quantified. *P*-values were determined using

one-way ANOVA; n = 30-50 axons per experiment, and results from two independent experiments were reported.

Immunostaining and quantification. Neural cultures were fixed with paraformaldehyde, permeabilized with 0.1% Triton X-100 in PBS, blocked with 1% BSA in PBS, and incubated with a mouse anti-βIII tubulin antibody (Sigma) overnight at 4 °C, followed by an Alexa Fluor 488-conjugated goat anti-mouse IgG secondary antibody (Invitrogen) for 1-2 h at room temperature for neurite outgrowth and boundary assays, or by rhodamine phalloidin (Pierce) for 1 h at room temperature for growth cone collapse assays. Cells were imaged using a Nikon TE2000-S fluorescent microscope or Zeiss LSM Pascal, and neurite outgrowth was quantified using NIH software ImageJ or MetaMorph software. Statistical analysis was performed using the one-way ANOVA; n = 50-500 cells per experiment, and results from at least three independent experiments were reported.

Protein expression and binding assays. For pull-down assays, full-length mouse PTPσ (Open Biosystems) was ligated into a pcDNA vector (Invitrogen) modified to fuse a myc-His tag to the 5' end of the insert. COS-7 cells were transfected using Lipofectamine (Invitrogen) and lysed two days after transfection with 1% Triton X-100 in PBS containing a protease inhibitor cocktail (Roche). Lysates were then incubated with streptavidin agarose resin (Pierce; 30 μl) with end-over-end mixing for 1 h at 4 °C to reduce nonspecific binding. The supernatant was collected, added to 30 μl of either CS-C or CS-E streptavidin agarose resin, and incubated with end-over-end mixing for 4 h at 4 °C. The supernatant was removed, and the resin was washed three times with PBS (500 μl). Resin was boiled

with 2X loading dye (30 μl of 100 mM Tris, 200 mM DTT, 4% SDS, 0.10% bromophenol blue, 20% glycerol), and the eluate was resolved by SDS-PAGE and transferred to PVDF membrane. PTPσ-myc was detected by immunoblotting with an anti-myc antibody (Cell Signaling) following the manufacturer's protocol. For ELISA and microarray assays, the extracellular domain of PTPσ was ligated into a pcDNA vector that had been modified to append a human Fc domain and myc-His tag to the expressed protein. HEK293T cells were transfected using Lipofectamine, and the conditioned media was collected and used for ELISA or subjected to Ni-NTA agarose purification for carbohydrate microarray assays.

ELISA and dot blot assays. To assay for PTPσ binding, PTPσ-Fc was incubated in 96-well protein A-coated plates (Pierce) overnight at 4 °C. The plates were washed with PBS containing 0.05% Tween-20 (PBST) and then incubated with biotinylated CS-A, CS-C, or CS-E polysaccharides in PBS for 2 h at room temperature. For the antibody blocking study, biotinylated CS-E (10 nM in PBS) was preincubated with the CS-C antibody[47] or CS-E antibody (10 μM) for 1 h at room temperature. The plates were then blocked with 1% BSA in PBS for 30 min at room temperature, incubated with horseradish peroxidase-conjugated streptavidin (Pierce; 1:25,000) for 1 h, and developed with TMB substrate (3,3′,5,5′-tetramethylbenzidine; Pierce) for 20 min and quenched with 2M H_2SO_4. The absorption at 450 nm was recorded on a PerkinElmer Victor plate reader. Experiments were performed in triplicate, and data represent the mean ± SEM, error bars.

For CS-E antibody binding to CSPGs, CSPGs (10 μg/ml; 25 μl) were incubated in a Nunc Maxisorp 384-well plate for 2 h. After blocking with 3% BSA in PBS, the anti-CS-

E antibody (at the indicated concentrations in 1% BSA in PBS) was incubated in each well for 2 h. For CS binding assays, streptavidin (20 µg/ml; 50 µl) was absorbed in each well for 1 hr, followed with biotinylated CS (20 µg/ml; 50 µl) for 1 hr. After blocking with 3% BSA in PBS, the anti-CS-E antibody (25 µl of 20 µg/ml or indicated concentrations in 1% BSA in PBS) was incubated in each well for 2 hr. Following incubation with horseradish peroxidase-conjugated anti-mouse IgG secondary antibody, the plates were developed and analyzed as described above. Dot blot assays for binding of CS-E Ab to CS polysaccharides were performed as described previously.[31]

Microarray assays. Microarrays were generated as described previously.[29] Arrays were blocked with 10% FBS in PBS with gentle rocking at 37 °C for 1 h, followed by a brief rinse with PBS. PTPσ-Fc, EphA2-Fc (R & D Systems), or Fc was reconstituted in 1% BSA in PBS, added to the slides in 100 µl quantities at a concentration of 1 µM, and incubated at room temperature for 3 h. The slides were briefly rinsed three times with PBS, and then incubated with a goat anti-human IgG antibody conjugated to Cy3 (Jackson ImmunoResearch; 1:5,000 in PBS) for 1 h in the dark with gentle rocking, and scanned at 532 nm using a GenePix 5000a scanner. Fluorescence quantification was performed using GenePix 6.0 software (Molecular Devices). Binding of the CS-E antibody was evaluated using 100 µl of a 1 µg/ml (or ~7 nM) solution of antibody and a goat anti-mouse IgG secondary antibody conjugated to Cy3. Experiments were performed in triplicate, and the data represent the average of 10 spots per concentration averaged from the three experiments (± SEM, error bars).

Mass spectrometry analysis. Brains were dissected from P7-P9 Sprague Dawley rats, homogenized in 0.32 M sucrose with protease inhibitors (Roche), and centrifuged at 1,000 g for 10 min. The supernatant was collected, and then centrifuged at 10,000 g for 20 min. The pellet was discarded, and the supernatant was centrifuged again at 12,000 g for 30 min. This supernatant was then ultra-centrifuged at 200,000 g for 1 h, and the pellet was saved and homogenized again in 0.32 M sucrose with protease inhibitors. The supernatant was again ultra-centrifuged at 200,000 g for 1 h and the pellet was saved, solubilized in 1% Triton X-100 (PBST) with protease inhibitors, and centrifuged at 12,000 g for 15 min. The final supernatant was obtained as the membrane protein-enriched fraction and incubated with CS-E or unsulfated CS conjugated to streptavidin agarose resin (described above) overnight at 4 ºC. The resin was washed with PBS, and the PBS was collected and measured until the OD_{280} was less than 0.05. The bound proteins were then eluted with PBS containing 500 mM NaCl. The eluted proteins were then dialyzed into PBS and subjected to SDS-PAGE. The resulting gel was stained with Coomassie Brilliant Blue, and the band at 206 kDa was cut out, subjected to tryptic digestion, and analyzed by liquid chromatography–mass spectrometry (LC-MS) analysis as reported.[48]

Surface plasmon resonance. All experiments were performed on a Biacore T100 at 25 ºC using a Sensor Chip CM5 with a running buffer composed of 0.01 M HEPES, pH 7.4, 0.15 M NaCl, 3 mM EDTA, 0.05% Surfactant P20 (HBS-EP+). To analyze the binding of the CS-E antibody to the CS-E tetrasaccharide, both control and active flow cells were exposed to a 1:1 mixture of *N*-hydroxysuccinimide (NHS) and 1-ethyl-3,3-dimethylaminopropyl-carbodiimide (EDC) for 3 min at a flow rate of 10 μl/min. Next, 5 mM carbohydrazine was

injected at the same flow rate for 7 min. Ligand was covalently attached to the surface by injecting a 0.5 mM solution of synthetic CS-E tetrasaccharide bearing an aldehyde group on a reducing-end linker, prepared as previously described,[47] onto the active flow cell briefly at a high flow rate (10 s, 60 μl/min), followed by a 20 min injection of 0.1 M sodium cyanoborohydride in 0.1 M sodium acetate pH 4.0 at 2 μl/min. Because of the low molecular weight of the CS-E tetrasaccharide, it was not possible to observe the amount of ligand bound to the surface. Instead, 500 nM of the CS-E antibody was injected into both the control and active flow cell to test the response. The amount of ligand was increased accordingly until an adequate response was observed. The kinetics of the CS-E antibody/CS-E tetrasaccharide interaction was determined by 300 s injections of the CS-E antibody at 30 μl/min. The dissociation was monitored for 900 s before the surface was regenerated with a 30 s injection of 6 M guanidine HCl. The resulting sensorgrams were fit to the bivalent analyte model. Affinity analysis was measured by injecting the antibody for 3600 s at 5 μl/min. After 600 s, the surface was regenerated with a 60 s injection at 10 μl/min. The data were analyzed by plotting the response at equilibrium versus concentration and fitting the resulting curve to the Langmuir equation.

CSPG purification. Adult brains from Chst15 knockout mice or WT controls were dissected and homogenized in PBS with 20 mM EDTA and protease inhibitors (Roche). The homogenates were centrifuged at 27,000x g for 1 h at 4 °C. The supernatant was collected, and the pellet was homogenized and centrifuged as before, and the second supernatant was added to the first (total volume: 8 ml). Urea (1 g) was added, and the supernatant was incubated at 4 °C for 1 h. For each brain, 2 ml of DEAE Sephacel beads

was added to a column, and the supernatant was incubated with these beads for 2 h at 4 °C. The column was then drained, and washed with 50 mM Tris HCl, pH 7.5, 2 mM EDTA, 2 M urea, 0.25 M NaCl. The CSPGs were eluted with the same buffer, with 0.75 M NaCl. The eluate was concentrated using 50 kDa filter columns (Amicon), and dialyzed into PBS. Protein concentrations were determined using the carbazole assay with commercial CSPGs (Millipore) as a concentration standard.

RhoA activation assay. COS-7 cells were cultured in DMEM supplemented with 10% FBS. The cells were then serum starved overnight, and then the medium was removed and replaced with serum-free medium containing CS-E polysaccharides or CSPGs (10 μg/ml). After 10 min, the cells were lysed, and RhoA activation was determined using the G-LISA kit (Cytoskeleton).

Immunostaining of retinal and optic nerve sections. At 14 days post-injury, mice were given an overdose of pentobarbital and were transcardially perfused with 4% PFA. Eyeballs still attached with the optic nerve were dissected and post-fixed in 4% PFA overnight. Following cryoprotection with 30% sucrose in PBS, tissues were embedded in O.C.T. and serial sectioned for 10 μm along the longitudinal direction of the nerve. For immunofluorescence labeling, the sections were washed with PBS, pre-incubated in a blocking buffer (1% BSA, 0.3% TX-100 in PBS) and followed by sequential incubations with primary antibodies, including mouse anti-CS-E (1:200), goat-anti-CTB (1:4,000), or rabbit anti-βIII-tubulin antibodies (Invitrogen). The sections were then reacted with biotinylated anti-goat IgG (1:200) and visualized with Alexa Fluor 546-conjugated

streptavidin (1:400) or with a Cy3-conjugated goat anti-mouse or -rabbit IgG. The retinal cryosections were mounted with Vectashield and visualized under a Nikon fluorescence microscope. To quantify the number of CTB-positive regenerating axons, the number of regenerating axons was counted at 125 μm stepwise from the crush site of the optic nerve. To quantify the number of surviving retinal ganglion cells, the total number of βIII-tubulin positive cells was counted in at least 3 retinal sections per retina.

Optic nerve regeneration assay. Immediately after crush injury in the optic nerve of adult mice, gelfoam soaked in a solution containing control IgG, CS-E antibody (1.7 mg/ml), chondroitinase ABC (ChABC; 50 U/ml), or ChABC (50 U/ml) plus CS-E antibody (1.7 mg/ml) was placed around the crush site of the nerve and replaced after three days. To analyze whether CS-E contributes primarily to the growth inhibition associated with CSPGs and acts extrinsic to neurons to block nerve regeneration, we also compared the effects of the CS-E antibody on optic nerve regeneration *in vivo* with that of CPT-cAMP, which is reported to stimulate the intrinsic growth status of retinal ganglion cell axons. Thus, in other groups of mice, mice that received an intravitreal injection of CPT-cAMP (100 mM, 2 μl) alone or CPT-cAMP plus CS-E antibody (1.7 mg/ml) treatment placed around the crush site of the nerve were studied. To label retinal ganglion cell axons, 2 μl of a solution containing an anterograde axon tracer, CTB, was injected intravitreally 3 days before mice were sacrificed. The extent of axonal regrowth was assessed 2 weeks after injury.

References

1. Yiu, G. & He, Z. Glial inhibition of CNS axon regeneration. *Nat. Rev. Neurosci.* **2006,** 7, (8), 617-627.

2. Busch, S. A. & Silver, J. The role of extracellular matrix in CNS regeneration. *Curr. Opin. Neurobiol.* **2007,** 17, (1), 120-127.

3. Carulli, D., Laabs, T., Geller, H. M. & Fawcett, J. W. Chondroitin sulfate proteoglycans in neural development and regeneration. *Curr. Opin. Neurobiol.* **2005,** 15, (1), 116-120.

4. Pizzorusso, T*., et al.* Structural and functional recovery from early monocular deprivation in adult rats. *Proc. Natl. Acad. Sci. U S A* **2006,** 103, (22), 8517-8522.

5. Cafferty, W. B*., et al.* Chondroitinase ABC-mediated plasticity of spinal sensory function. *J. Neurosci.* **2008,** 28, (46), 11998-12009.

6. Houle, J. D*., et al.* Combining an autologous peripheral nervous system "bridge" and matrix modification by chondroitinase allows robust, functional regeneration beyond a hemisection lesion of the adult rat spinal cord. *J. Neurosci.* **2006,** 26, (28), 7405-7415.

7. Bradbury, E. J*., et al.* Chondroitinase ABC promotes functional recovery after spinal cord injury. *Nature* **2002,** 416, (6881), 636-640.

8. Gilbert, R. J*., et al.* CS-4,6 is differentially upregulated in glial scar and is a potent inhibitor of neurite extension. *Mol. Cell. Neurosci.* **2005,** 29, (4), 545-558.

9. Wang, H*., et al.* Chondroitin-4-sulfation negatively regulates axonal guidance and growth. *J. Cell Sci.* **2008,** 121, (Pt 18), 3083-3091.

10. Properzi, F*., et al.* Chondroitin 6-sulphate synthesis is up-regulated in injured CNS, induced by injury-related cytokines and enhanced in axon-growth inhibitory glia. *Eur. J. Neurosci.* **2005,** 21, (2), 378-390.

11. Kitagawa, H., Tsutsumi, K., Tone, Y. & Sugahara, K. Developmental regulation of the sulfation profile of chondroitin sulfate chains in the chicken embryo brain. *J. Biol. Chem.* **1997,** 272, (50), 31377-31381.

12. Kusche-Gullberg, M. & Kjellen, L. Sulfotransferases in glycosaminoglycan biosynthesis. *Curr. Opin. Struct. Biol.* **2003,** 13, (5), 605-611.

13.   Lin, R., Rosahl, T. W., Whiting, P. J., Fawcett, J. W. & Kwok, J. C. F. 6-Sulphated Chondroitins Have a Positive Influence on Axonal Regeneration. *Plos One* **2011,** 6, (7).

14.   Olson, L. Medicine: clearing a path for nerve growth. *Nature* **2002,** 416, (6881), 589-590.

15.   Mckeon, R. J., Hoke, A. & Silver, J. Injury-Induced Proteoglycans Inhibit the Potential for Laminin-Mediated Axon Growth on Astrocytic Scars. *Exp. Neurol.* **1995,** 136, (1), 32-43.

16.   Sivasankaran, R.*, et al.* PKC mediates inhibitory effects of myelin and chondroitin sulfate proteoglycans on axonal regeneration. *Nat. Neurosci.* **2004,** 7, (3), 261-268.

17.   Kaneko, M., Kubo, T., Hata, K., Yamaguchi, A. & Yamashita, T. Repulsion of cerebellar granule neurons by chondroitin sulfate proteoglycans is mediated by MAPK pathway. *Neurosci. Lett.* **2007,** 423, (1), 62-67.

18.   Tom, V. J., Steinmetz, M. P., Miller, J. H., Doller, C. M. & Silver, J. Studies on the development and behavior of the dystrophic growth cone, the hallmark of regeneration failure, in an in vitro model of the glial scar and after spinal cord injury. *J. Neurosci.* **2004,** 24, (29), 6531-6539.

19.   Walenga, J. M.*, et al.* The inhibition of the generation of thrombin and the antithrombotic effect of a pentasaccharide with sole anti-factor Xa activity. *Thromb. Res.* **1988,** 51, (1), 23-33.

20.   Bishop, J. R., Schuksz, M. & Esko, J. D. Heparan sulphate proteoglycans fine-tune mammalian physiology. *Nature* **2007,** 446, (7139), 1030-1037.

21.   Rawat, M., Gama, C. I., Matson, J. B. & Hsieh-Wilson, L. C. Neuroactive chondroitin sulfate glycomimetics. *J. Am. Chem. Soc.* **2008,** 130, (10), 2959-2961.

22.   Gama, C. I.*, et al.* Sulfation patterns of glycosaminoglycans encode molecular recognition and activity. *Nat. Chem. Biol.* **2006,** 2, (9), 467-473.

23.   Ohtake-Niimi, S.*, et al.* Mice deficient in N-acetylgalactosamine 4-sulfate 6-o-sulfotransferase are unable to synthesize chondroitin/dermatan sulfate containing N-acetylgalactosamine 4,6-bissulfate residues and exhibit decreased protease activity in bone marrow-derived mast cells. *J. Biol. Chem.* **2010,** 285, (27), 20793-20805.

24.   Monnier, P. P., Sierra, A., Schwab, J. M., Henke-Fahle, S. & Mueller, B. K. The Rho/ROCK pathway mediates neurite growth-inhibitory activity associated with the chondroitin sulfate proteoglycans of the CNS glial scar. *Mol. Cell. Neurosci.* **2003,** 22, (3), 319-330.

25.   Aricescu, A. R., McKinnell, I. W., Halfter, W. & Stoker, A. W. Heparan sulfate proteoglycans are ligands for receptor protein tyrosine phosphatase sigma. *Mol. Cell. Biol.* **2002,** 22, (6), 1881-1892.

26.   Sapieha, P. S*., et al.* Receptor protein tyrosine phosphatase sigma inhibits axon regrowth in the adult injured CNS. *Mol. Cell. Neurosci.* **2005,** 28, (4), 625-635.

27.   Thompson, K. M*., et al.* Receptor protein tyrosine phosphatase sigma inhibits axonal regeneration and the rate of axon extension. *Mol. Cell. Neurosci.* **2003,** 23, (4), 681-692.

28.   McLean, J., Batt, J., Doering, L. C., Rotin, D. & Bain, J. R. Enhanced rate of nerve regeneration and directional errors after sciatic nerve injury in receptor protein tyrosine phosphatase sigma knock-out mice. *J. Neurosci.* **2002,** 22, (13), 5481-5491.

29.   Rogers, C. J*., et al.* Elucidating glycosaminoglycan-protein-protein interactions using carbohydrate microarray and computational approaches. *Proc. Natl. Acad. Sci. U S A* **2011,** 108, (24), 9747-9752.

30.   Fisher, D*., et al.* Leukocyte Common Antigen-Related Phosphatase Is a Functional Receptor for Chondroitin Sulfate Proteoglycan Axon Growth Inhibitors. *J. Neurosci.* **2011,** 31, (40), 14051-14066.

31.   Tully, S. E., Rawat, M. & Hsieh-Wilson, L. C. Discovery of a TNF-alpha antagonist using chondroitin sulfate microarrays. *J. Am. Chem. Soc.* **2006,** 128, (24), 7740-7741.

32.   Clement, A. M*., et al.* The DSD-1 carbohydrate epitope depends on sulfation, correlates with chondroitin sulfate D motifs, and is sufficient to promote neurite outgrowth. *J. Biol. Chem.* **1998,** 273, (43), 28444-28453.

33.   Pothacharoen, P*., et al.* Two related but distinct chondroitin sulfate mimetope octasaccharide sequences recognized by monoclonal antibody WF6. *J. Biol. Chem.* **2007,** 282, (48), 35232-35246.

34.   Park, K. K*., et al.* Promoting axon regeneration in the adult CNS by modulation of the PTEN/mTOR pathway. *Science* **2008,** 322, (5903), 963-966.

35.   Selles-Navarro, I., Ellezam, B., Fajardo, R., Latour, M. & McKerracher, L. Retinal ganglion cell and nonneuronal cell responses to a microcrush lesion of adult rat optic nerve. *Exp. Neurol.* **2001,** 167, (2), 282-289.

36.   Goldberg, J. L., Klassen, M. P., Hua, Y. & Barres, B. A. Amacrine-signaled loss of intrinsic axon growth ability by retinal ganglion cells. *Science* **2002,** 296, (5574), 1860-1864.

37.   Schwab, M. E. & Bartholdi, D. Degeneration and regeneration of axons in the lesioned spinal cord. *Physiol. Rev.* **1996,** 76, (2), 319-370.

38.   Cui, Q., Yip, H. K., Zhao, R. C., So, K. F. & Harvey, A. R. Intraocular elevation of cyclic AMP potentiates ciliary neurotrophic factor-induced regeneration of adult rat retinal ganglion cell axons. *Mol. Cell. Neurosci.* **2003,** 22, (1), 49-61.

39.   Geremia, N. M*., et al.* CD11d Antibody Treatment Improves Recovery in Spinal Cord-Injured Mice. *J. Neurotrauma* **2011**.

40.   Liebscher, T.*, et al.* Nogo-A antibody improves regeneration and locomotion of spinal cord-injured rats. *Ann. Neurol.* **2005,** 58, (5), 706-719.

41.   Yu, Y. J.*, et al.* Boosting brain uptake of a therapeutic antibody by reducing its affinity for a transcytosis target. *Sci. Transl. Med.* **2011,** 3, (84), 84ra44.

42.   Atwal, J. K.*, et al.* A therapeutic antibody targeting BACE1 inhibits amyloid-beta production in vivo. *Sci. Transl. Med.* **2011,** 3, (84), 84ra43.

43.   Yamauchi, S.*, et al.* Molecular cloning and expression of chondroitin 4-sulfotransferase. *J. Biol. Chem.* **2000,** 275, (12), 8975-8981.

44.   Ohtake, S., Ito, Y., Fukuta, M. & Habuchi, O. Human N-acetylgalactosamine 4-sulfate 6-O-sulfotransferase cDNA is related to human B cell recombination activating gene-associated gene. *J. Biol. Chem.* **2001,** 276, (47), 43894-43900.

45.   Taylor, K. A. & Buchanan-Smith, J. G. A colorimetric method for the quantitation of uronic acids and a specific assay for galacturonic acid. *Anal. Biochem.* **1992,** 201, (1), 190-196.

46.   Elchebly, M.*, et al.* Neuroendocrine dysplasia in mice lacking protein tyrosine phosphatase sigma. *Nat. Genet.* **1999,** 21, (3), 330-333.

47.   Gama, C. I.*, et al.* Sulfation patterns of glycosaminoglycans encode molecular recognition and activity. *Nat. Chem. Biol.* **2006,** 2, 467-473.

48.   Clark, P. M.*, et al.* Direct in-gel fluorescence detection and cellular imaging of O-GlcNAc-modified proteins. *J. Am. Chem. Soc.* **2008,** 130, 11576-11577.

Chapter 4: EphA4 is a Receptor for the Sulfated Carbohydrate Epitope CS-E*

Introduction

The Eph receptors (named after their identification in an **e**rythropoietin-**p**roducing human **h**epatocellular carcinoma cell line[1]) make up a large family of protein-tyrosine kinases. These receptors are involved in many different physiological properties, including cell patterning,[2, 3] guidance,[4, 5] attraction,[6, 7] and repulsion.[8-10] This first member of this family was identified over 25 years ago, and is now known as EphA1.[11] In the following years, multiple ligands for the Eph receptors (termed **Eph r**eceptor **in**teracting ligands, or ephrins; also referred to as Efns) were discovered.[12-14]

Soon after discovery of the first Eph receptor, a role of these proteins in cancer was established,[15] and this function has been extensively characterized since then. Both the ligands and receptors are often present in cancer cells, and changes in their expression levels have been linked with cancer progression.[16] The receptors and ligands are normally bound to the cell membrane, and signals can be transmitted to the cell expressing the Eph receptor or the ephrin ligand ("forward" signaling and "reverse" signaling, respectively[5, 17-19]). These interactions typically occur at a point where cells are in contact, with the ligand and the receptor expressed on opposing cells, i.e. *trans* interactions; however, some soluble

---

ephrins have been shown to retain their ability to activate their receptors,[20, 21] and ephrins and Eph receptors on the same cell surface can participate in *cis* interactions, sending a downstream signal in the cell expressing the ligand and the receptor.[22, 23]

The Eph receptors are grouped into two categories, based on sequence similarity: the EphA and EphB receptors, each with corresponding ligands that generally only interact with members of one of the receptor groups. In the human genome, there are nine EphA receptors with five ephrin-A ligands, and five EphB receptors with three ephrin-B ligands. The binding between the receptors and the ligands is promiscuous; in addition, there is some crossover of binding, in which ephrin-A ligands interact with EphB receptors, and ephrin-B ligands with EphA receptors.[16, 24-26] The ephrin-A ligands are
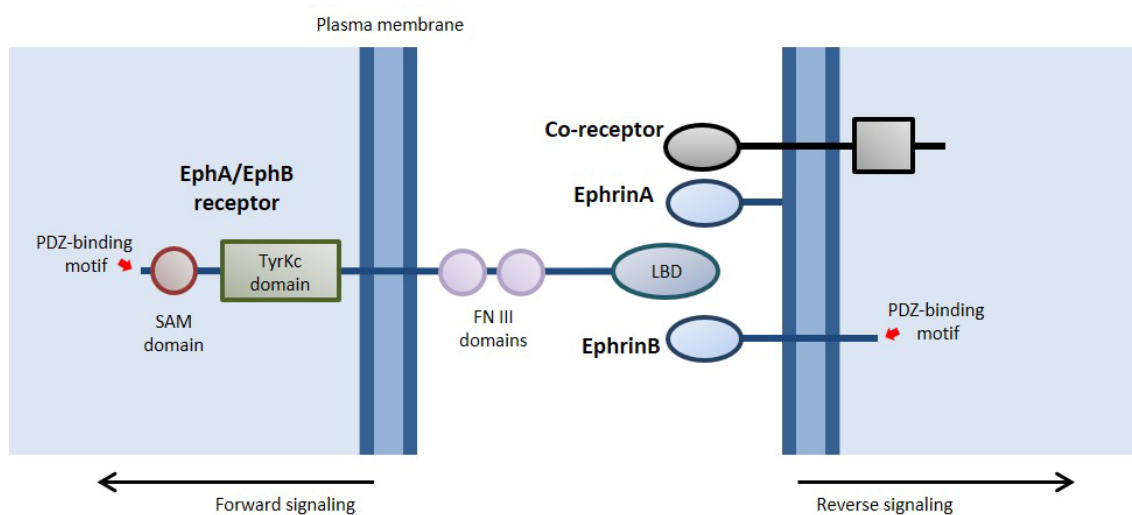

Figure 4.1. The Eph receptors and ephrin ligands. LBD: Ligand-binding domain; FN: Fibronectin; SAM: sterile alpha motif; TyrKc: Tyrosine kinase, catalytic; PDZ: PSD95/Dlg/ZO1.

linked to the cell surface via a glycosylphosphatidylinositol (GPI) linkage, while the ephrin-B ligands contain transmembrane and cytoplasmic regions (Figure 4.1). When Eph receptors are engaged by their ligands, autophosphorylation occurs on two tyrosine residues that are conserved among the EphA and EphB receptors – Y596 and Y602 in EphA4, and Y604 and Y610 in EphB2.[27, 28]

EphA and EphB receptors, as well as the ephrin-B ligands, have cytoplasmic domains that can initiate internal signaling cascades.[29, 30] Since ephrin-A ligands do not have cytoplasmic domains, they are dependent upon other membrane proteins that can serve as co-receptors for reverse signaling.[31-34] One such co-receptor is the p75 neurotrophin receptor, which was shown to be critical for reverse signaling of ephrin-A3 in the retina, forming a complex with ephrin-A3 that is necessary for the repulsive effect involved in axon guidance.[35] The p75 receptor is also involved in controlling dendrite and spine formation and function in hippocampal neurons,[36] a biological process that is dependent upon Eph-ephrin signaling.[37] This apparent convergence in function, as well as the p75 receptors' previously established role in inhibition of neurite outgrowth, [38] makes this receptor an intriguing candidate for further study in the context of ephrin signaling.

The Eph receptors and their ligands play a major role in the formation of the nervous system during development. Interactions between the ligands and receptors are frequently repulsive, such that cells containing a given Eph receptor are repelled by cells containing the ephrin ligand. These repulsive cues are involved in the regulation of axon guidance,[4, 5] axon fasciculation or bundling,[39, 40] formation of topgraphic maps,[41, 42] and vascularization of the developing nervous system.[43, 44] Ephs and ephrins are expressed in almost all embryonic tissues,[8, 24, 45] highlighting the importance of this group of proteins.

The Ephs and ephrins are also involved in the maintenance of the nervous system in the mature organism, and a role for these proteins has also been established in the prevention of regeneration of growth after injury in the nervous system. Members of the Eph receptor family, as well as the ephrin ligands, have been shown to be upregulated after injury to the adult nervous system.[46-48] Ephrin-A ligands and EphA receptors have been show to induce growth cone collapse via the activation of Rho and Rho kinase, members of a common signaling pathway that is involved in the inhibition of neurite outgrowth.[49, 50] One of the ephrin-B ligands, EphB3, has also been identified as a molecule inhibitory to recovery in the CNS after injury.[51]

Of particular interest to our group is the receptor EphA4, which has been shown to have a role in preventing recovery after spinal cord injury.[52] A recent study has shown that blocking activity of the EphA4 receptor after spinal cord injury allows axonal regrowth and recovery of function.[53] Our lab is interested in studying interactions between charged carbohydrates and the Eph receptors or ligands, which could potentially cause direct activation of receptors, or mediate the interaction between ligands and receptors. Heparan sulfate has previously been shown to modulate the interaction between Eph receptors and ephrin ligands,[54] supporting the possibility of other charged carbohydrates in mediating Eph/ephrin interactions.

In recent years, several receptors for chondroitin sulfate proteoglycans (CSPGs) have been discovered,[55-57] and our lab has identified CS-E as the crucial motif on CS chains that is likely to engage protein receptors.[58] Therefore, our lab has focused on targeting the Eph receptors and their ligands as potential receptors for the CS-E motif.

Results

EphA4 and Ephrin ligands interact with CS-E. As a general method for identifying novel CS receptors, our lab has used affinity chromatography and mass spectrometry to find CS-E-interacting proteins in tissues of the nervous system. To do this, we first generated affinity columns by immobilizing biotinylated CS-E-enriched or unsulfated CS polysaccharides on streptavidin-coated agarose beads. The membrane protein-enriched fraction of rat brain lysate was passed over the affinity columns, and bound proteins were identified by high-throughput mass spectrometry (LC-MS/MS) analysis. From this analysis, EphA4 was identified as a CS-E-interacting protein. Three unique peptides (34 amino acids, 3% total amino acid coverage) were identified in the pull-down, confirming the identity of EphA4 (Figure 4.2).

355 G G R **Q D I S Y N V V C K** K C G A G

728 A A R **N I L V N S N L V C K** V S D F

767 M S R **V L E D D P E A A Y T T R** G G

Tax_Id=10116 Gene_Symbol=RGD1560587_predicted similar to Eph receptor A4
3 unique peptides, 3 unique spectra, 3 total spectra, 34/986 amino acids (3% coverage)

Figure 4.2. EphA4 peptides identified by LC-MS/MS analysis. EphA4 from rat brain lysates was pulled down using CS-E and resolved by SDS-PAGE. In-gel tryptic digestion and LC-MS/MS analysis revealed three unique peptides within EphA4.

A commercially available set of EphA Fc chimera proteins containing EphA1, EphA2, EphA3, EphA4, EphA5, EphA6, EphA7, and EphA8 was purchased, and these proteins were tested on the carbohydrate microarray to screen for binding to CS motifs (Figure 4.3). These results showed that the receptors EphA1, EphA4, and EphA6 show an appreciable amount of binding to the CS-E motif, with the strongest binding seen with
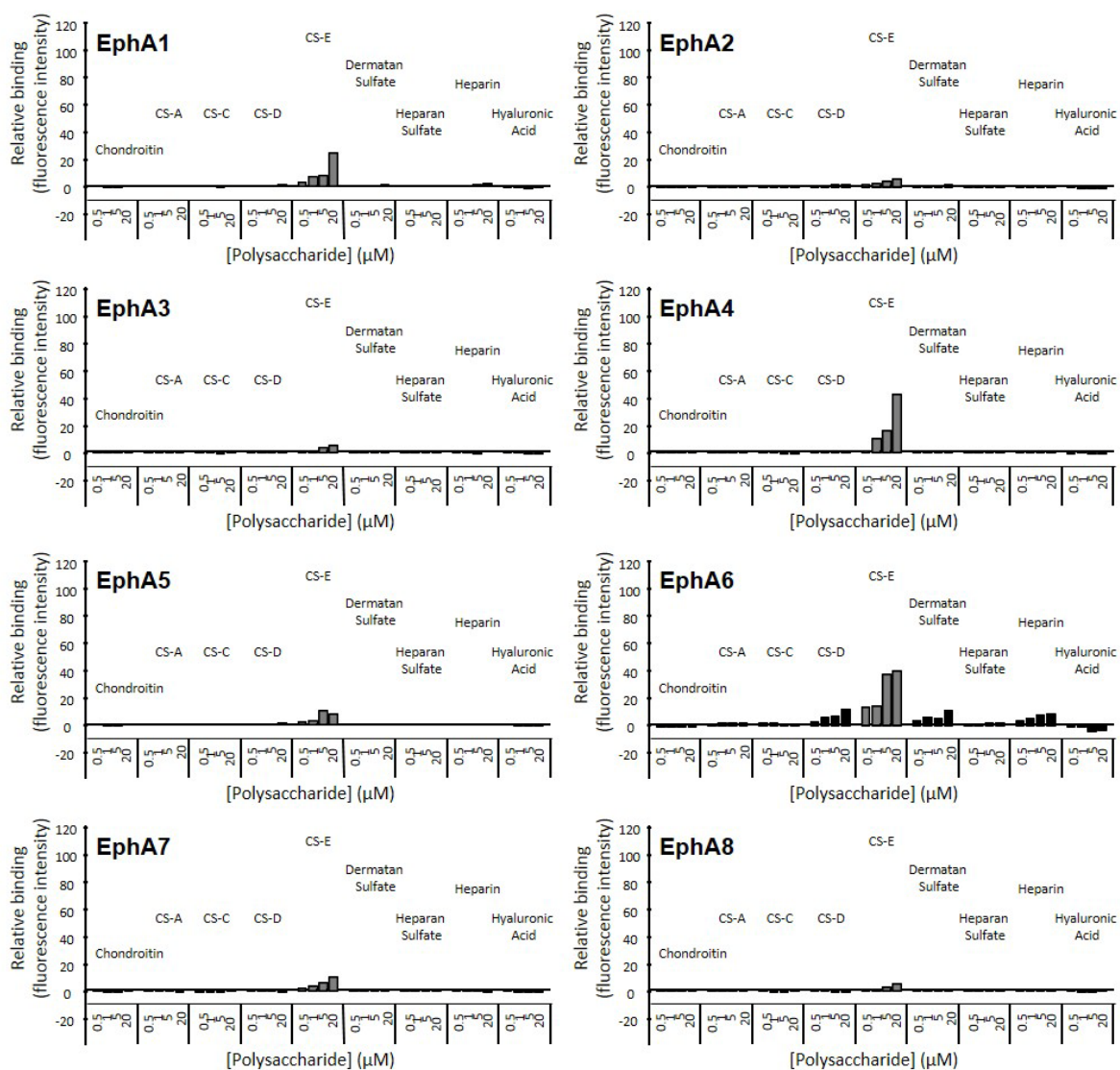
Figure 4.3. EphA1, EphA4, and EphA6 bind to CS-E on the array. Experiments were repeated in triplicate. Representative results are shown.
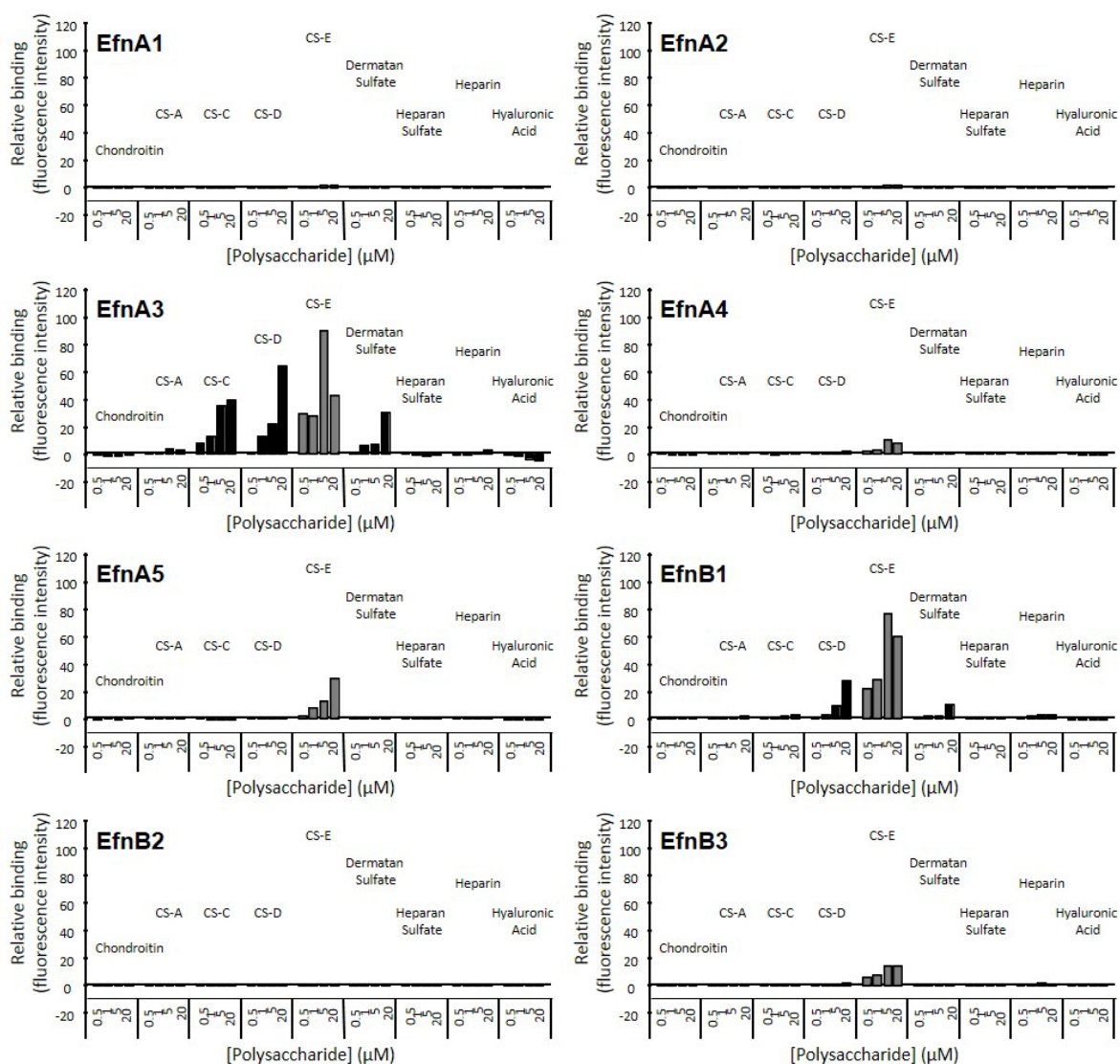
Figure 4.4. EphrinA3, EphrinA5, and EphrinB1 bind to CS-E on the array. Experiments were repeated in triplicate. Representative results are shown.

EphA4 and EphA6. A kit containing the soluble portions of the ephrin-A ligands EfnA1, EfnA2, EfnA3, EfnA4, and EfnA5, as well as the ephrin-B ligands EfnB1, EfnB2, and EfnB3 was also screened (Figure 4.4). These results showed that the ligands ephrin-A3 and ephrin-B1 have an appreciable amount of binding to the CS-E motif, with a smaller amount of binding observed with ephrin-A5. Additional testing of the EphA4 protein showed that the protein binds to both CS-E and a mixed CS preparation containing CS-A, -C, -D, and – E motifs (Figure 4.5). A small degree of possible binding to heparin and heparan sulfate was also observed.
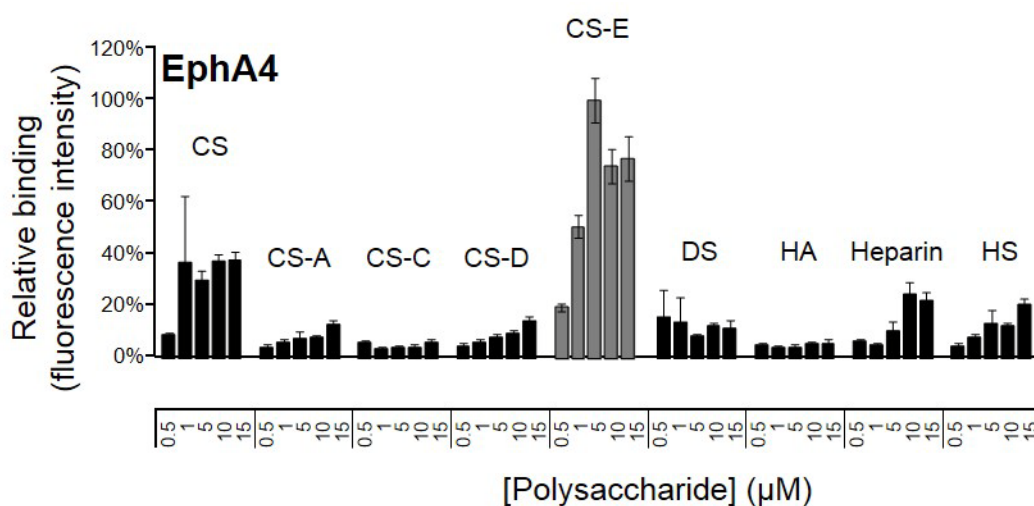
Figure 4.5. EphA4 is specific to CS-E on the microarray. The experiment was repeated three times; combined results are shown. Error bars = standard error of the mean for 10 array spots per experiment, for three experiments.
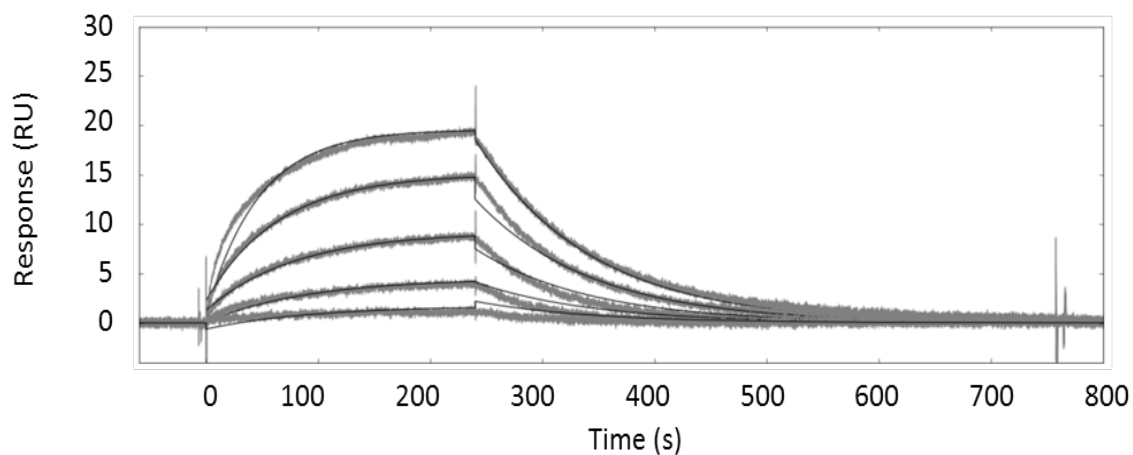
Figure 4.6. Sensorgram of the interaction of EphA4 with CS-E polysaccharide. EphA4 had a dissociation constant of 856 nM.
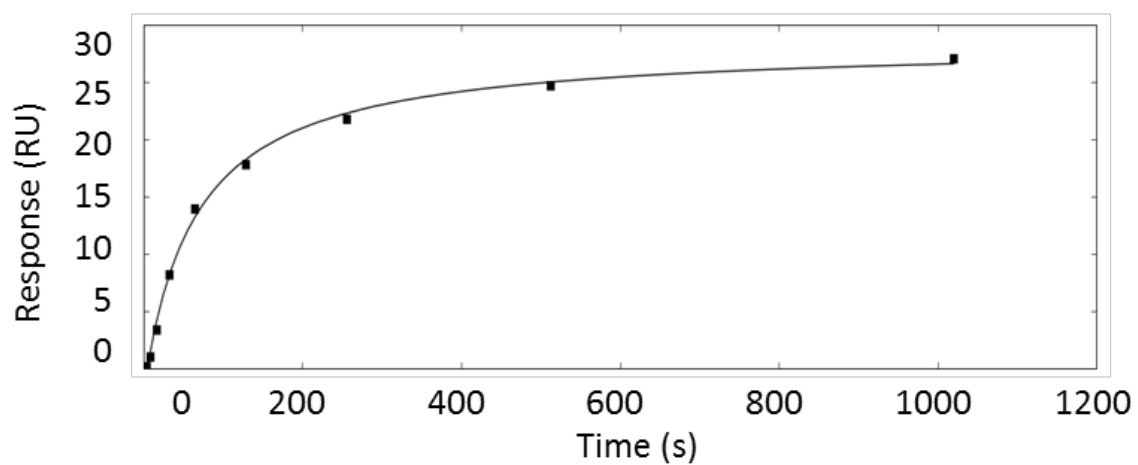
Figure 4.7. Affinity analysis of the ephrin-A3/CS-E polysaccharide interaction gives an apparent K_D of 65 nM.

After screening by microarray, the kinetics of binding between EphA4 and CS-E was analyzed by surface plasmon resonance (SPR). EphA4 interacted with CS-E according to a one-to-one binding model, with a calculated K_D of 856 nM (Figure 4.6). Out of the EfnA lignads screened by microarray, EfnA3 appeared to bind to CS-E particularly strongly. After performing the SPR analysis, it was found that the interaction between EfnA3 and CS-E could not be described using the one-to-one binding model. To obtain an overall K_D for the interaction, an affinity analysis was performed. EfnA3 was found to bind to CS-E with an apparent K_D of 65 nM (Figure 4.7).

Next, expression vectors were constructed containing the entire sequence of promising genes of interest: the ligands EfnA3 and EfnB1, and the receptor EphA4. These vectors were transfected into cells to express the proteins on the cell surface, and the cells were lysed to isolate the expressed proteins. These proteins were then incubated with CS that had been biotinylated and conjugated to streptavidin beads. We found that these full-length constructs were co-precipitated with CS-E, but not other CS motifs (Figure 4.8). The receptor EphA4 was co-precipitated only with the CS-E motif, with no observable protein capture with the other motifs. The ligands EfnA3 and EfnB1 were also shown to mainly interact with the CS-E motif, with minimal interaction with other motifs. However, there is some amount of co-precipitation with other CS motifs, suggesting that there may be a small amount of non-specific CS binding, which was also seen in the microarray results. In experiments that involved co-expressing the proteins, we found that the receptor EphA4 and the ligand EfnA3 were both co-precipitated by CS-E, allowing the possibility of simultaneous ligand-receptor and CS-E interaction.
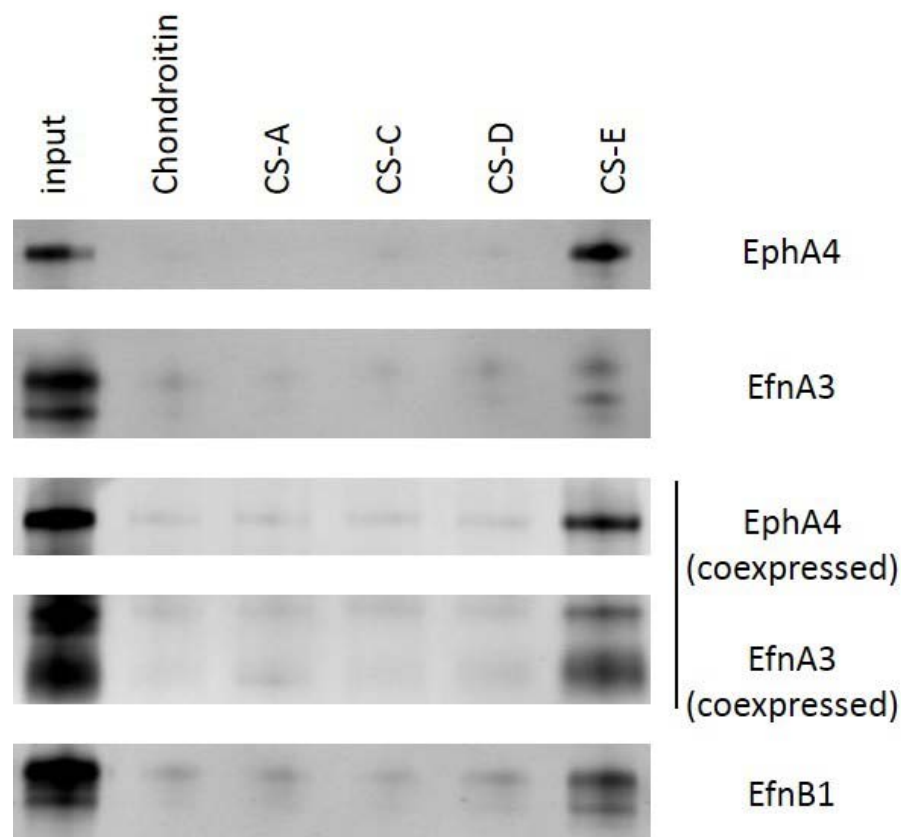
Figure 4.8. EphrinA3, EphrinB1, and EphA4 are pulled down specifically by CS-E.

EphA4 is activated in response to CS-E. Next, we sought to determine if activation of the EphA4 receptor could be observed in response to CS-E. Engagement with ephrin-A ligands causes autophosphorylation of Eph receptors on tyrosine residues, which is the first step leading to activation of downstream signaling pathways.[19, 26] Since CS-E binds to EphA4, and likely has multiple protein binding sites on each molecule, we hypothesized that the addition of CS-E to EphA4-expressing cells could induce the oligomerization and subsequent phosphorylation of EphA4. To test this hypothesis, EphA4 was overexpressed in cells, and CS-E was added to the culturing medium for various amounts of time.

Afterwards, the cells were lysed, EphA4 was immunoprecipitated, and the enriched EphA4 protein was assayed for phosphorylation via western blot. We found that CS-E was capable of inducing EphA4 phosphorylation (Figure 4.9). The phosphorylation of EphA4 in response to CS-E was found to occur in a time-dependent manner, with maximal effects observed 15 min after application of CS-E. These levels reduced to control levels after 30 min.
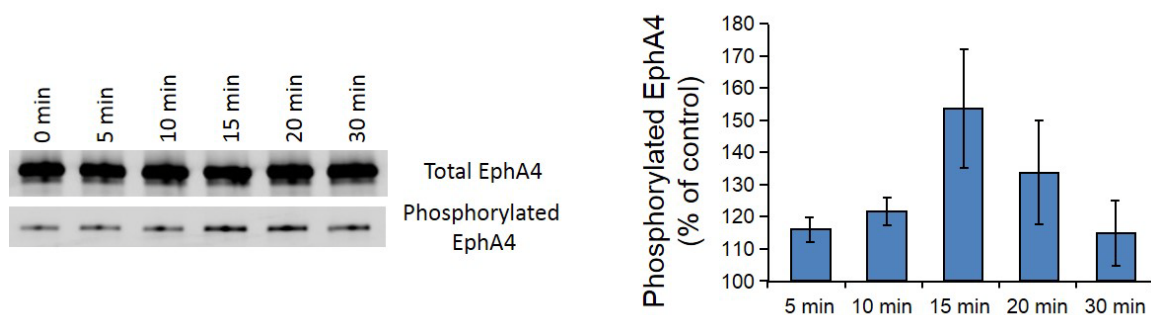
Figure 4.9. Overexpressed EphA4 is phosphorylated in response to CS-E treatment.

Abolishment of CS-E expression reduces activity of EphA4 *in vivo*. In order to further determine the effect of CS-E on the EphA4 receptor, we analyzed the endogenous phosphorylation of EphA4 in mice deficient in CS-E.[59] Adult CS-E KO mice or wild-type controls were euthanized, and their hippocampi were extracted and homogenized. This homogenate was incubated with EphA4 antibody to enrich the protein, and phosphorylation of EphA4 was analyzed via western blot. Our results indicated that basal phosphorylation of EphA4 was significantly reduced in the CS-E KO animals, supporting the physiological role of CS-E in EphA4 activation (Figure 4.10).
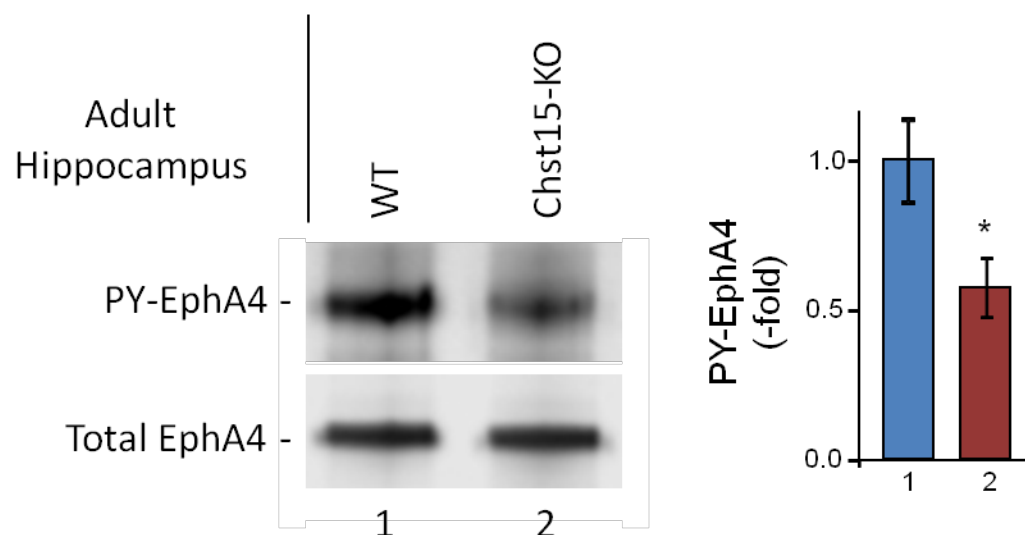
Figure 4.10. **Effect of the absence of the CS-E motif on EphA4 phosphorylation *in vivo*. Phosphorylation of endogenous EphA4 in the hippocampus is compared between Chst15 KO (lane 2) and control mice (lane 1). Bar graphs represent fold-changes in the intensity of immunoreactive bands. Error bars represent standard error of the mean of the relative intensity from six control and six knockout mice. *, P < 0.01.**

CGN Neurite Outgrowth is mediated by Eph receptors. Since EphA4 is expressed in many regions of the nervous system during different stages of development,[60] we targeted several different cell types that could serve as a model for CS-E inhibition in the nervous system to be analyzed for involvement of the EphA4 receptor. Using reverse transcriptase PCR (RT-PCR) we sought to determine the relative mRNA levels present in postnatal cerebellar granule neurons (CGNs), a commonly used neuron type for neurite outgrowth experiments, that we previously found to be inhibited in response to CS-E.[58] Using this

method, we determined that the ligands EfnA1, EfnA3, EfnA5, and EfnB1, and the receptor EphA4, were all likely to be expressed based on the presence of their respective mRNA (Figure 4.11).
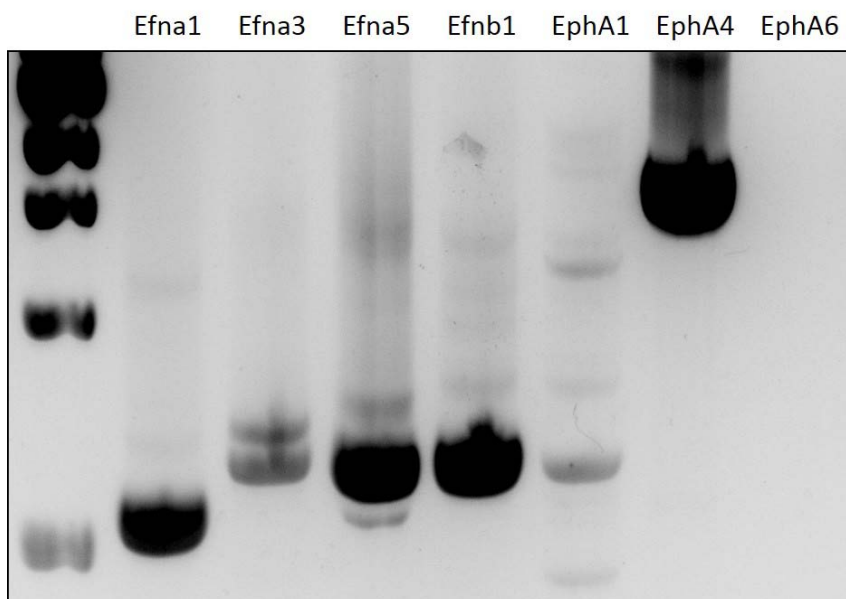
Figure 4.11. RT-PCR showing the presence of Efn and Ephs in the postnatal cerebellum.

After determining the likely expression of Ephs and ephrins in CGNs, we next measured CGN neurite outgrowth in response to CS-E, in the presence of dasatinib (BMS-354825), a tyrosine kinase inhibitor that has been shown to inhibit Ephs.[16, 61] We found that neurite outgrowth inhibition by CS-E and CSPG in CGNs was rescued when cells were cultured with dasatinib added to the medium (Figure 4.12). At 20 nM, dasatinib appeared to completely abolish the inhibitory effect of CS-E. The control growth of neurites was reduced upon the addition of higher concentrations of dasatinib, however, suggesting that

this compound may be somewhat toxic to cells. Furthermore, this molecule is not specific

to EphA4, allowing for multiple tyrosine kinase receptors being involved in mediating the

inhibitory signal of CS-E in this cell type.
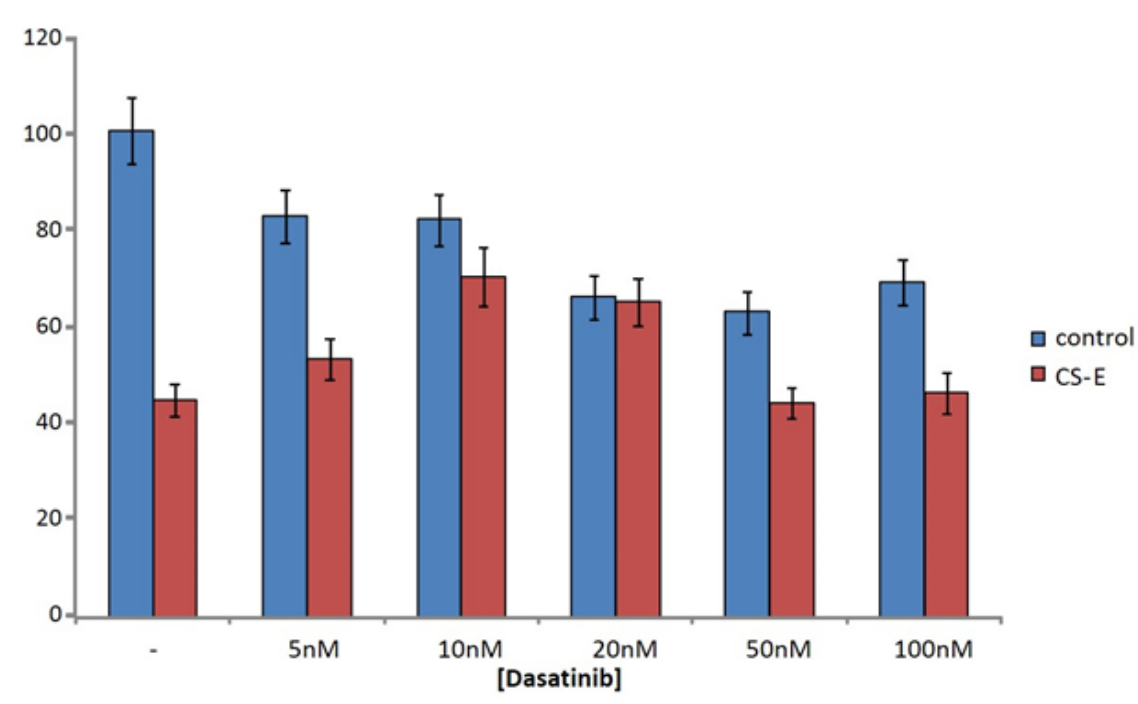
Figure 4.12. Inhibition of CGN neurite outgrowth by CS-E is attenuated by dasatinib.
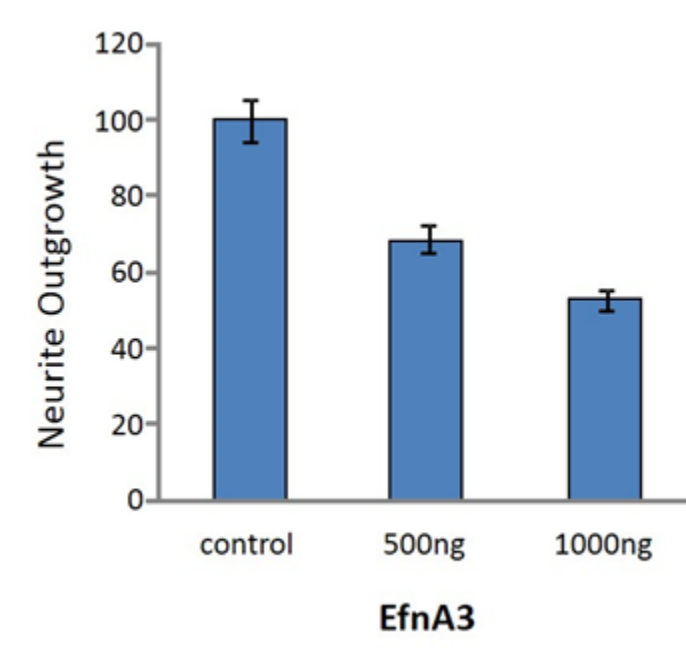
Figure 4.13. CGN neurite outgrowth is inhibited by EfnA3.

We also investigated the effect of the ephrin ligands on neurite outgrowth of CGNs. The ligand EfnA3 was coated in the wells of a plastic culture dish, upon which CGNs were cultured for 24 h. We found that EfnA3 inhibits the neurite outgrowth of CGNs in a concentration-dependent manner (Figure 4.13). Similar experiments were performed with EfnA5, and this ligand was found to be a potent inhibitor of CGN outgrowth (Figure 4.14). This inhibition was partially overcome upon the addition of KYL, a 12-amino acid peptide identified via phage display that binds preferentially to EphA4 compared to other EphA receptors, and blocks ephrin binding to the receptor.[62, 63]
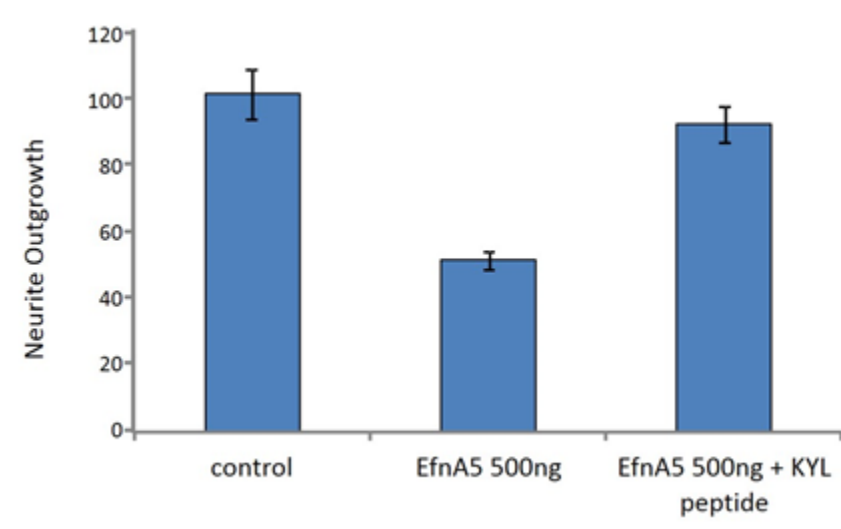
Figure 4.14. CGN neurite outgrowth is inhibited by EfnA5, and is reduced with the addition of KYL peptide.

We next wanted to see if neurite outgrowth inhibition caused by CS-E and CSPG was reduced in cells lacking the EphA4 receptor. CGNs from EphA4 KO mice[64] or wild type controls were cultured on a substrate of coated CS-E or CSPG. We observed only a small degree of possible rescue in the case of CSPG coating, but not with CS-E, suggesting other receptors/mechanisms for the inhibition in this cell type (Figure 4.15). Since there was only a negligible effect, we reasoned that other receptors expressed in these neurons are responsible for mediating the inhibitory effects of CS-E and CSPG.
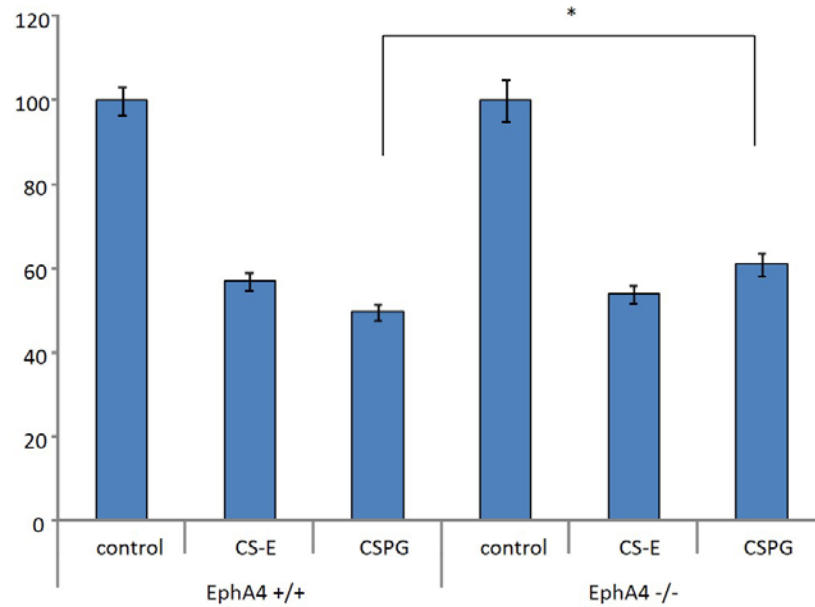
Figure 4.15. CGN neurite outgrowth inhibition by CSPG is slightly attenuated in EphA4 KO neurons, but no difference in CS-E inhibition is observed. *: P<0.005.

Functions of EphA4 and EfnA3 in the developing cortex. We next tested the response of cortical neurons, which have high levels of expression of EphA4.[60] It was also previously shown that the interaction between ephrinA3 and EpA4 in these neurons is dependent on heperan sulfate, and this interaction leads to an inhibitory effect.[54] We found that cortical neurons were highly inhibited by CS-E and CSPG (Figure 4.16), making these cells an attractive target for the investigation of the effects of EphA4 and CS-E interaction on neuron growth.
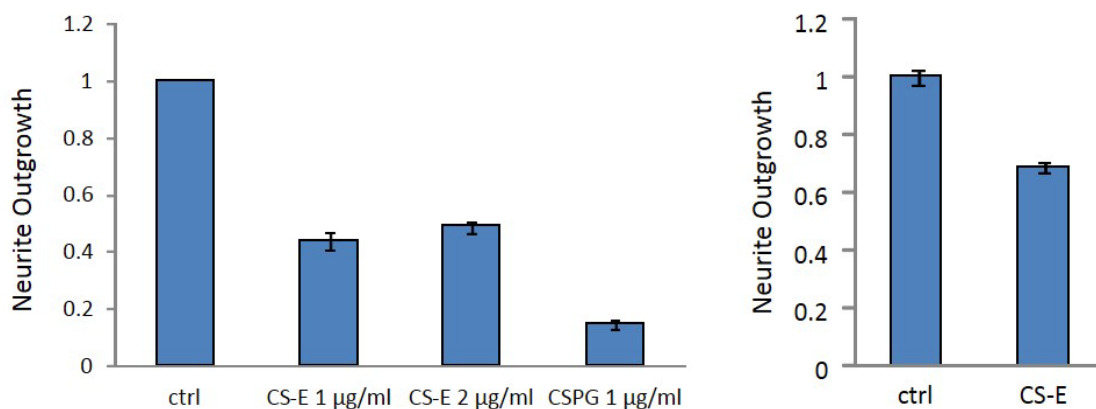
Figure 4.16. Cortical neurite outgrowth is inhibited by CS-E and CSPG coated on the culture surface (left), and by CS-E linked to agarose beads (right).

We next tested the phosphorylation of EphA4 in these neurons in response to CS-E. These neurons have a very high level of EphA4 expression that is comparable to the overexpressed EphA4 described previously, making this measurement feasible in this cell type. As with the overexpressed EphA4, the endogenous EphA4 in cortical neurons was phosphorylated in response to CS-E treatment in a time-dependent manner (Figure 4.17).
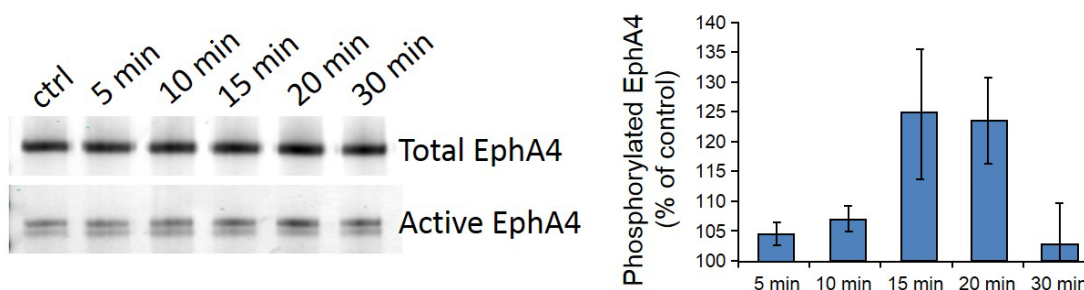
Figure 4.17. Endogenous cortical EphA4 is phosphorylated in response to CS-E treatment.

Next, we tested the effects of Efn ligands in neurons deficient in CS-E.[59] We reasoned that if CS-E was involved in mediating the interaction of EphA4 and its ligands, we should observe less phosphorylation of EphA4 upon addition of ligand in the absence of endogenous CS-E. We found that in wild-type neurons, the Efn ligands EfnA2, EfnA3, and EfnA5 all resulted in increased phosphorylation of EphA4, as expected (Figure 4.18). However, we were surprised to observe that in the CS-E KO neurons, the activation induced by EfnA3 and EfnA5 was increased, suggesting a higher degree of activation of the receptor by its ligands when CS-E is absent. Because CS-E binds to both the EphA4 receptor and the EfnA3 and EfnA5 ligands, it is possible that CS-E serves to sequester the proteins away from each other in this cell type. Activation of EphA4 in response to the EfnA2 ligand, which was not found to bind to CS-E in our array screening, was similar in the wild-type and CS-E KO neurons.
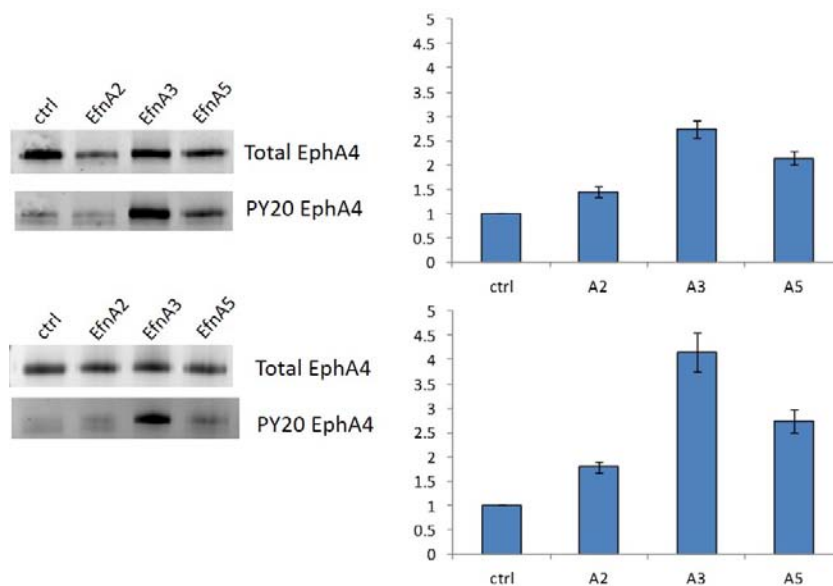
Figure 4.18. Activation of EphA4 in response to Efn ligands in CS-E $^{+/+}$ (top) and CS-E $^{-/-}$ (bottom) cortical neurons. The average of three experiments is shown.
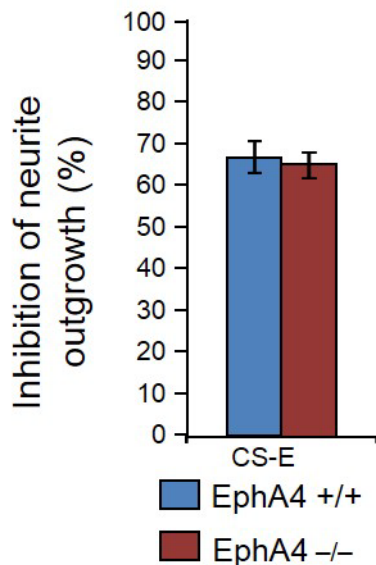
Figure 4.19. No difference in CS-E inhibition is observed in cortical neurons deficient in EphA4. The results of three experiments are shown, >300 neurons per experiment. Error bars represent standard error of the mean (SEM) for all neurons.

We next wanted to see if neurite outgrowth inhibition by CS-E and CSPG was rescued in cells lacking the EphA4 receptor. Cortical neurons from EphA4 knockout mice or wild type controls were cultured on a substrate of coated CS-E. We found that there was no rescue of outgrowth in the KO neurons, which showed the same degree of inhibition as seen in the control (Figure 4.19). This result suggests that EphA4 is not primarily responsible for CS-E inhibition in cortical neurons.

We next sought to investigate the possible role of EfnA3 in these neurons, using mice deficient in this protein.[65] As this ligand bound very strongly to CS-E via microarray and SPR analysis, we reasoned that neurons lacking this protein might show some difference in response to CS-E. EfnA3 was also an intriguing target for analysis, as it has been found to be crucial for biological functions in conjunction with EphA4, such as spine morphology.[37, 65] Cortical neurons from EfnA3 knockout mice or wild type controls were

cultured on a substrate of coated CS-E, as with the EphA4 KO neurons. We found that the neurons deficient in EfnA3 were much less inhibited that the control (Figure 4.20). As mentioned previously, EfnA3 (and other EfnAs) are not independently capable of transmitting inhibitory signals, as they lack an intracellular domain. However, this result shows a strong role for EfnA3 in CS-E-mediated inhibition in cortical neurons, and further studies may reveal the critical co-receptor for this effect.
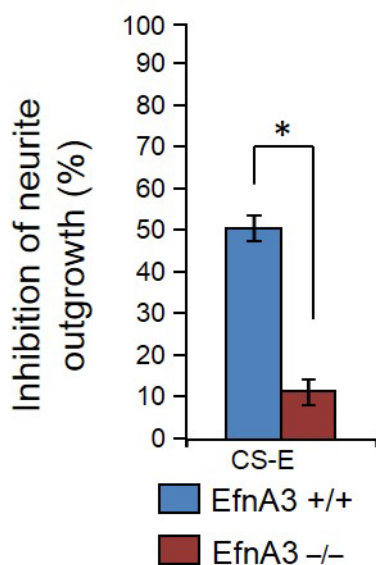
Figure 4.20. Significant rescue of CS-E inhibition is observed in cortical neurons deficient in EfnA3. The results of three experiments are shown, >300 neurons per experiment. Error bars represent standard error of the mean (SEM) for all neurons. Statistical analysis was performed using the one-way ANOVA (*$P < 0.001$, relative to control).

DRG Neurite Outgrowth is mediated by EphA4 and the ligand EfnA3. Next, we investigated dorsal root ganglion (DRG) neurons, which allow us to approximate the growth conditions of the spinal cord *in vitro*. As EphA4 and CS have both been previously shown to be involved in the inhibition of recovery after spinal cord injury, we reasoned that

the observed interaction between these two molecules may be able to explain the effect. Using RT-PCR we determined the relative mRNA levels of both EphA4 and EfnA3 present in postnatal DRGs, and found that both EphA4 and EfnA3 are likely to be expressed in both pup and adult DRGs based on the presence of their mRNA (Figure 4.21).
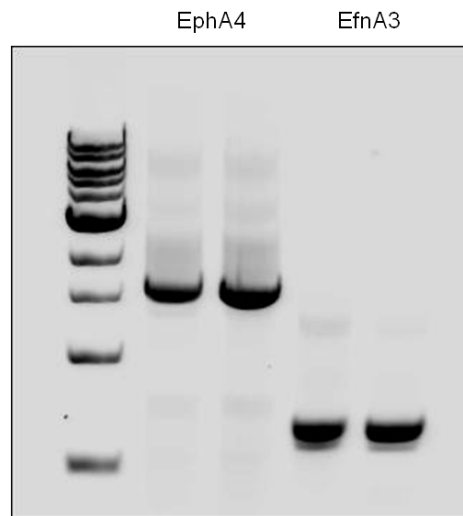
Figure 4.21. EphA4 and EfnA3 are expressed in postnatal mouse DRGs. For each pair, cDNA from P7 pups (left) and adult (right) were used.

Although the neuron-bound Eph receptors typically interact with ephrins expressed by glial cells, we hypothesized that the EphA4 and EfnA3 expressed by DRGs could be inhibiting cellular growth by interacting with CS-E, either separately or cooperatively. To determine the role of EphA4 and EfnA3 in DRG outgrowth, we measured the outgrowth of neurons deficient in either protein in the presence of CS-E. Deletion of EphA4 significantly attenuated CS-E-induced inhibition of neurite outgrowth (Figure 4.22), indicating that

EphA4 is required for CS-E to inhibit neurite outgrowth. Interestingly, deletion of EfnA3 also significantly attenuated CS-E-induced inhibition of neurite outgrowth (Figure 4.23), suggesting that these proteins are both involved in mediating the inhibitory signal of CS-E in this cell type.
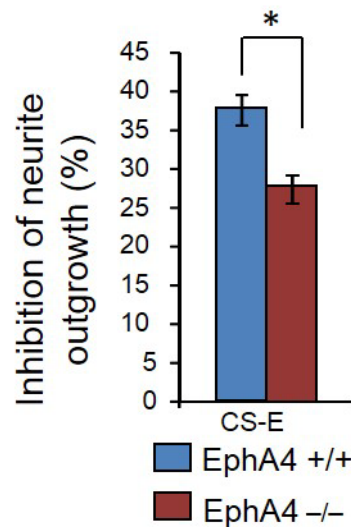
Figure 4.22. Inhibition of DRG neurite outgrowth by CS-E is attenuated in EphA4 KO neurons. The results of three experiments are shown, >300 neurons per experiment. Error bars represent standard error of the mean (SEM) for all neurons. Statistical analysis was performed using the one-way ANOVA (*P < 0.005, relative to control).
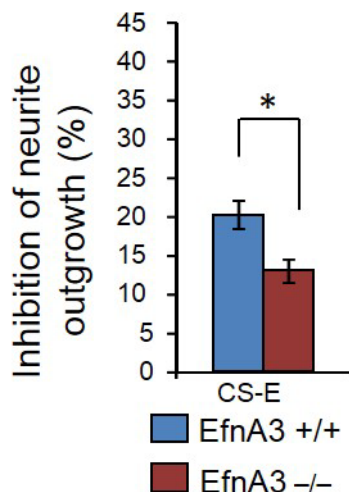
Figure 4.23. Inhibition of DRG neurite outgrowth by CS-E is attenuated in EfnA3 KO neurons. The results of three experiments are shown, >300 neurons per experiment. Error bars represent standard error of the mean (SEM) for all neurons. Statistical analysis was performed using the one-way ANOVA (*P < 0.005, relative to control).

Conclusions

Previous evidence has shown that the EphA4 receptor has various roles in the development and regulation of the nervous system, and plays a role in inhibiting regrowth after injury in the adult. We found that EphA4 binds directly and with high affinity to CS-E to operate as a receptor for this sulfated motif. Our results support the role of EphA4 in mediating the inhibition of axon outgrowth in DRG neurons, which replicate the growth conditions of the spinal cord. EphA4 deletion in transgenic mice promotes significant neurite and axon outgrowth in mature DRG neurons cultured on CS-E substrates.

Furthermore, we have found that EfnA3, a ligand for EphA4, also binds directly and with high affinity to the CS-E motif, and has a crucial role for the inhibition caused by

CS-E in cortical neurons and in DRGs. In DRGs, both the ligand and the receptor are critical for CS-E interaction, suggesting that they are both interacting on these cells, in an example of *cis* Eph activation. In cortical neurons, EfnA3 seems to be mediating the effect independently of EphA4, either via other EphA receptors or through another unidentified co-receptor.

The identification of a novel protein that mediates the inhibitory effect of CS-E advances our understanding of inhibition after injury in the CNS when CS-E expression is upregulated, and provides us with the opportunity to develop therapies for the recovery of axonal outgrowth after damage to the nervous system. Future work in our lab will explore the molecular basis of interactions between CS-E and the EphA4 receptor and EfnA3 ligand. The identification of a specific site on these proteins that binds CS-E may provide leads for potential drug design to treat spinal cord injury. Alternative blocking approaches targeting the CS motifs, such as the CS-E antibody, could be used, and such approaches could potentially be combined with blocking agents of other regeneration inhibitors. Identifying a receptor for the inhibitory CS-E motif provides new pathways for research into mechanisms and therapeutic interventions to enhance regeneration after nervous system injury.

Materials and Methods

Mass spectrometry analysis. Brains were dissected from P7-P9 Sprague Dawley rats, homogenized in 0.32 M sucrose with protease inhibitors (Roche), and centrifuged at 1,000 g for 10 min. The supernatant was collected, and then centrifuged at 10,000 g for 20 min. The pellet was discarded, and the supernatant was centrifuged again at 12,000 g for 30 min. This supernatant was then ultra-centrifuged at 200,000 g for 1 h, and the pellet was saved and homogenized again in 0.32 M sucrose with protease inhibitors. The supernatant was again ultra-centrifuged at 200,000 g for 1 h and the pellet was saved, solubilized in 1% Triton X-100 (PBST) with protease inhibitors, and centrifuged at 12,000 g for 15 min. The final supernatant was obtained as the membrane protein-enriched fraction and incubated with CS-E or unsulfated CS conjugated to streptavidin agarose resin (described above) overnight at 4 ºC. The resin was washed with PBS, and the PBS was collected and measured until the OD_{280} was less than 0.05. The bound proteins were then eluted with PBS containing 500 mM NaCl. The eluted proteins were then dialyzed into PBS and subjected to SDS-PAGE. The resulting gel was stained with Coomassie Brilliant Blue, and the band at 206 kDa was cut out, subjected to tryptic digestion, and analyzed by liquid chromatography–mass spectrometry (LC-MS) analysis as reported.[68]

Microarray assays. Microarrays were generated as described previously.[69] Arrays were blocked with 10% FBS in PBS with gentle rocking at 37 °C for 1 h, followed by a brief rinse with PBS. Fc chimera proteins (R & D Systems) were reconstituted in 1% BSA in PBS, added to the slides in 100 µl quantities at a concentration of 250 nM, and incubated at room temperature for 3 h. The slides were briefly rinsed three times with PBS, and then incubated with a goat anti-human IgG antibody conjugated to Cy3 (Jackson

ImmunoResearch; 1:5,000 in PBS) for 1 h in the dark with gentle rocking, and scanned at 532 nm using a GenePix 5000a scanner. Fluorescence quantification was performed using GenePix 6.0 software (Molecular Devices). Experiments were performed in triplicate, and the data represent the average of 10 spots per concentration averaged from the three experiments (± SEM, error bars).

Molecular Cloning. EphA4, EfnA3, and EfnB1 genes were subcloned from mouse cDNA (Open Biosystems) into a pCAX Myc6 vector using the restriction enzymes FseI (N-terminal) and AscI (C-terminal) to place an N-terminal 6X Myc tag on the expressed proteins. The vector contained a secretion peptide coding sequence upstream of the myc tag; thus, the endogenous signal peptide coding sequences were excluded from the cloning sequence.

EphA4 sense primer: AATGCTGGCCGGCCAGTCACCGGTTCTAGGGTATACCCC

EphA4 antisense primer: ATTGGCGCGCCTCAGACAGGAACCATCCTGCCATG

EfnA3 sense primer: AATGCTGGCCGGCCACAGGGGCCTGGGGGCGCACTGGGA

EfnA3 antisense primer: ATTGGCGCGCCCTAGGAGGCCAAGAGCGTCATGAG

EfnB1 sense primer: AATGCTGGCCGGCCAAAGAACCTGGAGCCCGTGTCCTGG

EfnB1 antisense primer: ATTGGCGCGCCTCAAACCTTGTAGTAGATGTTCGC

RT-PCR. Total RNA was prepared from P7 or adult (~6 weeks old) mouse tissues using the RNeasy Mini Kit (Qiagen). First-strand cDNA was synthesized using iScript cDNA synthesis Kit (Bio-rad). 1 μg of total RNA, 4 μl of 5x iScript reaction mix and 1 μl iScript reverse transcriptase were mixed together and adjusted to a total volume of 20 μl with

nuclease-free water. The reaction mixture was incubated at 25 °C for 5 min, followed by incubation at 42 °C for 30 min and, finally, at 85 °C for 5 min. The reaction mixture was diluted 1:10 with nuclease-free water. PCR was carried out using One Taq Hot Start DNA Polymerase (New England Biolabs) for 30 cycles. A first round of PCR was performed using the first round primer sets. 2 µl of cDNA, 5 µl of OneTaq standard reaction buffer, 0.5 µl of 10mM dNTPs, 0.5 µl of each 10 µM forward and reverse primer solutions and 0.125 µl One Taq Hot Start DNA Polymerase were mixed and adjusted to a total volume of 25 µl. A second round of PCR was performed using the second round primer sets. 10 µl of template DNA from round 1, 10 µl of OneTaq standard reaction buffer, 1 µl of 10mM dNTPs, 1 µl of each 10µM forward and reverse primer solutions and 0.25 µl One Taq Hot Start DNA Polymerase were mixed and adjusted to a total volume of 50 µl. Samples were analyzed using electrophoresis on a 2% (w/v) agarose gel containing ethidium bromide.

First round:

EphA1 sense primer: 5'-ATGGAGCGGCGCTGGCCCCTGGGG-3'

EphA1 antisense primer: 5'-CTCTCCTCCGGTCAGGCTTCTGGA-3'

EphA4 sense primer: 5'-ATGGCTGGGATTTTCTATTTCATC-3'

EphA4 antisense primer: 5'-AGTGGAGTTGGCTCCATCGCCAAT-3'

EphA6 sense primer: 5'-ATGCAATTCCCCTCGCCTCCAGCC-3'

EphA6 antisense primer: 5'-AATCTGCCCTTGTTCTGCCGCCAT-3'

EphB6 sense primer: 5'-ATGGCTACTGAGGGCACGACTGGC-3'

EphB6 antisense primer: 5'-CACCAAGGACAGCTTCTCTGGAAG-3'

EfnA1 sense primer: 5'-ATGGAGTTCCTTTGGGCCCCTCTC-3'

EfnA1 antisense primer: 5'-TCACTGAGATTGCAGCAGCAGCAG-3'

EfnA3 sense primer: 5'-ATGGCGGCGGCTCCGCTGCTGCTG-3'

EfnA3 antisense primer: 5'-CTAGGAGGCCAAGAGCGTCATGAG-3'

EfnA5 sense primer: 5'-ATGTTGCACGTGGAGATGTTGACG-3'

EfnA5 antisense primer: 5'-CTATAATGTCAAAAGCATCGCCAG-3'

EfnB1 sense primer: 5'-ATGGCCCGGCCTGGGCAGCGTTGG-3'

EfnB1 antisense primer: 5'-GTCCCCGCTGCCACCGCCACCTGC-3'

Second round:

EphA1 sense primer: 5'-CTTGCATTGCTGCTGCTGCTGCTC-3'

EphA1 antisense primer: 5'-AACTGGTGGGCTTGTCCGAAACTC-3'

EphA4 sense primer: 5'-CTCTTTTCGTTTCTCTTTGGAATT-3'

EphA4 antisense primer: 5'-GATGCGGGAAGGCACTGTATTAGT-3'

EphA6 sense primer: 5'-GCCAGGAGCTCCCCGGCGGCGCAG-3'

EphA6 antisense primer: 5'-GTCAGAAGTTTCATCTCCTGTTTC-3'

EphB6 sense primer: 5'-TCAGGGAGCAGAGTGGTGGCGGGC-3'

EphB6 antisense primer: 5'-CTGGGAGGACAGCTCACCTTGAGG-3'

EfnA1 sense primer: 5'-TTGGGTCTGTGCTGCAGTCTGGCC-3'

EfnA1 antisense primer: 5'-TGGTAGGAGCAATACTGCCCAGAC-3'

EfnA3 sense primer: 5'-CTGCTGCTGCTGCTGCTCGTGCCC-3'

EfnA3 antisense primer: 5'-GAAGAAGGCGATGCCCACGGCCAG-3'

EfnA5 sense primer: 5'-CTGCTCTTTCTGGTGCTCTGGATG-3'

EfnA5 antisense primer: 5'-GAGGAACAGTAGGATTGCCAAAAG-3'

EfnB1 sense primer: 5'-CTCAGCAAGTGGCTTGTGGCTATG-3'

EfnB1 antisense primer: 5'-ACCTGGGCCACTCTTCTCTTCCTG-3'

Immunoprecipitation. COS-7 cells were transfected with constructed vectors using Lipofectamine (Invitrogen) and lysed two days after transfection with 1% Triton X-100 in PBS containing a protease inhibitor cocktail (Roche). Lysates were then incubated with streptavidin agarose resin (Pierce; 30 μl) with end-over-end mixing for 1 h at 4 °C to reduce nonspecific binding. The supernatant was collected, added to 30 μl of either CS-C or CS-E streptavidin agarose resin, and incubated with end-over-end mixing for 4 h at 4 °C. The supernatant was removed, and the resin was washed three times with PBS (500 μl). Resin was boiled with 2X loading dye (30 μl of 100 mM Tris, 200 mM DTT, 4% SDS, 0.10% bromophenol blue, 20% glycerol), and the eluate was resolved by SDS-PAGE and transferred to PVDF membrane. Proteins were detected by immunoblotting with an anti-myc antibody (Cell Signaling) following the manufacturer's protocol.

Cellular Culture. For assays using CGNs, Poly-D-Lysine Cellware plates were coated with laminin (10 μg/ml) in Neurobasal medium (Invitrogen) for 2 h at 37 °C and 10% CO_2. Cerebella were dissected, incubated in 0.125% trypsin w/ EDTA for 10 min at 37 °C, triturated to dissociate to single cell suspensions, purified on discontinuous 35%/60% Percoll gradient, and cultured on the coated coverslips in Neurobasal medium supplemented with B27, GlutaMAX™ (Invitrogen), and 40 ng/ml bFGF (R&D) at a density of 25,000 cells/well for 24 h. Cells were fixed in 4% PFA with 10% sucrose, immunostained using an anti-β tubulin III antibody (TUJ1; Covance), imaged using a Nikon TE2000-S fluorescent microscope and quantified using the NIH software ImageJ.

Statistical analysis was performed using the one-way ANOVA; n = 50–200 cells per experiment, and results from at least three independent experiments were reported. For Efn inhibition studies, Ephrin ligand was coated on Poly-D-Lysine Cellware plates (500 ng/well) overnight at 37 °C and 10% CO_2. Laminin was added (10 µg/ml) in Neurobasal medium (Invitrogen) for 2 h at 37 °C, and CGNs were cultured for 24 h. KYL peptide (KYLPYWPVLSSL) was synthesized by GenScript USA Inc., and was added to the culture medium at the start of culturing (10 µM).

For inhibition studies using DRG neurons from EphA4-/- and EfnA3-/- mice, Poly-D-Lysine Cellware Plates were coated with laminin (10 µg/ml) in Neurobasal medium (Invitrogen) for 2 h at 37 °C and 10% CO_2. DRGs were dissected from adult knockout (KO) mice or WT controls, incubated in 0.125% trypsin w/ EDTA for 15 min at 37 °C, followed by collagenase (Worthington; 4 mg/ml) for 15 min at 37 °C, triturated to dissociate to single cell suspensions, filtered using a 40-µm cell strainer (Fisher) to remove non-dissociated cells, and seeded at approximately 2,000 cells per well. Cells were cultured for two days in Neurobasal medium supplemented with B27 and GlutaMAX™ (Invitrogen). CS-E was biotinylated as described[70] and conjugated to streptavidin agarose beads (200 µg of CS in 400 µl PBS incubated with 100 µl agarose resin for 1 h at room temperature), which were then co-plated with the cells (5 µg of 50% slurry per well). Unconjugated beads at the same concentration were used as a control. Cells were grown in Neurobasal medium supplemented with B27 and GlutaMAX™ (Invitrogen) for two days. For all neurite outgrowth experiments, we performed statistical analysis using the one-way ANOVA; n = 50-200 cells per experiment, and results from at least three independent experiments were reported.

For cortical neuron experiments, Poly-D-Lysine Cellware plates were coated with laminin (10 µg/ml) in Neurobasal medium (Invitrogen) for 2 h at 37 °C and 10% CO_2. Pregnant E16 EphA4-/- and EfnA3-/- knockout (KO) mice or WT controls were euthanized, and embryos were extracted into cold HBSS. The brains were removed from the embryos, and the cortices were separated from the rest of the tissue. Meninges were carefully removed, and the cortices were incubated in trypsin (Life Technologies) at 37 °C for 15 min. Tissue was quenched with DMEM with 10% FBS, pelleted, and resuspended in DMEM with 10% FBS. The tissue was triturated to dissociate to single cell suspensions, filtered using a 40-µm cell strainer (Fisher) to remove non-dissociated cells, and seeded at approximately 20,000 cells per well. Cells were cultured for 24 h in Neurobasal medium supplemented with B27 and GlutaMAX™ (Invitrogen). For activation assays, neurons were dissected as described above, and cultured in 10 cm dishes (~10 million cells/dish).

Immunostaining and quantification. All neuronal cultures were fixed with paraformaldehyde, permeabilized with 0.1% Triton X-100 in PBS, blocked with 1% BSA in PBS, and incubated with a mouse anti-βIII tubulin antibody (Sigma) overnight at 4 °C, followed by an Alexa Fluor 488-conjugated goat anti-mouse IgG secondary antibody (Invitrogen) for 1-2 h at room temperature for neurite outgrowth assays. Cells were imaged using a Nikon TE2000-S fluorescent microscope or Zeiss LSM Pascal, and neurite outgrowth was quantified using NIH software ImageJ or MetaMorph software. Statistical analysis was performed using the one-way ANOVA; n = 50-500 cells per experiment, and results from at least three independent experiments were reported.

Activation Assays. COS-7 or HEK293T cells were transfected with EphA4 using Lipofectamine (Life Technologies). Cells were cultured for two days in DMEM

supplemented with 10% FBS. For cortical activation assays, cortical neurons were dissected and cultured as described above. After 24 h, cells were stimulated by changing their medium to fresh medium containing CS-E (Seikagaku; 10 μg/ml) or Efn-Fc proteins (R&D systems; 1 μg/ml) and incubating for the time described at 37 °C. Cells were lysed with cold lysis buffer consisting of PBS with 1% Triton X-100 with protease inhibitor cocktail (Roche) and phosphatase inhibitor mixture. Lysates were clarified via centrifugation. For each sample, 50 μl of protein A/G agarose (Pierce) was added to an Eppendorf along with 3 μg of EphA4 antibody (Invitrogen). Clarified lysate was added, and incubated at 4 °C with rotation for 2 h. Agarose was washed three times with lysis buffer, boiled with 2X loading dye (30 μl of 100 mM Tris, 200 mM DTT, 4% SDS, 0.10% bromophenol blue, 20% glycerol), and the eluate was resolved by SDS-PAGE and transferred to PVDF membrane. Phosphorylated EphA4 was detected by immunoblotting with an anti-phosphotyrosine antibody (BD Biosciences) following the manufacturer's protocol. After scanning, membranes were stripped (NewBlot 5X PVDF stripping buffer; LI-COR) and re-blotted with anti-EphA4 antibody (Invitrogen). For analysis of Jak2/Stat1 phosphorylation, COS-7 cells were transfected with EphA4 expression vector, and cultured for two days in DMEM supplemented with 10% FBS. After two days, cells were serum-starved by culturing in DMEM with 0.5% FBS for 6 h. After serum starvation, cells were stimulated with CS-E or other molecules in reduced-serum medium as indicated. The cells were then lysed with RIPA buffer (25 mM Tris-HCl, pH 7.6; 150 mM NaCl; 1% NP-40; 1% sodium deoxycholate; 0.1% SDS; protease and phosphatase inhibitor cocktail) and sonicated. The lysed were clarified by centrifugation at 12,000 rpm for 4 min. Loading dye was added to the lysate, and the lysate was resolved by SDS-PAGE and transferred to

PVDF membrane. Phosphorylated Jak2 and Stat1 were detected by immunoblotting with an anti-phosphotyrosine Jak2 antibody (Millipore) or anti-phosphotyrosine Stat1 antibody (Cell Signaling) following the manufacturer's protocol. After scanning, membranes were stripped (NewBlot 5X PVDF stripping buffer; LI-COR) and re-blotted with anti-Jak2 or Stat1 antibodies (Santa Cruz).

References

1.   Flanagan, J. G., Gale, N. W., Hunter, T., Pasquale, E. B. & Tessier-Lavigne, M. Unified nomenclature for Eph family receptors and their ligands, the ephrins. *Cell* **1997,** 90, (3), 403-404.

2.   Adams, R. H. Vascular patterning by Eph receptor tyrosine kinases and ephrins. *Semin. Cell Dev. Biol.* **2002,** 13, (1), 55-60.

3.   Drescher, U. The Eph family in the patterning of neural development. *Curr. Biol.* **1997,** 7, (12), R799-807.

4.   Egea, J. & Klein, R. Bidirectional Eph-ephrin signaling during axon guidance. *Trends Cell Biol.* **2007,** 17, (5), 230-238.

5.   Klein, R. Bidirectional modulation of synaptic functions by Eph/ephrin signaling. *Nat. Neurosci.* **2009,** 12, (1), 15-20.

6.   Holmberg, J., Clarke, D. L. & Frisen, J. Regulation of repulsion versus adhesion by different splice forms of an Eph receptor. *Nature* **2000,** 408, (6809), 203-206.

7.   Dravis, C.*, et al.* Bidirectional signaling mediated by ephrin-B2 and EphB2 controls urorectal development. *Dev. Biol.* **2004,** 271, (2), 272-290.

8.   Flanagan, J. G. & Vanderhaeghen, P. The ephrins and Eph receptors in neural development. *Annu. Rev. Neurosci.* **1998,** 21, 309-345.

9.   Wilkinson, D. G. Multiple roles of EPH receptors and ephrins in neural development. *Nat. Rev. Neurosci.* **2001,** 2, (3), 155-164.

10.   Knoll, B. & Drescher, U. Ephrin-As as receptors in topographic projections. *Trends Neurosci.* **2002,** 25, (3), 145-149.

11.   Hirai, H., Maru, Y., Hagiwara, K., Nishida, J. & Takaku, F. A Novel Putative Tyrosine Kinase Receptor Encoded by the Eph Gene. *Science* **1987,** 238, (4834), 1717-1720.

12.   Bartley, T. D.*, et al.* B61 Is a Ligand for the Eck Receptor Protein-Tyrosine Kinase. *Nature* **1994,** 368, (6471), 558-560.

13.   Beckmann, M. P.*, et al.* Molecular Characterization of a Family of Ligands for Eph-Related Tyrosine Kinase Receptors. *Embo. J.* **1994,** 13, (16), 3757-3762.

14.   Cheng, H. J. & Flanagan, J. G. Identification and cloning of ELF-1, a developmentally expressed ligand for the Mek4 and Sek receptor tyrosine kinases. *Cell* **1994,** 79, (1), 157-168.

15. Maru, Y., Hirai, H. & Takaku, F. Overexpression Confers an Oncogenic Potential Upon the Eph Gene. *Oncogene* **1990,** 5, (3), 445-447.

16. Pasquale, E. B. Eph receptors and ephrins in cancer: bidirectional signalling and beyond. *Nat. Rev. Cancer* **2010,** 10, (3), 165-180.

17. Holland, S. J*., et al.* Bidirectional signalling through the EPH-family receptor Nuk and its transmembrane ligands. *Nature* **1996,** 383, (6602), 722-725.

18. Mellitzer, G., Xu, Q. L. & Wilkinson, D. G. Control of cell behaviour by signalling through Eph receptors and ephrins. *Curr. Opin. Neurobiol.* **2000,** 10, (3), 400-408.

19. Murai, K. K. & Pasquale, E. B. 'Eph'ective signaling: forward, reverse and crosstalk. *J. Cell Sci.* **2003,** 116, (14), 2823-2832.

20. Alford, S. C., Bazowski, J., Lorimer, H., Elowe, S. & Howard, P. L. Tissue transglutaminase clusters soluble A-type ephrins into functionally active high molecular weight oligomers. *Exp. Cell Res.* **2007,** 313, (20), 4170-4179.

21. Wykosky, J*., et al.* Soluble monomeric EphrinA1 is released from tumor cells and is a functional ligand for the EphA2 receptor. *Oncogene* **2008,** 27, (58), 7260-7273.

22. Kao, T. J. & Kania, A. Ephrin-Mediated cis-Attenuation of Eph Receptor Signaling Is Essential for Spinal Motor Axon Guidance. *Neuron* **2011,** 71, (1), 76-91.

23. Arvanitis, D. & Davy, A. Eph/ephrin signaling: networks. *Gene Dev.* **2008,** 22, (4), 416-429.

24. Pasquale, E. B. Eph receptor signalling casts a wide net on cell behaviour. *Nat. Rev. Mol. Cell. Biol.* **2005,** 6, (6), 462-475.

25. Gale, N. W*., et al.* Eph receptors and ligands comprise two major specificity subclasses and are reciprocally compartmentalized during embryogenesis. *Neuron* **1996,** 17, (1), 9-19.

26. Himanen, J. P. & Nikolov, D. B. Eph signaling: a structural view. *Trends Neurosci.* **2003,** 26, (1), 46-51.

27. Ellis, C*., et al.* A juxtamembrane autophosphorylation site in the Eph family receptor tyrosine kinase, Sek, mediates high affinity interaction with p59fyn. *Oncogene* **1996,** 12, (8), 1727-1736.

28. Holland, S. J*., et al.* Juxtamembrane tyrosine residues couple the Eph family receptor EphB2/Nuk to specific SH2 domain proteins in neuronal cells. *Embo. J.* **1997,** 16, (13), 3877-3888.

29.   Dail, M., Richter, M., Godement, P. & Pasquale, E. B. Eph receptors inactivate R-Ras through different mechanisms to achieve cell repulsion. *J. Cell Sci.* **2006,** 119, (7), 1244-1254.

30.   Mann, F., Miranda, E., Weinl, C., Harmer, E. & Holt, C. E. B-type Eph receptors and ephrins induce growth cone collapse through distinct intracellular pathways. *J. Neurobiol.* **2003,** 57, (3), 323-336.

31.   Huai, J. S. & Drescher, U. An ephrin-A-dependent signaling pathway controls integrin function and is linked to the tyrosine phosphorylation of a 120-kDa protein. *J. Biol. Chem.* **2001,** 276, (9), 6689-6694.

32.   Sharfe, N.*, et al.* EphA and ephrin-A proteins regulate integrin-mediated T lymphocyte interactions. *Mol. Immunol.* **2008,** 45, (5), 1208-1220.

33.   Davy, A.*, et al.* Compartmentalized signaling by GPI-anchored ephrin-A5 requires the Fyn tyrosine kinase to regulate cellular adhesion. *Gene Dev.* **1999,** 13, (23), 3125-3135.

34.   Davy, A. & Robbins, S. M. Ephrin-A5 modulates cell adhesion and morphology in an integrin-dependent manner. *Embo. J.* **2000,** 19, (20), 5396-5405.

35.   Lim, Y. S.*, et al.* p75(NTR) mediates ephrin-A reverse signaling required for axon repulsion and mapping. *Neuron* **2008,** 59, (5), 746-758.

36.   Zagrebelsky, M.*, et al.* The p75 neurotrophin receptor negatively modulates dendrite complexity and spine density in hippocampal neurons. *J. Neurosci.* **2005,** 25, (43), 9989-9999.

37.   Murai, K. K., Nguyen, L. N., Irie, F., Yamaguchi, Y. & Pasquale, E. B. Control of hippocampal dendritic spine morphology through ephrin-A3/EphA4 signaling. *Nat. Neurosci.* **2003,** 6, (2), 153-160.

38.   Wang, K. C., Kim, J. A., Sivasankaran, R., Segal, R. & He, Z. G. p75 interacts with the Nogo receptor as a co-receptor for Nogo, MAG and OMgp. *Nature* **2002,** 420, (6911), 74-78.

39.   Coate, T. M.*, et al.* Otic Mesenchyme Cells Regulate Spiral Ganglion Axon Fasciculation through a Pou3f4/EphA4 Signaling Pathway. *Neuron* **2012,** 73, (1), 49-63.

40.   Chen, Z. Y.*, et al.* Abnormal hippocampal axon bundling in EphB receptor mutant mice. *J. Neurosci.* **2004,** 24, (10), 2366-2374.

41. Yue, Y.*, et al.* Mistargeting hippocampal axons by expression of a truncated Eph receptor. *Proc. Natl. Acad. Sci. U S A* **2002,** 99, (16), 10777-10782.

42. Dearborn, R., He, Q., Kunes, S. & Dai, Y. Eph receptor tyrosine kinase-mediated formation of a topographic map in the Drosophila visual system. *J. Neurosci.* **2002,** 22, (4), 1338-1349.

43. Kuijper, S., Turner, C. J. & Adams, R. H. Regulation of angiogenesis by Eph-Ephrin interactions. *Trends Cardiovas. Med.* **2007,** 17, (5), 145-151.

44. Zhang, J. & Hughes, S. E. Role of the ephrin and Eph receptor tyrosine kinase families in angiogenesis and development of the cardiovascular system. *J. Pathol.* **2006,** 208, (4), 453-461.

45. Adams, R. H. & Klein, R. Eph receptors and ephrin ligands. essential mediators of vascular development. *Trends Cardiovasc. Med.* **2000,** 10, (5), 183-188.

46. Moreno-Flores, M. T. & Wandosell, F. Up-regulation of Eph tyrosine kinase receptors after excitotoxic injury in adult hippocampus. *Neuroscience* **1999,** 91, (1), 193-201.

47. Rodger, J.*, et al.* Expression of ephrin-A2 in the superior colliculus and EphA5 in the retina following optic nerve section in adult rat. *Eur. J. Neurosci.* **2001,** 14, (12), 1929-1936.

48. Willson, C. A.*, et al.* Upregulation of EphA receptor expression in the injured adult rat spinal cord. *Cell Transplant.* **2002,** 11, (3), 229-239.

49. Wahl, S., Barth, H., Ciossek, T., Aktories, K. & Mueller, B. K. Ephrin-A5 induces collapse of growth cones by activating Rho and Rho kinase. *J. Cell Biol.* **2000,** 149, (2), 263-270.

50. Shamah, S. M.*, et al.* EphA receptors regulate growth cone dynamics through the novel guanine nucleotide exchange factor ephexin. *Cell* **2001,** 105, (2), 233-244.

51. Liu, X., Hawkes, E., Ishimaru, T., Tran, T. & Sretavan, D. W. EphB3: An endogenous mediator of adult axonal plasticity and regrowth after CNS injury. *J. Neurosci.* **2006,** 26, (12), 3087-3101.

52. Goldshmit, Y., Galea, M. P., Wise, G., Bartlett, P. F. & Turnley, A. M. Axonal regeneration and lack of astrocytic gliosis in EphA4-deficient mice. *J. Neurosci.* **2004,** 24, (45), 10064-10073.

53. Goldshmit, Y.*, et al.* EphA4 blockers promote axonal regeneration and functional recovery following spinal cord injury in mice. *PLoS One* **2011,** 6, (9), e24636.

54. Irie, F., Okuno, M., Matsumoto, K., Pasquale, E. B. & Yamaguchi, Y. Heparan sulfate regulates ephrin-A3/EphA receptor signaling. *Proc. Natl. Acad. Sci. U S A* **2008,** 105, (34), 12307-12312.

55. Shen, Y.*, et al.* PTPsigma is a receptor for chondroitin sulfate proteoglycan, an inhibitor of neural regeneration. *Science* **2009,** 326, (5952), 592-596.

56. Fisher, D.*, et al.* Leukocyte Common Antigen-Related Phosphatase Is a Functional Receptor for Chondroitin Sulfate Proteoglycan Axon Growth Inhibitors. *J. Neurosci.* **2011,** 31, (40), 14051-14066.

57. Dickendesher, T. L.*, et al.* NgR1 and NgR3 are receptors for chondroitin sulfate proteoglycans. *Nat. Neurosci.* **2012,** 15, (5), 703-712.

58. Brown, J. M.*, et al.* A sulfated carbohydrate epitope inhibits axon regeneration after injury. *Proc. Natl. Acad. Sci. U S A* **2012,** 109, (13), 4768-4773.

59. Ohtake-Niimi, S.*, et al.* Mice Deficient in N-Acetylgalactosamine 4-Sulfate 6-O-Sulfotransferase Are Unable to Synthesize Chondroitin/Dermatan Sulfate containing N-Acetylgalactosamine 4,6-Bissulfate Residues and Exhibit Decreased Protease Activity in Bone Marrow-derived Mast Cells. *J. Biol. Chem.* **2010,** 285, (27), 20793-20805.

60. Greferath, U., Canty, A. J., Messenger, J. & Murphy, M. Developmental expression of EphA4-tyrosine kinase receptor in the mouse brain and spinal cord. *Mech. Develop.* **2002,** 119, S231-S238.

61. Chang, Q., Jorgensen, C., Pawson, T. & Hedley, D. W. Effects of dasatinib on EphA2 receptor tyrosine kinase activity and downstream signalling in pancreatic cancer. *Br. J. Cancer* **2008,** 99, (7), 1074-1082.

62. Noberini, R.*, et al.* Small Molecules Can Selectively Inhibit Ephrin Binding to the EphA4 and EphA2 Receptors. *J. Biol. Chem.* **2008,** 283, (43), 29461-29472.

63. Murai, K. K.*, et al.* Targeting the EphA4 receptor in the nervous system with biologically active peptides. *Mol. Cell. Neurosci.* **2003,** 24, (4), 1000-1011.

64. Dottori, M.*, et al.* EphA4 (Sek1) receptor tyrosine kinase is required for the development of the corticospinal tract. *Proc. Natl. Acad. Sci. U S A* **1998,** 95, (22), 13248-13253.

65. Carmona, M. A., Murai, K. K., Wang, L., Roberts, A. J. & Pasquale, E. B. Glial ephrin-A3 regulates hippocampal dendritic spine morphology and glutamate transport. *Proc. Natl. Acad. Sci. U S A* **2009,** 106, (30), 12524-12529.

66.   Hornberger, M. R*., et al*. Modulation of EphA receptor function by coexpressed EphrinA ligands on retinal ganglion cell axons. *Neuron* **1999,** 22, (4), 731-742.

67.   Marcus, R. C., Gale, N. W., Morrison, M. E., Mason, C. A. & Yancopoulos, G. D. Eph family receptors and their ligands distribute in opposing gradients in the developing mouse retina. *Dev. Biol.* **1996,** 180, (2), 786-789.

68.   Clark, P. M*., et al.* Direct in-gel fluorescence detection and cellular imaging of O-GlcNAc-modified proteins. *J. Am. Chem. Soc*. **2008,** 130, (35), 11576-11577.

69.   Rogers, C. J*., et al.* Elucidating glycosaminoglycan-protein-protein interactions using carbohydrate microarray and computational approaches. *Proc. Natl. Acad. Sci. U S A* **2011,** 108, (24), 9747-9752.

70.   Saito, A. & Munakata, H. Detection of chondroitin sulfate-binding proteins on the membrane. *Electrophoresis* **2004,** 25, (15), 2452-2460.

Appendix 1: The myelin protein inhibitors and their receptors interact with CS-E[*]

Introduction

Following injury to the central nervous system (CNS), a variety of inhibitory molecules prevent neuronal regeneration. These inhibitory molecules exist in two categories: the myelin-associated inhibitory proteins and proteoglycans associated with the glial scar.[1-4] There are several myelin-associated proteins involved in inhibiting neuronal growth after injury to the central nervous system, including the reticulon protein Nogo-A, myelin-associated glycoprotein (MAG), and oligodendrocyte myelin glycoprotein (OMgp), all of which converge on common receptors.[4] One of the first receptors identified for these inhibitory proteins is the Nogo-66 receptor[5] (NgR), which binds Nogo-66, a 66-amino acid loop near the C-terminal region of Nogo-A which is expressed on the neuronal cell surface. It was later found that MAG and OMgp are also ligands for this receptor.[4, 6, 7] NgR is linked to the cell surface via a glycosylphosphatidylinositol (GPI) anchor at its C-terminus, and thus must form a receptor complex with a transmembrane protein in order to transmit its inhibitory signal. This critical co-receptor was identified as the p75 neurotrophin receptor[8] (p75NTR/p75). This NgR/p75 receptor complex was later found to also include Lingo-1,

---

[*] Experiments using signaling molecule inhibitors were performed by Dr. Cristal Gama, a former graduate student in the Hsieh-Wilson laboratory. Surface plasmon resonance (SPR) analysis was performed by Dr. Claude Rogers, a former graduate student in the Hsieh-Wilson laboratory.

and these three proteins together are sufficient to transmit the inhibitory signal of Nogo-66, MAG, and OMgp.[9] It was later discovered that the more broadly expressed TNF receptor TAJ/TROY could replace p75 in this complex, and may be more likely to be found in the complex at later developmental stages, when it is more highly expressed compared to p75.[10] Furthermore, a recent study showed that the mostly uncharacterized protein Amigo3 can substitute for Lingo1 in the complex, and is upregulated soon after injury (compared to the delayed upregulation of Lingo1) supporting a functional role for this protein in inhibiting growth after injury.[11]

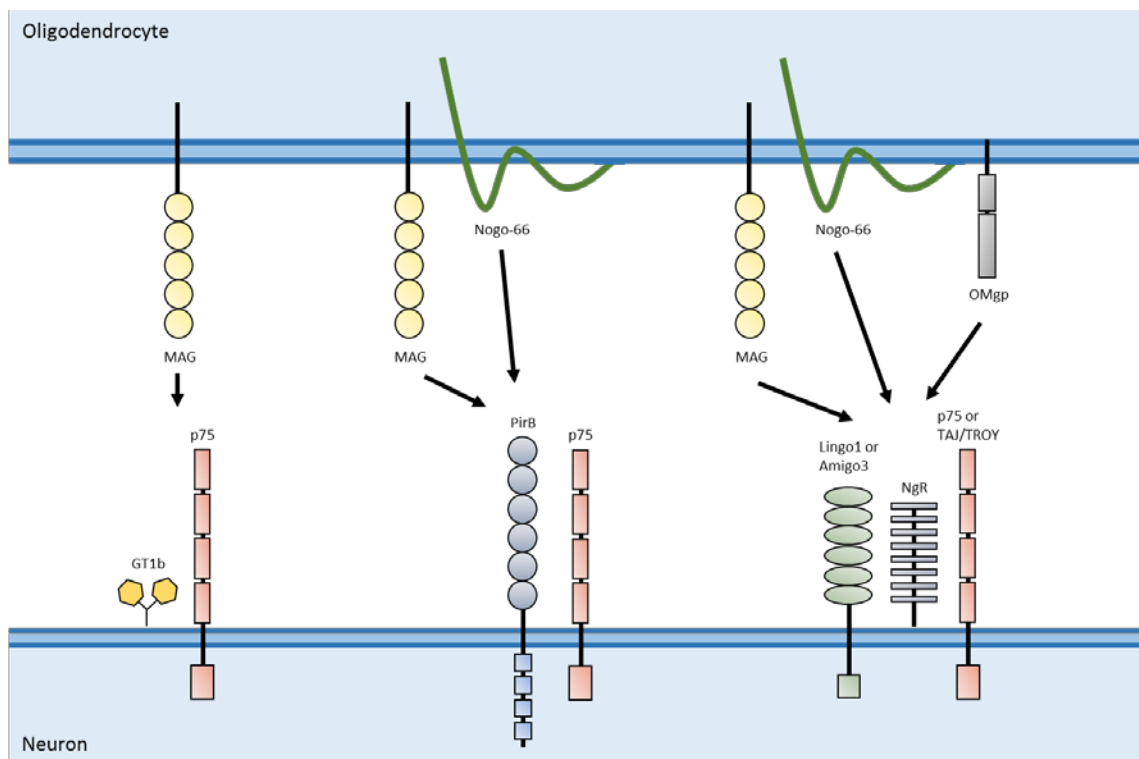**Figure A1.1. Myelin-associated inhibitors and their receptor(s). Nogo-66, MAG (myelin-associated glycoprotein) and OMgp (oligodendrocyte myelin glycoprotein) all bind to NgR with high affinity. NgR associates with transmembrane coreceptors to transduce the signal across the plasma membrane. Nogo-66 and MAG also bind to PirB (paired immunoglobulin-like receptor B), while MAG also binds to the ganglioside GT1b.**

An additional recognition element, the ganglioside GT1b, was also found to associate with the inhibitory protein MAG, and it was further found that GT1b associates with the p75 receptor to form a complex to transmit the inhibitory signal from MAG.[12, 13] Finally, a novel receptor, PirB, was recently discovered as a binder and mediator of the inhibitory signal of both MAG and Nogo-66.[14] It was later found that the p75 receptor is required for the inhibitory signaling of PirB, highlighting the seemingly crucial role of this protein in mediating the inhibitory signaling of the myelin inhibitory proteins.[15] These ligand and receptor interactions described above are summarized in Figure A1.1.

In the NgR receptor complex, NgR alone has been shown to be the critical binding element which binds to the ligands Nogo-66, MAG, and OMgp, while the other components are needed for signaling and do not seem to engage the ligands.[9] Upon ligand binding to the NgR receptor complex, Rho and Rho-kinase (ROCK) are activated to trigger actin depolymerization, which ultimately leads to growth cone collapse and the inhibition of neurite outgrowth.[2, 16] Further demonstrating the effect of this receptor complex, neurons from mice deficient in p75 show reduced inhibition of neurite outgrowth by the myelin inhibitory proteins.[8]

Until recently, receptors mediating the effect of the second group of inhibitory molecules, the proteoglycans, were unknown. However, in the last several years, specific receptors involved in CSPG-mediated axon inhibition after CNS injury have been identified.[17-19] Our lab has shown that a specific CS motif, CS-E, serves as a recognition element to facilitate interactions of CSPGs with inhibitory receptors (see Chapters 3 and 4). As a general approach to learn about the downstream pathways mediating this inhibition, and to establish a role for receptors in mediating this effect, our lab cultured neurons on

CSPG or CS-E polysaccharides with or without inhibitors to various downstream signaling molecules. These included inhibitors to Rho/Rho-kinase (ROCK; Y27632), mitogen-activated protein kinase (MEK; PD98059), and epidermal growth factor receptor (EGFR; AG1478), all of which have been shown to be activated by CSPGs and myelin inhibitors.[16, 20-22] As a control, an inhibitor to JNK (JNK inhibitor II) was also included (Figure A1.2). As shown in the figure, ROCK, MEK, and EGFR are involved in mediating the inhibitory signal of both CSPG and CS-E, as inhibiting these molecules reduces the inhibitory effect on neurite outgrowth. Thus, proteins known to activate these signaling molecules are likely candidates for CSPG receptors, which specifically engage the CS-E motif.
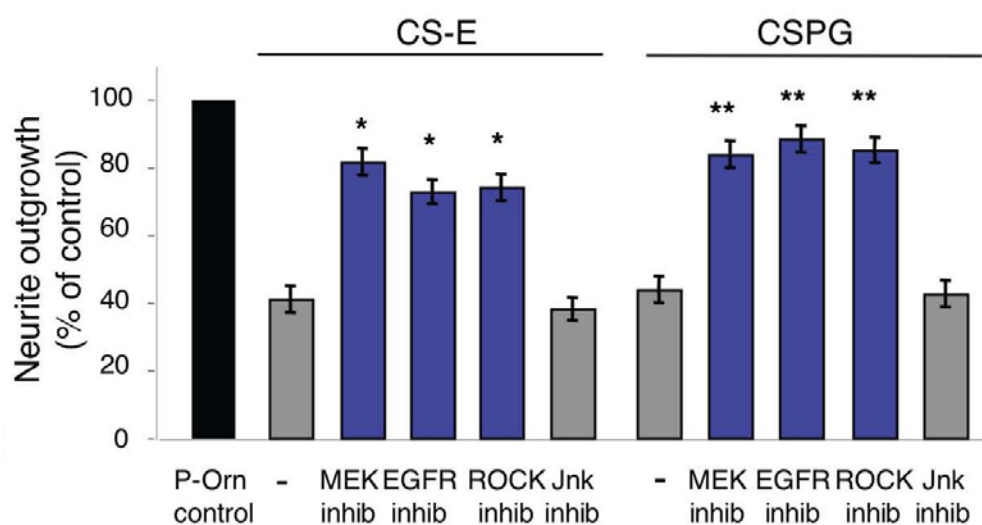
Figure A1.2. Inhibitors to MEK, EGFR, and ROCK, but not Jnk, attenuate the inhibitory effects of both CSPG and CS-E, to a similar degree. (A) Inhibitors to MEK, EGFR, ROCK, and JNK alone have no effect on CGN outgrowth. Dissociated rat P5-9 CGN neurons were cultured on a P-Orn substratum in the presence or absence of inhibitors against MEK (PD98059, 25 μM), EGFR (AG1478, 15 nM), ROCK (Y27632, 5 μM), and JNK inhibitor II (10 μM) for 24 h. Neurites were visualized by staining with an anti-β-tubulin III antibody, and quantification from at least three independent experiments is reported (n = 50–200 cells per experiment).

Results

Interestingly, the signaling molecules ROCK, MEK, and EGFR are involved in the inhibitory signaling of both the myelin inhibitors Nogo-66, MAG, and OMgp as well as CSPGs and CS-E.[2, 4, 20, 21] Because of this convergence of signaling molecules, it is possible that there is also a convergence in the receptors mediating this signal. Our lab first targeted the NgR receptor complex, as this complex mediates the signal of all three myelin inhibitory proteins. To investigate possible interactions between proteins in this complex and chondroitin sulfate, we first tested the binding of the receptor proteins that were available as soluble, Fc hybrid proteins to various CS motifs first via microarray assay to look for evidence of interactions. We found that soluble NgR Fc-fusion protein selectively binds to CS-E on the microarray, while an Fc control protein did not show any binding (Figure A1.3).
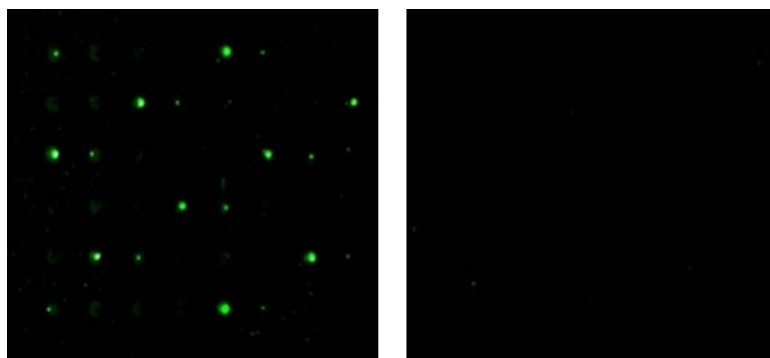
Figure A1.3. Representative portions of microarrays tested with NgR (left) or Fc control (right).

NgR-Fc and p75-Fc were also tested to determine the relative binding of each of these components of the receptor complex. The experiments were repeated five or six times (p75 and NgR, respectively) and each experiment yielded binding data for 10 spots of each polysaccharide at each concentration. Graph bars represent all spots from all array

experiments for the shown concentrations. For each microarray experiment, values were normalized relative to the highest binding signal for that particular array, and these results were averaged to produce the final result. This interaction appears to be selective to CS-E, as minimal binding was observed to other highly sulfated GAGs such as heparin and heparan sulfate. Although both proteins specifically bind CS-E, the interaction between CS-E and NgR was greater than that of CS-E and p75 (Figure A1.4).
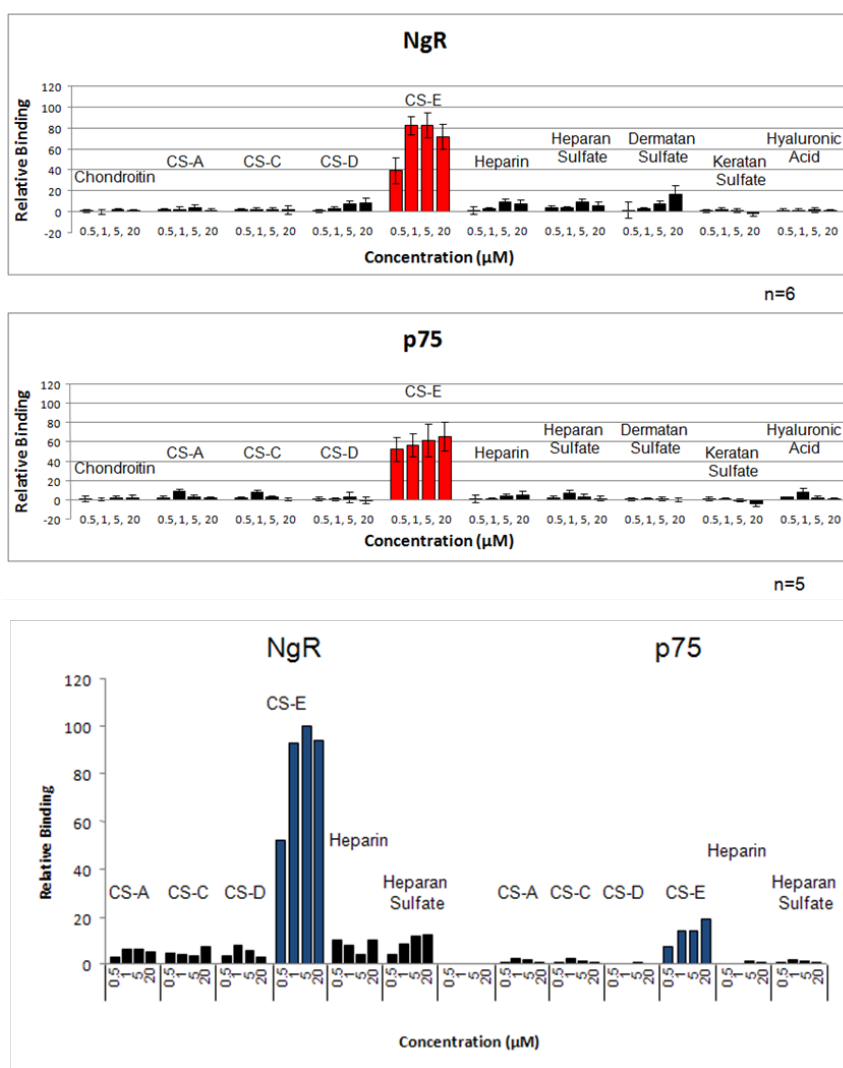

Figure A1.4. NgR and p75 bind preferentially to CS-E enriched polysaccharides on the microarray. Comparitive binding of NgR and p75. Each bar represents the average of ten spots on one typical array. The binding intensity is relative to that of NgR binding to 5μM CS-E.
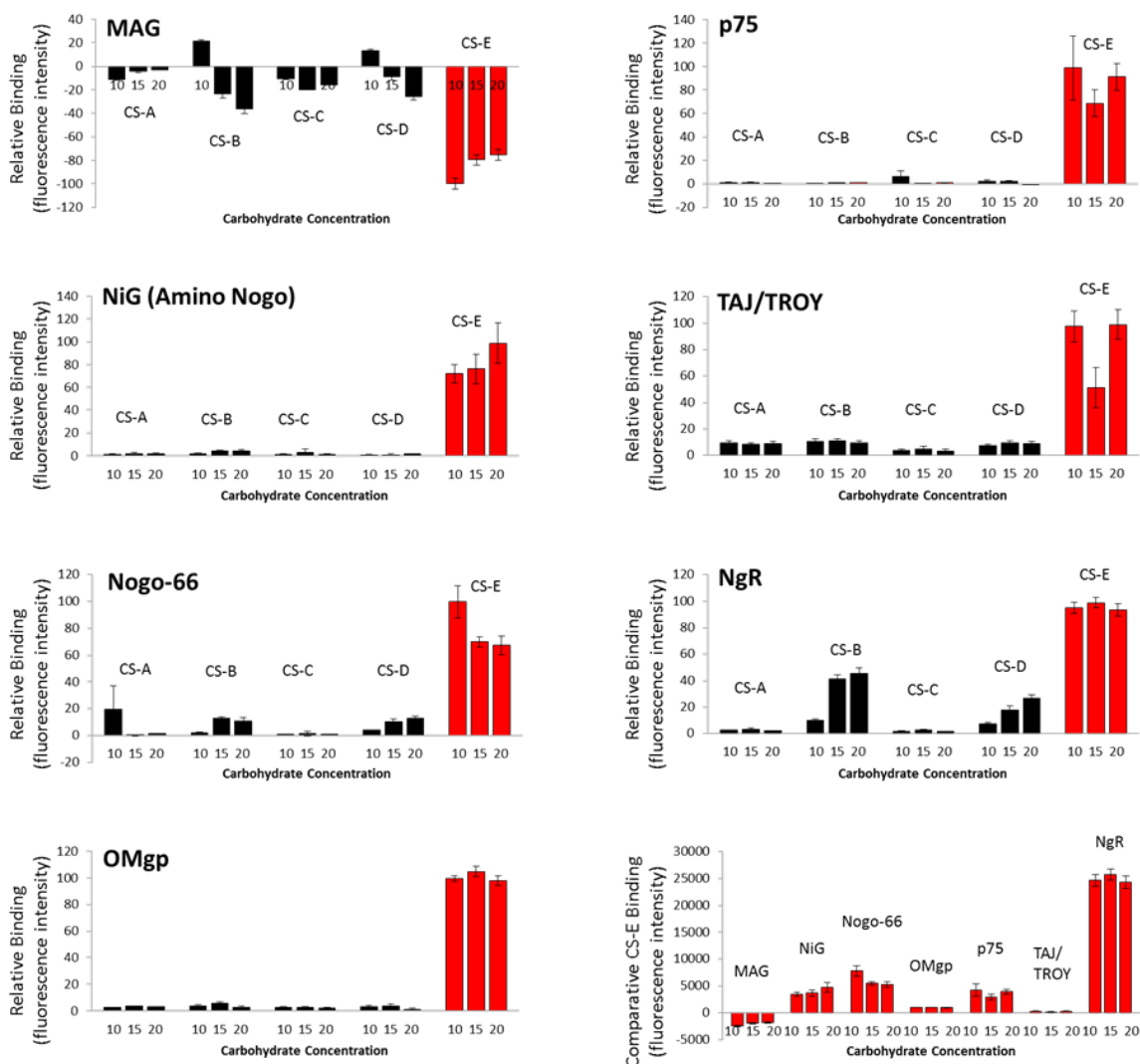
Figure A1.5. Myelin inhibitory proteins (left) and associated receptors (right) on the carbohydrate microarray. Amino Nogo, Nogo-66, and OMgp selective bid to CS-E, compared to other CS motifs. MAG did not bind to any motifs. All of the receptors tested (p75, TAJ/TROY, and NgR) selectively bound to the CS-E motif. The lower right shows the comparative binding of all proteins to CS-E.

After determining that both NgR and p75 seemed to bind specifically to CS-E, additional available myelin inhibitory ligands or receptors were tested. Of the myelin protein ligands, we found that amino Nogo/NiG (a region of the NogoA protein that is

inhibitory to neurite outgrowth and acts via RhoA activation, but is independent of the NgR/p75 receptor complex[23]), Nogo-66, and OMgp all bound preferentially to the CS-E motif, compared to other CS motifs (Figure A1.5). MAG did not bind to any of the CS motifs on the array, and in fact appeared to display repulsion to the CS spots on the surface, which is indicated by a negative value in the graph. MAG has a lower theoretical isoelectric point, calculated based on amino acid sequence, and thus is expected to have a net negative charge at physiological pH which causes it to be repelled by the negatively charged CS on the microarray surface.

Of the receptors tested, p75, TAJ/TROY, and NgR all appeared to preferentially bind CS-E, with little or no binding to the other CS motifs. Figure A1.5 shows a scaled graph comparing the relative binding of each of the proteins tested to CS-E. NgR in particular bound to CS-E to a very high degree, and most of the other proteins demonstrate some level of affinity for the CS-E motif. This high level of binding of CS-E by the soluble NgR-Fc protein was further demonstrated by surface plasmon resonance (SPR). Kinetic analysis using SPR revealed that NgR binds to CS-E polysaccharides with remarkably high affinity and specificity (Figure A1.6). At least two independent, high-affinity NgR binding sites were observed within CS-E polysaccharides (K_D1 = 8.7 nM; K_D2 = 1.8 pM), whereas binding CS-C polysaccharides was not detected.
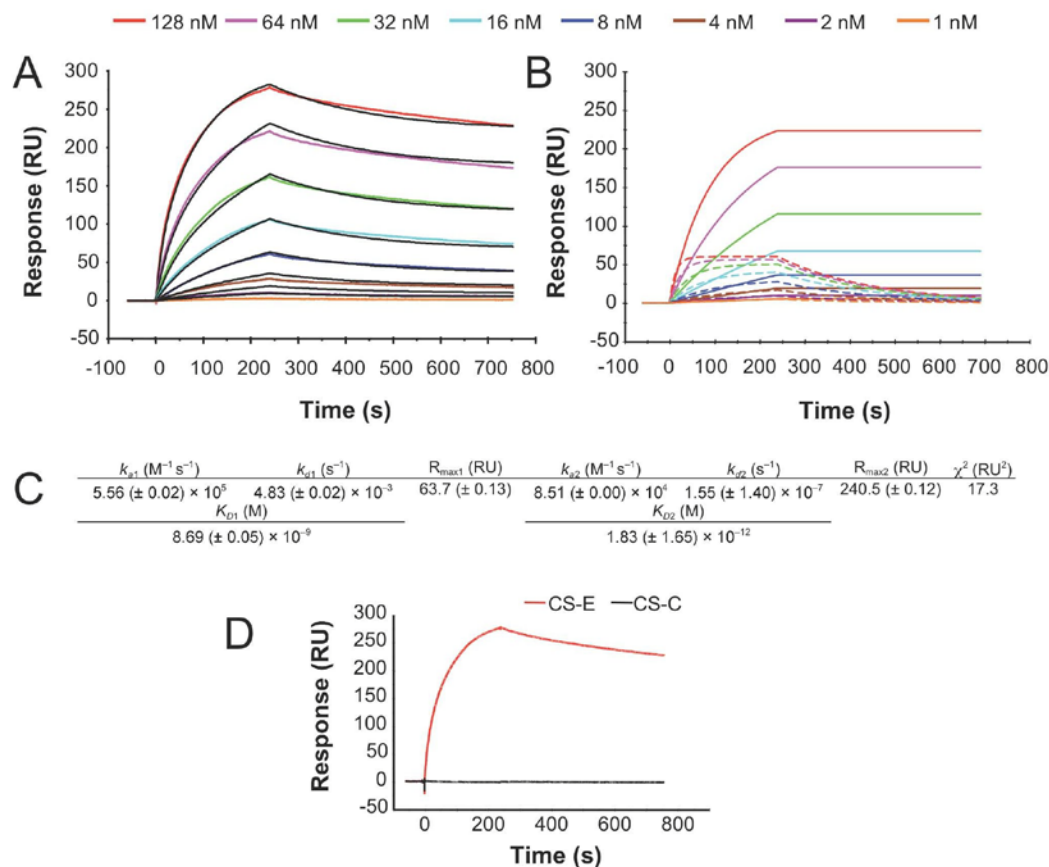
Figure A1.6. Kinetic analysis of NgR-binding to CS-E-enriched polysaccharides by surface plasmon resonance. (A) Biotinylated CS-E polysaccharides were immobilized onto the surface via streptavidin capture (R_L = 25 RU). NgR was passed over the surface at 80 µL/min at 25 ºC for 240 s. After monitoring the dissociation for 600 s, the surface was regenerated by three successive injections of 2.5 M MgCl$_2$ of 90 s at 30 µL/min. The resulting sensorgrams were fit to the heterogeneous ligand model (black lines), where the bulk refractive index (RI) was set as a constant value of zero. The model predicts two independent binding sites. The kinetic parameters derived from the fitting are tabulated in (C), with the standard error in parentheses. (B) Simulation of curves representing the individual binding components of the heterogeneous ligand model. A binding site with picomolar affinity (solid lines) binds approximately 6 molecules of NgR per polysaccharide, based on solving the equation $R_{max} = R_L(MW_A/MW_L)S_m$ for S_m, the number of binding sites. The observed nanomolar binding site (dashed lines) binds approximately 2 molecules of NgR per polysaccharide. (D) No binding of NgR to CS-C polysaccharides was observed (black line).

This specific binding of the receptor protein ectodomains to CS-E on the microarrays gave the first possible indication that these proteins could serve as a receptor for CS-E and thus for CSPG. However, these soluble proteins represent only a portion of the total protein, and lack the C-terminal end of NgR and the transmembrane and intracellular portions of p75. Additionally, several of the myelin inhibitory proteins were not commercially available as soluble proteins, and thus need to be cloned and expressed. The next step was to confirm the microarray binding results by testing for specific binding to CS-E with the native, full-length proteins. We generated full-length expression vectors for NgR and p75, as well as the receptors Lingo-1 and PirB, which were not available as soluble fusion proteins for testing on the array. These constructs were transfected into COS-7 cells, which were later lysed to solubilize membrane proteins.

After establishing expression of the full-length proteins, the next step was to try to confirm the specific binding to CS-E as seen with the microarrays, using CS that had been biotinylated as described previously.[24] This technique yields a one-to-one ratio of biotin to CS, and produces CS molecules that can be immobilized via one end, allowing the rest of the molecule to remain free to interact with proteins of interest.
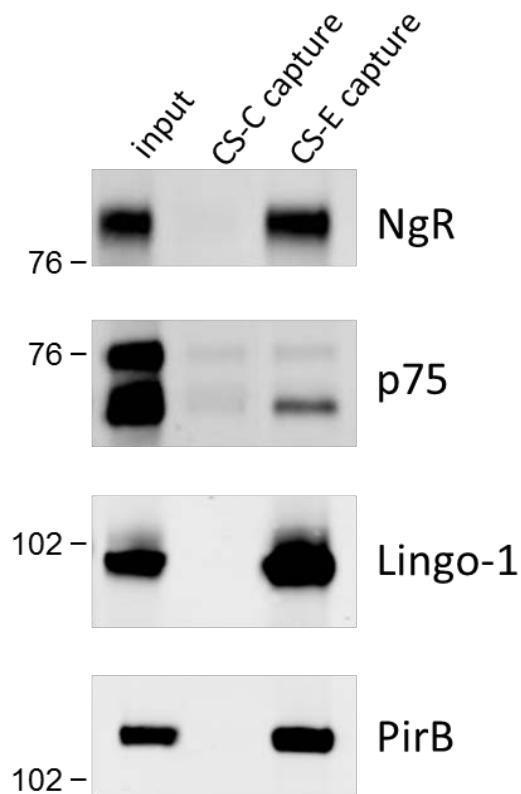
Figure A1.7. Full-length expressed proteins bind to CS-E.

After biotinylation, the concentrations of the biotinylated CS samples were determined by carbazole assay.[25] The biotinylated CS-C or CS-E samples were then conjugated to streptavidin agarose beads, and cell lysates from COS-7 cells expressing NgR, p75, Lingo1, or PirB were incubated with the beads. The streptavidin-CS beads, and any proteins bound to the beads, were then pelleted and washed. The bound proteins were eluted from the beads, and the eluates were analyzed by western blot for NgR-myc. This assay showed that CS-E (but not CS-C) is able to pull NgR out of solution, confirming that NgR binds preferentially to CS-E (Figure A1.7).

The salt concentration of the lysis buffer, as well as the overall protein concentration, was critical for binding, as lysates diluted with water showed stronger

pulldown of NgR by CS-E, as compared with lysates diluted with phosphate buffered saline (PBS) or undiluted lysates (data not shown). The observed importance of salt concentration is consistent with previous results examining protein binding to glycosaminoglycans.[26]
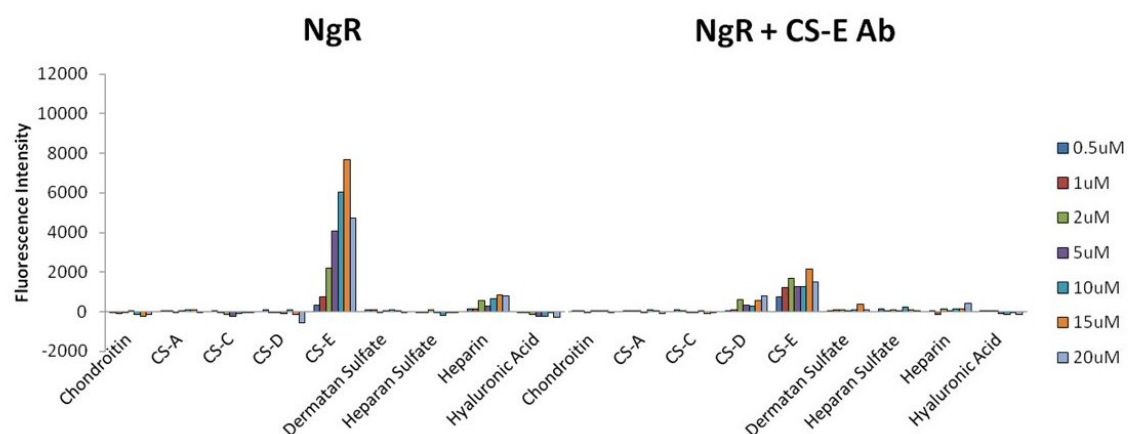
Figure A1.8. The CS-E monoclonal antibody (mAb) attenuates binding of CS-E polysaccharides to NgR-Fc. NgR-Fc (400 nM) was added to microarrays alone or with the CS-E mAb (20 µM).

An important implication of these results is that blocking CS-E interactions may prevent the inhibition caused by CSPGs and promote axon regeneration. Our lab previously raised a monoclonal antibody against a pure synthetic CS-E tetrasaccharide,[27] and experiments showed that the antibody generated in this manner was highly selective for the CS-E sulfation motif on polysaccharides, as measured by dot blot, ELISA, carbohydrate microarrays, and surface plasmon resonance.[28] This antibody was able to block the interaction of CS-E polysaccharides with NgR on the array (Figure A1.8).

The microarray, SPR, and pulldown experiments show evidence that NgR and possibly other components of the receptor complex bind preferentially to CS-E. To determine if the NgR complex is in fact mediating the inhibitory signal of CS-E, we tested cerebellar granule neurons (CGNs) from p75 knockout (KO) mice to find if the inhibitory effect of CS-E would be attenuated in these neurons. Because NgR lacks an intracellular signaling domain and requires formation of a complex with the neurotrophin receptor p75, a receptor critical for the inhibitory activity of CNS myelin,[8, 29, 30] we next investigated the contribution of p75 to CS-E activity. Mice lacking the p75 receptor have normal lifespans and are generally healthy, but lack sensation in their extremities and develop digital lesions as a result.[31] We reasoned that p75 knockout mice would effectively lack a functional NgR/p75 receptor complex, as the NgR has no intracellular domain and thus depends on p75 to transmit its inhibitory signal. Neurons from either p75 -/- or wild-type control mice were cultured on substrates of poly-ornithine (P-Orn) alone or P-Orn coated with CS-E or CSPG for 24 h. We found that p75 -/- neurons do not display significant rescue on surfaces of CS-E or CSPG (Figure A1.9). This result may be explained by other proteins that can fulfill the role of p75 in the signaling complex, such as TAJ/TROY.
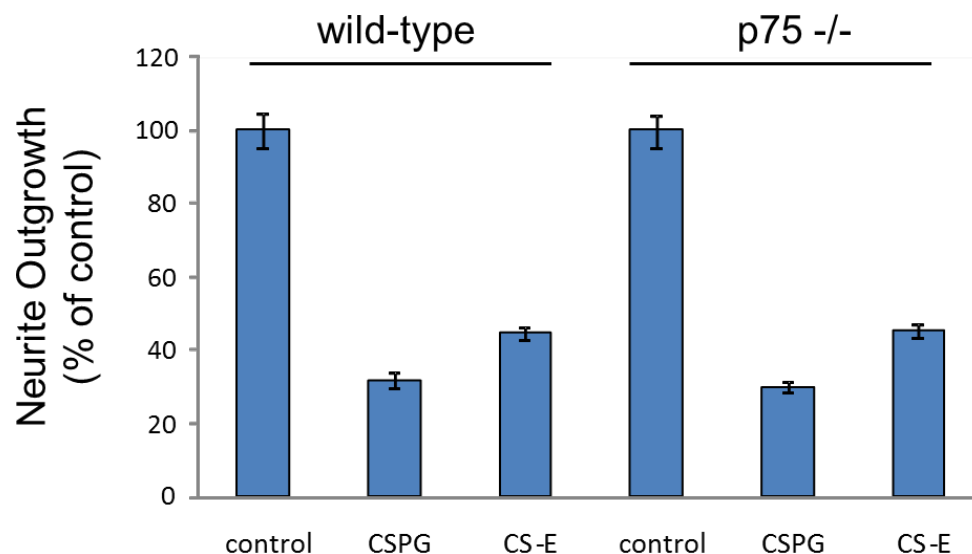
Figure A1.9. Neurite outgrowth inhibition mediated by CS-E and CSPGs is not significantly attenuated in p75^{NTR}-deficient neurons. CGN neurons from wild type or p75^{NTR}-deficient mice were cultured on a substratum of P-Orn and CS-E or CSPGs. Neurites were visualized by staining with an anti-βIII-tubulin antibody, and the percent neurite outgrowth is quantified relative to the wild-type control. Quantification from three experiments is reported. (n = 50-200 cells per experiment).

Conclusions

A major obstacle to axonal regeneration is the inhibitory environment encountered by injured axons. This activity is principally attributable to the myelin-associated inhibitory proteins and proteoglycans associated with the glial scar. The three proteins MAG, OMgp, and Nogo-66 account for the majority of myelin-based inhibition, and these proteins activate several receptor complexes, some of which are common to the different proteins. Several receptors for CSPGs have recently been identified, and these receptors engage the chondroitin sulfate component of CSPGs. The diverse sulfation patterns of CS have further complicated the study of these interactions, and our lab has focused on the CS-E motif which seems most responsible for the activity of CS.

Our binding results suggest that NgR may be the member of a receptor complex responsible for binding CS-E. This means that NgR is a possible point of convergence for binding both groups of inhibitory molecules responsible from preventing neuronal recovery after injury in the CNS: the myelin inhibitory proteins and CSPGs. Recently, another group demonstrated that two variants of the NgR, NgR1 and NgR3, can serve as receptors for CSPGs.[19] This supports our initial findings, and CS-E likely serves as the recognition element for NgR binding to CSPGs. Furthermore, our findings demonstrate that most of the ligands and receptors involved in myelin inhibition show preferred binding to the CS-E motif. As CS-E is upregulated during injury, this motif may act as a recruiting mechanism for these inhibitory molecules. Furthermore, this shared binding of the CS-E motif by the ligands and receptors may act as a mechanism to enhance the effect of binding.

Genetic methods removing individual receptors have not been able to account for the inhibitory effect observed in vivo. Genetic removal of the receptors PirB or p75, which should remove receptors for both groups of inhibitory molecules, do not allow substantial growth past the injury site.[32, 33] However, there may be an effect in certain systems and cell types, as deletion of the p75 receptor has been shown to allow recovery in the injured optic nerve.[34] In the studies described here, p75-deficient neurons did not have enhanced growth capability of substrates of CS-E or CSPG.

Materials and Methods

Microarray assays. Carbohydrate microarrays were generated by spotting 1 nl of the heparin (Sigma), hyaluronic acid (Sigma), dermatan sulfate (Sigma), heparan sulfate (Neoparin), chondroitin (Seikagaku) chondroitin sulfate (Seikagaku), or keratan sulfate (Seikagaku) polysaccharide solutions onto poly-L-lysine-coated slides using a Microgrid II arrayer (Biorobotics; Cambridge, UK) at room temperature and 50% humidity. The concentrations of the solutions ranged from 500 nM to 20 μM, and were calibrated to one another using the carbazole assay for uronic acid residues.[25] A given concentration of each polysaccharide was spotted ten times at different positions on the array. A boundary was created around the polysaccharide spots on the slides using a hydrophobic slide marker (Super Pap Pen, Research Products International) and the slides were blocked with 10% fetal bovine serum (FBS) in PBS with gentle rocking at 37 °C for 1 h, followed by a brief rinse with PBS. Human NgR-Fc, p75-Fc, or Fc control (R & D Systems) were reconstituted in 1% BSA in PBS, added to the bound region on the slides in 100 μl quantities at a concentration of 1-2 μM, and incubated at room temperature for 3 h. The slides were briefly rinsed three times with PBS, and then incubated with a goat anti-human IgG antibody conjugated to Cy3 (1:5000 in PBS) for 1 h in the dark with gentle rocking. After rinsing two times with PBS and once with H_2O, the microarray was analyzed at 532 nm using a GenePix 5000a scanner, and fluorescence quantification was performed using GenePix 6.0. The experiments were repeated 5-6 times, and data representing the average of all spots (± SE, error bars) for all spots were shown.

Expression plasmids and cell lysis. Full-length human p75 cDNA (amino acids 1-427; Open Biosystems) was ligated into a pcDNA3 vector (Invitrogen), modified to fuse an HA tag to the 5' end of the insert using the restriction enzymes NotI (N-terminal) and BamHI (C-terminal). Human NgR (amino acids 27-473; imaGenes) was ligated into a modified pAPtag-5 vector (GenHunter) which fuses a secretion signal sequence and a c-myc tag to the 3' end of the insert using the restriction enzymes NotI (N-terminal) and BamHI (C-terminal). Lingo-1 and PirB genes were subcloned from mouse cDNA (Open Biosystems) into a pCAX Myc6 vector using the restriction enzymes HindIII (N-terminal) and XhoI (C-terminal) to place an N-terminal 6X Myc tag on the expressed proteins. The vector contained a secretion peptide coding sequence upstream of the myc tag; thus, the endogenous signal peptide coding sequences were excluded from the cloning sequence.

p75 sense primer:

GTGGCGGCCGCCATGTATCCATATGATGTTCCAGATTATGCTATGGGGGCAGGTGCCACC

p75 antisense primer:

GCGGGATCCTCACACCGGGGATGTGGCAGTGGACTCACTGCACAGACTCTCCACG

NgR sense primer: GTGGCGGCCGCCATGAAGAGGGCGTCCGCTGGAGGGAGC

NgR antisense primer:

GCGGGATCCTCACAGATCCTCTTCAGAGATGAGTTTCTGCTCGCAGGGCCCAAGCACAGTCC

Lingo-1 sense primer: CCCAAGCTTACACGGGCTGCCCGCCCCGCTGCGAG

Lingo-1 antisense primer: CCGCTCGAGTATCATCTTCATGTTGAACTTGCG

PirB sense primer: CCCAAGCTTACTCCCTCCCTAAGCCTATCCTCAGA

PirB antisense primer: CCGCTCGAGTTGCTCCATGTCCTTGGGAACAGC

COS-7 cells were transfected using the Lipofectamine (Invitrogen) method. Cells were lysed two days after transfection with 1% Triton X-100 in PBS containing a protease inhibitor mixture (Roche) by rocking for 30 min at 4 °C. The lysates were clarified by centrifugation at 13,000 rpm for 5 min.

CS biotinylation. Biotin was attached to the free amino group of the residual core peptides of CS-C and CS-E polysaccharides (Seikagaku) with minor modifications to Saito *et al.*[24] Briefly, CS-C and CS-E (2 mg each) were dissolved in 1 ml of 0.05M $NaHCO_3$ for 30 min at room temperature. EZ-Link Sulfo-NHS-LC-LC-Biotin (0.25 mg; Pierce) was dissolved in 1 ml of H_2O and added to each CS sample. The solution was mixed at room temperature for 3 h, lyophilized, resuspended in H_2O, and subjected to gel filtration using Sephadex G-50 (Amersham) to remove excess biotin.

Pull-down assays with biotinylated CS. Biotinylated CS-C and CS-E (280 μg each) in 300 μl of PBS were added to 140 μl of settled streptavidin agarose resin (Pierce), and incubated at room temperature for 1 h. The supernatant was removed and the resin was washed twice with 500 μl PBS to remove unconjugated CS. Clarified COS-7 cell lysates

were diluted 1:10 with PBS, and further diluted 1:2 with H_2O. Diluted lysate (500 μl, 0.8 mg/ml total protein) was incubated with 30 μl of unconjugated streptavidin agarose resin with mixing for 1 h at 4°C. The supernatant was collected, added to 30 μl of either CS-C or CS-E streptavidin agarose resin, and incubated with mixing for 4 h at 4°C. The supernatant was removed, and the resin was washed three times with 500 μl PBS. Resin was boiled with 30 μl 2X loading dye (100mM Tris, 200mM DTT, 4% SDS, 0.10% bromophenol blue, 20% glycerol) and the eluates were collected and separated by SDS-PAGE. NgR-myc, Lingo-1-myc, PirB-myc, and p75-HA were detected by immunoblotting with monoclonal myc-tag (Cell Signaling) or HA-tag (Sigma) antibodies.

CGN neurite outgrowth assays. Nitric acid-treated, 15-mm round German glass coverslips were coated with P-Orn in borate buffer, pH 8.5 (50 µg/ml) for 1 h at 37 °C and 5% CO_2. CSPGs (1 µg/ml) or polysaccharides enriched in the CS-A, CS-C, or CS-E sulfation motifs (1 µg/ml) were coated on the P-Orn-coated coverslips overnight at 37 °C and 5% CO_2. For neurite outgrowth experiments from p75 knockout mice, cerebella from P5-7 mice, either C57BL/6 wild-type or p75-/- knockout mice, were dissected, incubated in 0.125% trypsin w/ EDTA for 10 min at 37 °C, triturated to dissociate to single cell suspensions, purified on discontinuous 35%/60% Percoll gradient, and cultured on the coated coverslips in Neurobasal medium supplemented with B27, GlutaMAX™ (Invitrogen), and 40 ng/ml bFGF (R&D) at a density of 200-300 cells/mm^2 for 24 h. Cells were fixed in 4% PFA with 10% sucrose, immunostained using an anti-β tubulin III antibody (TUJ1; Covance), imaged using a Nikon TE2000-S fluorescent microscope and

quantified using the NIH software ImageJ. Statistical analysis was performed using the

one-way ANOVA; n = 50–200 cells per experiment, and results from at least three

independent experiments were reported.

References

1.   Filbin, M. T. Myelin-associated inhibitors of axonal regeneration in the adult mammalian CNS. *Nat. Rev. Neurosci.* **2003,** 4, (9), 703-713.

2.   Yiu, G. & He, Z. Glial inhibition of CNS axon regeneration. *Nat. Rev. Neurosci.* **2006,** 7, (8), 617-627.

3.   Busch, S. A. & Silver, J. The role of extracellular matrix in CNS regeneration. *Curr. Opin. Neurobiol.* **2007,** 17, (1), 120-127.

4.   McGee, A. W. & Strittmatter, S. M. The Nogo-66 receptor: focusing myelin inhibition of axon regeneration. *Trends Neurosci.* **2003,** 26, (4), 193-198.

5.   Fournier, A. E., GrandPre, T. & Strittmatter, S. M. Identification of a receptor mediating Nogo-66 inhibition of axonal regeneration. *Nature* **2001,** 409, (6818), 341-346.

6.   Liu, B. P., Fournier, A., GrandPre, T. & Strittmatter, S. M. Myelin-associated glycoprotein as a functional ligand for the Nogo-66 receptor. *Science* **2002,** 297, (5584), 1190-1193.

7.   Wang, K. C*., et al.* Oligodendrocyte-myelin glycoprotein is a Nogo receptor ligand that inhibits neurite outgrowth. *Nature* **2002,** 417, (6892), 941-944.

8.   Wang, K. C., Kim, J. A., Sivasankaran, R., Segal, R. & He, Z. G. p75 interacts with the Nogo receptor as a co-receptor for Nogo, MAG and OMgp. *Nature* **2002,** 420, (6911), 74-78.

9.   Mi, S*., et al.* LINGO-1 is a component of the Nogo-66 receptor/p75 signaling complex. *Nat. Neurosci.* **2004,** 7, (3), 221-228.

10.   Shao, Z*., et al.* TAJ/TROY, an orphan TNF receptor family member, binds Nogo-66 receptor 1 and regulates axonal regeneration. *Neuron* **2005,** 45, (3), 353-359.

11.   Ahmed, Z., Douglas, M. R., John, G., Berry, M. & Logan, A. AMIGO3 Is an NgR1/p75 Co-Receptor Signalling Axon Growth Inhibition in the Acute Phase of Adult Central Nervous System Injury. *PLoS One* **2013,** 8, (4), e61878.

12.   Vinson, M*., et al.* Myelin-associated glycoprotein interacts with ganglioside GT1b. A mechanism for neurite outgrowth inhibition. *J. Biol. Chem.* **2001,** 276, (23), 20280-20285.

13. Yamashita, T., Higuchi, H. & Tohyama, M. The p75 receptor transduces the signal from myelin-associated glycoprotein to Rho. *J. Cell Biol.* **2002,** 157, (4), 565-570.

14. Atwal, J. K.*, et al.* PirB is a functional receptor for myelin inhibitors of axonal regeneration. *Science* **2008,** 322, (5903), 967-970.

15. Fujita, Y., Takashima, R., Endo, S., Takal, T. & Yamashita, T. The p75 receptor mediates axon growth inhibition through an association with PIR-B. *Cell Death Dis.* **2011,** 2.

16. Monnier, P. P., Sierra, A., Schwab, J. M., Henke-Fahle, S. & Mueller, B. K. The Rho/ROCK pathway mediates neurite growth-inhibitory activity associated with the chondroitin sulfate proteoglycans of the CNS glial scar. *Mol. Cell. Neurosci.* **2003,** 22, (3), 319-330.

17. Shen, Y.*, et al.* PTPsigma is a receptor for chondroitin sulfate proteoglycan, an inhibitor of neural regeneration. *Science* **2009,** 326, (5952), 592-596.

18. Fisher, D.*, et al.* Leukocyte common antigen-related phosphatase is a functional receptor for chondroitin sulfate proteoglycan axon growth inhibitors. *J. Neurosci.* **2011,** 31, (40), 14051-14066.

19. Dickendesher, T. L.*, et al.* NgR1 and NgR3 are receptors for chondroitin sulfate proteoglycans. *Nat. Neurosci.* **2012,** 15, (5), 703-712.

20. Sivasankaran, R.*, et al.* PKC mediates inhibitory effects of myelin and chondroitin sulfate proteoglycans on axonal regeneration. *Nat. Neurosci.* **2004,** 7, (3), 261-268.

21. Koprivica, V.*, et al.* EGFR activation mediates inhibition of axon regeneration by myelin and chondroitin sulfate proteoglycans. *Science* **2005,** 310, (5745), 106-110.

22. Kaneko, M., Kubo, T., Hata, K., Yamaguchi, A. & Yamashita, T. Repulsion of cerebellar granule neurons by chondroitin sulfate proteoglycans is mediated by MAPK pathway. *Neurosci. Lett.* **2007,** 423, (1), 62-67.

23. Schweigreiter, R.*, et al.* Versican V2 and the central inhibitory domain of Nogo-A inhibit neurite growth via p75NTR/NgR-independent pathways that converge at RhoA. *Mol. Cell. Neurosci.* **2004,** 27, (2), 163-174.

24. Saito, A. & Munakata, H. Detection of chondroitin sulfate-binding proteins on the membrane. *Electrophoresis* **2004,** 25, (15), 2452-2460.

25. Taylor, K. A. & Buchanansmith, J. G. A Colorimetric Method for the Quantitation of Uronic-Acids and a Specific Assay for Galacturonic Acid. *Anal. Biochem.* **1992,** 201, (1), 190-196.

26. Moss, J. M., VanDamme, M. P. I., Murphy, W. H. & Preston, B. N. Dependence of salt concentration on glycosaminoglycan-lysozyme interactions in cartilage. *Arch. Biochem. Biophys.* **1997,** 348, (1), 49-55.

27. Tully, S. E., Rawat, M. & Hsieh-Wilson, L. C. Discovery of a TNF-alpha antagonist using chondroitin sulfate microarrays. *J. Am. Chem. Soc.* **2006,** 128, (24), 7740-7741.

28. Brown, J. M.*, et al.* A sulfated carbohydrate epitope inhibits axon regeneration after injury. *Proc. Natl. Acad. Sci. U S A* **2012,** 109, (13), 4768-4773.

29. Wong, S. T.*, et al.* A p75(NTR) and Nogo receptor complex mediates repulsive signaling by myelin-associated glycoprotein. *Nat. Neurosci.* **2002,** 5, (12), 1302-1308.

30. Zheng, B.*, et al.* Genetic deletion of the Nogo receptor does not reduce neurite inhibition in vitro or promote corticospinal tract regeneration in vivo. *Proc. Natl. Acad. Sci. U S A* **2005,** 102, (4), 1205-1210.

31. Lee, K. F., Bachman, K., Landis, S. & Jaenisch, R. Dependence on P75 for Innervation of Some Sympathetic Targets. *Science* **1994,** 263, (5152), 1447-1449.

32. Nakamura, Y., Fujita, Y., Ueno, M., Takai, T. & Yamashita, T. Paired immunoglobulin-like receptor B knockout does not enhance axonal regeneration or locomotor recovery after spinal cord injury. *J. Biol. Chem.* **2011,** 286, (3), 1876-1883.

33. Omoto, S., Ueno, M., Mochio, S., Takai, T. & Yamashita, T. Genetic deletion of paired immunoglobulin-like receptor B does not promote axonal plasticity or functional recovery after traumatic brain injury. *Neurosci. Res.* **2010,** 68, E254-E254.

34. Uesugi, N., Kimura, Y. & Yamashita, T. Suppression of the p75 receptor signal attenuates the effect of ephrin-B3 and promotes axonal regeneration of the injured optic nerve. *Cell Death Dis.* **2013,** 4, e557.